ROLE OF LPS AND PEPTIDOGLYCAN MONOMERS IN THE SYMBIOTIC INTERACTIONS BETWEEN VIBRIO FISCHERI AND EUPRYMNA SCOLOPES

by

DAWN MICHELLE ADIN

(Under the Direction of Eric V. Stabb)

ABSTRACT

The symbiosis between the bioluminescent bacterium Vibrio fischeri and the Hawaiian squid Euprymna scolopes allows for the study of how beneficial bacteria communicate with and colonize a mutualistic host. This dissertation work focuses on two signaling molecules within the symbiosis, lipid A and peptidoglycan (PG) monomers. The first goal was to determine the role of secondary acylations of lipid A in colonization of the host by examining V. fischeri lipid A acyltransferase mutants. While mutations in htrB2 and msbB had no effect on host colonization, a deletion of htrB1 resulted in delayed initiation of symbiotic colonization suggesting secondary acylations of lipid A may be important during initial infection. The next goal focused on the genetic basis for PG monomer release in V. fischeri. PG monomer, Nacetylglucosaminyl-1,6-anhydro-*N*-acetylmuramylalanyl-y-glutamyldiaminopimelylalanine, stimulates normal light-organ morphogenesis in the host, resulting in regression of infectionpromoting ciliated appendages. Genomic analysis suggested V. fischeri has a functional PG recycling system including the PG monomer permease AmpG, which most Gram-negative bacteria use to recycle PG monomer. Deletion of ampG resulted in a 100-fold increase in PG monomer release and this enhanced PG monomer release induced regression in animals exposed

to a V. fischeri strain that is unable to colonize the light organ, demonstrating that regression of

the ciliated appendages can be independent of colonization. Mutant analysis further suggested

that PG monomer release in culture is mediated by three lytic transglycosylases; LtgA1, LtgA2,

and LtgD, and a ltgA1 ltgA2 ltgD mutant released low levels of PG monomers. This mutant

colonized squid and stimulated light-organ morphogenesis; however, animals infected with this

mutant were more susceptible to secondary V. fischeri colonists, suggesting attenuated triggering

of ciliated appendage regression. To analyze the regulation behind PG monomer release,

transposon mutagenesis on an ampG::lacZ reporter strain was performed. Surprisingly, mutants

were isolated that cleave 5-bromo-4-chloro-3-indolyl-β-D-galactoside independent of the

engineered ampG lacZ reporter. This phenotype resulted from cryptic galactosidase activity of

the celCBGKAI gene cluster, which allows V. fischeri to grow on cellobiose. Constructs for

mutating celG or introducing celI may enable future applications of lacZ as a reporter for

studying regulation of genes underpinning symbiotic signaling.

INDEX WORDS:

LOS, lpxM, lpxL, tracheal cytotoxin, peptidoglycan cytotoxin, TCT,

PGCT, Photobacterium, chitin, cellulose, Aliivibrio

ROLE OF LPS AND PEPTIDOGLYCAN MONOMERS IN THE SYMBIOTIC INTERACTIONS BETWEEN VIBRIO FISCHERI AND EUPRYMNA SCOLOPES

by

DAWN MICHELLE ADIN

B.S., Jacksonville University, 2001

A Dissertation Submitted to the Graduate Faculty of The University of Georgia in Partial Fulfillment of the Requirements for the Degree

DOCTOR OF PHILOSOPHY

ATHENS, GEORGIA

2008

© 2008

Dawn Michelle Adin

All Rights Reserved

ROLE OF LPS AND PEPTIDOGLYCAN MONOMERS IN THE SYMBIOTIC INTERACTIONS BETWEEN VIBRIO FISCHERI AND EUPRYMNA SCOLOPES

by

DAWN MICHELLE ADIN

Major Professor: Eric V. Stabb

Committee: Russell W. Carlson

Anna C. Karls MaryAnn Moran Lawrence J. Shimkets

Electronic Version Approved:

Maureen Grasso Dean of the Graduate School The University of Georgia August 2008

DEDICATION

I dedicate this thesis to my family and to my sweet husband. My mother, who kept me in graduate school through some of the darkest days, encouraging me to see the positives in this experience. My father, who I knew would be there to back me up no matter what happened. My grandparents, who were so supportive and willing to do almost anything to make sure things were ok. And my dear husband, John, who has rode this part of the road with me through it all. I do not know how I could have made it through this without all of your support.

ACKNOWLEDGEMENTS

This whole experience has been a growing and ever evolving journey. They say it takes a village to raise a child; well it definitely takes a small army to help someone get through a dissertation and defense. I would like to thank my graduate mentor, Eric, for making sure that I stuck to the plan and not letting me wander down to many dead end paths. I have learned a great deal from his persistence and vision and I finally fully understand the reason for our weekly meetings. My committee, Anna, Larry, MaryAnn and Russ are the nicest people a person could have on a committee. They each challenged me and pushed me to think about things more than I thought I could. I am honored to have each of then as a member and I am so thankful for all their help. I need to also thank our collaborator Margaret McFall-Ngai for her willingness to help and come to my rescue with any questions that I had about the squid. Her quick responses and advice were a welcome sight in these past few months. Josh Troll, a graduate student in the McFall-Ngai lab, has been not only a useful resource for squid experiments, but also a supportive colleague for understanding the painful days of squid experiments and the frustration of a laboratory squid famine. Susie Engle, formerly in Bill Goldman's lab, ran the HPLC and put up with countless emails asking questions. I thank her for putting up with me when I went to St. Louis and her patience is undeniable.

My lab family have been not only been fantastic role models, but also good friends. Those that have gone forward with their careers, Anne Dunn and Jeff Bose, went above and beyond with helping me look at the next step of my research. I especially want to thank Jeff for

putting up sharing my desk half with me. More than once he had to listen to me talking to myself and I appreciate him humoring my endless "what do you think about this" questions. My current labmates: Noreen and Alecia, are some of the hardest working people I know and I will miss working with them every Saturday and Sunday. I thank them for dealing with me through this last stretch of graduate school and smiling when my neuroticism was a little out of control. Deanna, our newest member, has only be part of the last leg of this journey and I hope that I have not scared her off of graduate school too much..

Marcel Proust said "Let us be grateful to people who make us happy; they are the charming gardeners who make our souls blossom". I have been lucky enough to form some wonderful friendships with some of the smartest gardeners then that I've ever known. I cannot list everyone, but there are a few that I want to particularly point out. I want to thank Pam Bonner Brown, Tiffany Major and Stephanie Ross Bose for being so supportive my first few years here. I need to also mention the best class ever: Praveen Alamuri, John Buchner, Patrick Curtis, and James Henriksen. If it were not for them, I never would have made it through any of our classes. Chandra Carpenter, who has been my sounding board, my "oh my god you won't believe what just happened", and my Sonic Happy Hour buddy. I thank her for her honesty and her friendship. She is truly one of my closest and dearest friends. I need to thank my neglected friends from college, Angela, Amber, Trisha, and Samantha, who have dealt with my sporadic emails and half crazy phone calls (ok, fully crazy phone calls). I also need to acknowledge the thesis reading group (ie. dissertation group therapy), John Buchner, Chandra Carpenter, Emily DeCrescenzo Henriksen and James Henriksen. It has been a difficult last few months, but 11 days and 5 defenses later; we are going to finish together.

I truly need to thank my family for their support and understanding in these past 7 years. It has not always been the most fun time for them or me, but the end is finally here and I owe them more than I could even imagine. I just hope that hugs and kisses are enough to pay them back for all the love they have bestowed upon me.

I thank my husband, John Buchner. St. Thomas Aquinas said, "Love takes up where knowledge leaves off." We were lucky enough to meet during this time and I could not imagine having anyone else more wonderful to be part of my life. It has not been the easiest 6 years, but going through this has shown us that we are an awesome team. I am unbelieveably proud of him and all that he has accomplished. I truly believe he is the other half of my soul and I am honored to be his wife and friend.

And finally, one last quote from Daniel Boorstin, "Education is learning what you didn't even know you didn't know." I have learned a tremendous amount in these past 7 years and am now more aware then ever all the things I still do not know. I thank each and every one of my family, friends, faculty, and department staff for being part of this educational chapter in my life. I hope they all play a part in the next chapter as it unfolds.

TABLE OF CONTENTS

	Pag	ţе.
ACKNO	OWLEDGEMENTS	V
LIST OF	F TABLES	κi
LIST OF	F FIGURESx	ii
CHAPT	ER	
1	INTRODUTION AND LITERATURE REVIEW	1
	Overview	1
	The Vibrio fischeri-Euprymna scolopes symbiosis	1
	V. fischeri-E. scolopes symbiosis is a model system	2
	E. scolopes light organ development of the symbiosis	3
	Signals in the symbiosis	8
	LPS biosynthesis	0
	Importance of LPS in innate immunity	3
	PG biosynthesis and recycling	4
	Importance of PG in innate immunity1	8
	LPS and PG as signaling molecules in other symbioses	9
	Rhizobium-legume symbiosis and the role of LPS and PG in the symbiosis2	0
	Complex gut microbiota symbioses and the role of LPS in maintenance of the	
	microbial community2	23

	Future aims of research with PG and LPS	24
	Rationale and objectives of this study	24
2	CHARACTERIZATION OF HTRB AND MSBB MUTANTS OF THE LIGHT	
	ORGAN SYMBIONT VIBRIO FISCHERI	27
	Abstract	28
	Introduction	29
	Materials and Methods	30
	Results	40
	Discussion	53
	Acknowledgements	57
3	MUTATIONS IN AMPG AND LYTIC TRANSGLYCOSYLASE GENES	
	AFFECT THE NET RELEASE OF PEPTIDOGLYCAN MONOMERS FRO	M
	VIBRIO FISCHERI	58
	Abstract	59
	Introduction	60
	Materials and Methods	62
	Results	71
	Discussion	82
	Acknowledgements	85
4	IDENTIFICATION OF A CELLOBIOSE UTILIZATION GENE CLUSTER W	ITH
	CRYPTIC β-GALACTOSIDASE ACTIVITY IN <i>VIBRIO FISCHERI</i>	87
	Abstract	88
	Introduction	89

Materials and Methods	90
Results	98
Discussion	112
Acknowledgements	116
5 CONCLUSIONS AND FUTURE DIRECTIONS	117
LPS and Lipid A	118
Peptidoglycan	120
MAMP signal perception by hosts	121
REFERENCES	
APPENDICES	151
A CHADACTEDIZATION OF CENES THAT AT TED VIRRIO FISCHERIT DS	151

LIST OF TABLES

Page
Table 2.1: Bacterial strains, plasmids and oligonucleotides
Table 2.2: Percent fatty acid composition of partially purified lipid A from V. fischeri ES114 and
mutant derivatives
Table 2.3: Effects of htrB and msbB mutations on V. fischeri sensitivity to SDS, polymyxin B
and kanamycin46
Table 3.1: Bacterial strains, plasmids, and oligonucleotides
Table 3.2: Peptidoglycan biosynthesis and recycling protein homologs in <i>V. fischeri</i> 72
Table 4.1: Bacterial strains, select plasmids, and oligonucleotides94
Table 4.2: Growth and acid production of <i>Vibrio</i> strains on glucose and cellobiose
Table 4.3: Colonization competitiveness of <i>V. fischeri cel</i> mutants relative to ES114112
Table A.1: <i>V. fischeri</i> strains, select plasmids, and oligonucleotides
Table A.2: Percent fatty acid composition of partially purified lipid A from V. fischeri ES114
and DMA370 (bacA)164

LIST OF FIGURES

Page
Figure 1.1: The <i>V. fischeri-E. scolopes</i> light organ symbiosis
Figure 1.2: <i>E. scolopes</i> light organ morphogenesis
Figure 1.3: Simplified illustration of major LPS components
Figure 1.4: Modifications to the Kdo ₂ -lipid A in <i>E. coli</i> K-12 and <i>Salmonella</i>
Figure 1.5: Schematic illustration of peptidoglycan synthesis and recycling
Figure 2.1: Chromosomal location and orientation of htrB1, htrB2, and msbB in V. fischeri
ES11441
Figure 2.2: Complementation of <i>E. coli</i> MKV15 with putative lipid A secondary acyltransferase
genes from <i>V. fischeri</i> 43
Figure 2.3: Motility of <i>V. fischeri htrB1</i> , <i>htrB2</i> , and <i>msbB</i> mutants
Figure 2.4: Morphology of <i>htrB2</i> mutants
Figure 2.5: Effects of <i>htrB1</i> , <i>htrB2</i> , and <i>msbB</i> mutations on bioluminescence
Figure 2.6: Symbiotic luminescence and colonization for <i>V. fischeri</i> wild type and an <i>htrB1</i>
mutant51
Figure 2.7: Competition between ES114 and its <i>htrB1</i> mutant EVS300 in culture and in
squid53
Figure 3.1: Mutation in <i>V. fischeri ampG</i> increases PG monomer release in log-phase
cultures

Figure 3.2: Mutations in V. fischeri lytic transglycosylases results in a decrease in PG mon	iomer
release in log phase cultures	77
Figure 3.3: A non-motile $ampG$ mutant triggers regression of the ciliated appendages of the	e light
organ	80
Figure 3.4: Animals infected with DMA388 (ΔltgA1 ΔltgD ltgA2::pDMA90) are more	
susceptible to a secondary infection	81
Figure 4.1: Schematic representation of the genetic organization around the <i>cel</i> gene cluster	er in V.
fischeri ES114	99
Figure 4.2: <i>celG</i> -dependent enzymatic activity	102
Figure 4.3: Specific fluorescence generated from P_{cel} -gfp reporter in ES114 (wt), mutant	
DMA420 (cel ^T), or mutant DMA401 (celΓ celG ⁻)	104
Figure 4.4: Homologs of the <i>V. fischeri</i> cellobiose-utilization genes	109
Figure 4.5: Comparison of V. fischeri CelB, CelC, CelK, and CelG to proteins encoded by	other
bacteria with similar gene clusters	110
Figure A.1: Motility of ptgA1, pgtA2, pgtA3 and bacA mutants	161
Figure A.2: Morphology of <i>pgtA3</i> mutant	161
Figure A.3: Alterations of the O-deacylated LPS by mutations in <i>pgtA1</i> and <i>pgtA2</i>	163

CHAPTER 1: INTRODUCTION AND LITERATURE REVIEW

Overview

Most animals have a persistent consortium of cooperative bacteria that provides important metabolic functions for the hosts and triggers normal host tissue development (222). These interactions are often initiated when a juvenile animal is first exposed to environmental bacteria, triggering complex signaling programs that orchestrate the establishment of the host-symbiont relationship. The complexity of multispecies microbial associations with hosts, such as those found in the mammalian intestinal tract, has hampered investigations into the mechanisms involved in symbiont-host signaling. The *Euprymna scolopes - Vibrio fischeri* symbiosis is an experimentally tractable association (21), and studying this interaction may shed light on the components of recognition, signaling, and persistence in a symbiont-host interaction. Studies of this symbiosis may also complement studies of pathogenesis, and together they may provide approaches for fighting microbial disease with less disruption of the host's native microbiota.

The Vibrio fischeri - Euprymna scolopes symbiosis

V. fischeri is a bioluminescent marine bacterium (143) that forms a symbiosis with the Hawaiian bobtail squid, E. scolopes, a nocturnal shallow-water invertebrate (18). Reports of bioluminescent symbioses with squid go back to the early 20th century (110). In 1928, Kishitani sectioned a Euprymna morsei light organ and drew detailed diagrams showing sac-like "glands" (now referred to as "crypts") caused by invaginations of an epithelial lining. These light organ

crypts were filled with bioluminescent bacteria, and he noted that the architecture of the whole organ seemed to be suited to produce and emit light (110). Later, *V. fischeri*, a Gram-negative, facultative anaerobe with polar flagella (143), was identified as the colonist of the *Euprymna* light organs and the source of luminescence (111, 294).

In this symbiosis, *E. scolopes* provides nutrients that support the growth and bioluminescence of *V. fischeri* (102). The light produced by the symbionts may be used by the squid in a camouflaging behavior known as counterillumination, whereby light is emitted ventrally, matching the intensity of moon and starlight thus cloaking itself from predators below it in the water column by obscuring its silhouette (132, 225). Other potential functions for the luminescence are suggested by reports of *E. scolopes* emitting flashes of light (120, 172, 185). The squid release a portion of their symbionts each day, regrowing the remainder in the light organ, and presumably as a result of this behavior *V. fischeri* is more abundant in waters where *E. scolopes* is present, reinforcing the idea that the relationship is beneficial for both host and symbiont (151).

V. fischeri - E. scolopes symbiosis is a model system

The mutualistic association between *E. scolopes* and *V. fischeri* is an excellent model system for studying interactions between bacteria and host tissues, because even though it is a simple and experimentally tractable system, it has many characteristics similar to relationships that are abundant in nature, most of which are more complex and less tractable. This host-symbiont relationship facilitates research into the mechanisms of establishing a cooperative symbiosis because: i) *E. scolopes* has a monospecific association with *V. fischeri* (i.e. no other bacteria colonize the light organ) even though other bioluminescent bacteria co-occur in the

same environment (174); ii) *V. fischeri* is horizontally transmitted, so juveniles are aposymbiotic and the symbiosis can be reconstituted in a controlled manner (294); iii) the absence of *V. fischeri* does not negatively affect lab-reared hosts (44); iv) numerous juvenile *E. scolopes* can be maintained in an experimental setting; and v) *V. fischeri* can be cultured independently of its host and is genetically manipulable.

E. scolopes light organ and development of the symbiosis

The E. scolopes light organ is bilobed and embedded in the ink sac on the ventral side of the mantle cavity (Figure 1.1A). Hatchling E. scolopes increase water flow across the light organ using ciliated appendages (170, 191, 195) with the effective stroke of the superficial cilia on the appendages toward six pores on the surface of the light organ (173) (Figure 1.1B-C). In the first hour after hatching, the light organ goes through a "permissible" stage where environmental bacteria, or experimentally added bacteria and 1 µm polystyrene beads, are drawn into the light organ (191). In nature, the few cells drawn in are unlikely to be V. fischeri, which comprises <0.1% of environmental bacterial populations (150). Furthermore, any bacteria sampled by the host in this way, including V. fischeri, are cleared after the hour and do not establish an infection (191). After the permissible stage, the squid's epithelial appendages begin shedding mucus that contains both sialomucin and neutral mucin (195). V. fischeri marked with green fluorescent protein were observed adhering to the mucus and forming aggregates on the surface of the light organ (192). These aggregates may contain other Gram-negative bacteria (195), but V. fischeri outcompetes them (192). Aggregates can contain fewer than twenty bacterial cells (177), but larger aggregates occur with denser inocula (192).

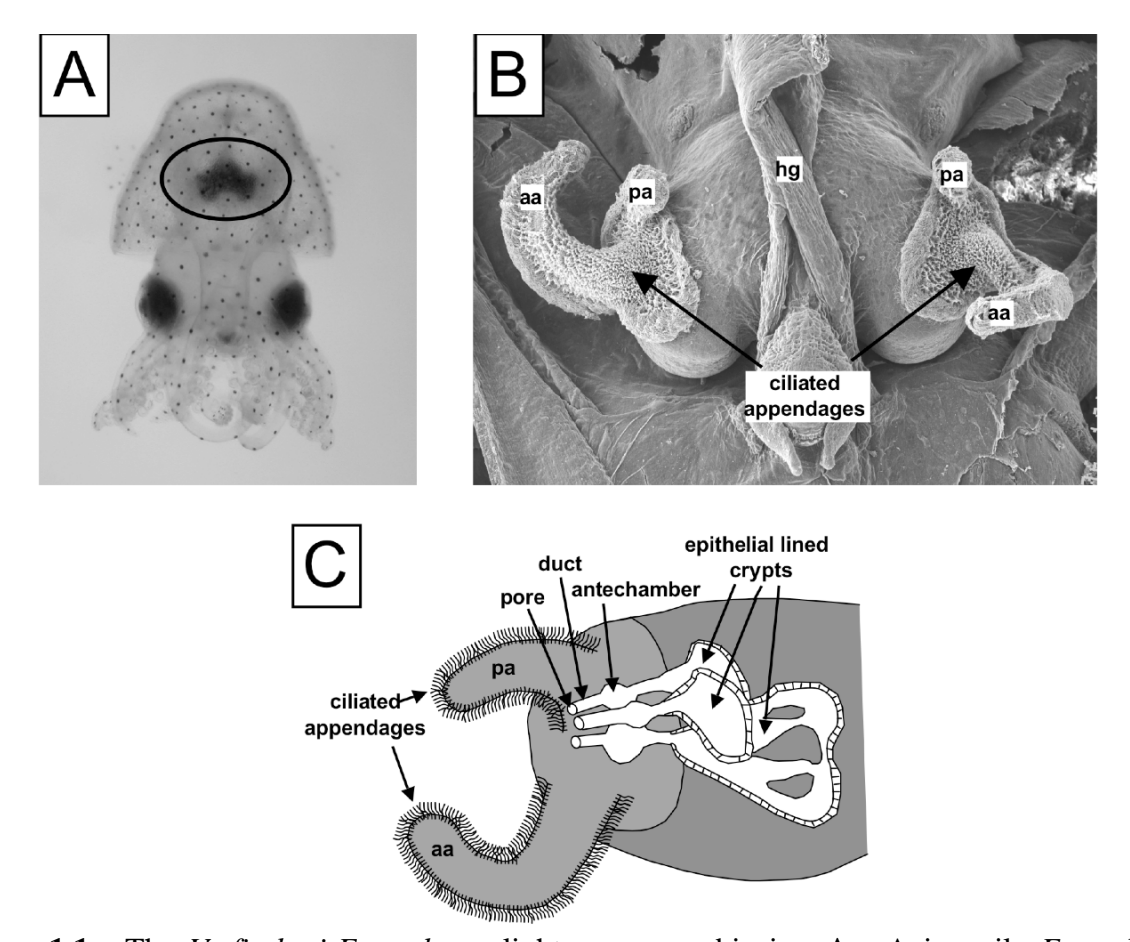


Figure 1.1. The *V. fischeri-E. scolopes* light organ symbiosis. **A.** A juvenile *E. scolopes* oriented ventral side up to show the light organ which is on top of the ink sac (circled in black) in the center of the mantle cavity. **B.** Scanning electron micrograph of an aposymbiotic juvenile *E. scolopes* in which the mantle has been removed to reveal the bilobed light organ with a pair of ciliated epithelial appendages one either side. The anterior (aa) and posterior (pa) ciliated appendages are indicated as well as the hindgut (hg). **C.** Cartoon illustration of one side of the symmetric bilobed light organ of an aposymbiotic juvenile *E. scolopes* light organ. Panels B and C are courtesy of Eric Stabb.

As early as 2 hours after inoculation, *V. fischeri* cells migrate through the mucus into pores, through ducts, and finally enter the epithelium-lined crypts in the light organ (Figure 1.1C) (195, 257). The ducts leading to the crypts contain cilia that beat outwards toward the pores, and the bacterial cells must be motile to traverse these passages (173). Non-motile mutants are unable to colonize (101, 195), and chemotaxis may also play a role in the initial colonization by directing migration toward the pores. *V. fischeri* is able to recognize and swim toward *N*-acetylneuraminic acid, a component of the mucus (60) that may act as an attractant.

Other bacteria also migrate toward the pores, but upon entry they are rarely found in the ducts or the crypt spaces (195). Nitric oxide in the duct and mucus is believed to be partially responsible for inhibiting large aggregate formation and colonization by other bacteria (57, 192). Apparently only a subset of the *V. fischeri* from the original aggregate survive the gauntlet of the ducts and reach the light-organ crypts to establish infection (69, 168).

Once *V. fischeri* reaches the crypts, the bacteria grow rapidly (223), filling the extracellular space (193), and begin producing luminescence approximately 8-12 hours after hatching (174). Bacteria that are unable to luminesce do not persist as well as the wild type in the light organ, suggesting the squid is selectively maintaining only bacteria that are useful to the symbiosis (282). Each morning, the light of dawn cues the squid to expel 90-95% of the bacteria in the light organ as a thick paste into the environment (151, 193). The remaining bacteria repopulate the light organ over the day to prepare for the next night (22).

During the establishment of the symbiosis, numerous morphological changes occur that are triggered by *V. fischeri*. Some of these changes require the continued presence of *V. fischeri* while others are irreversibly triggered by even a transient *V. fischeri* infection; however, none of these changes occur in aposymbiotic animals kept in water that does not contain *V. fischeri*. The epithelial cells within the light organ begin to branch and elongate their microvilli, making more contact with the symbiont (144). The epithelial cells also begin to swell, shifting from columnar to cuboidal-shaped cells (257, 282). There is a change in abundance of at least 48 proteins (152), including an increase in myeloperoxidase, causing elevated levels of specific reactive oxygen species, (243, 269, 296) and irreversible down-regulation of nitric oxide synthase (57), both of which are thought to be part of challenging colonizing bacteria before they reach the light-organ crypt spaces. Symbionts also trigger the increase of p53 family proteins, which are implicated in

the induction of apoptosis and morphogenesis (99). Some effects are not related to protein expression, such as an increase in abundance of filamentous actin, which may be a result of posttranscriptional action on the protein (139). These changes in actin could assist the bacteria in reshaping the crypt space epithelial cells to increase interactions with the host tissue. Remodeling of actin also constricts the pores potentially minimizing the possiblity further infection by other bacteria (139). These large scale morphological and molecular changes in the juvenile *E. scolopes* are also reflected in cDNA libraries of symbiotic and aposymbiotic light organs (43).

The most visible alteration to the juvenile squid infected with *V. fischeri* is an extensive tissue remodeling resulting in the regression of the ciliated appendages (Figure 1.2). The regression occurs through a series of events. Between 4-6 hours after exposure to *V. fischeri*, the ciliated appendages begin to develop pycnotic nuclei from the condensation of DNA within each cell indicative of apoptotic cell death (76). The number of intact cells in the appendages decreases over the next 72 to 96 hours (182). A transient exposure to *V. fischeri* (4 hours or less) does not induce regression, although after 12 hours the regression program appears irreversible (64). Over the next 3-5 days, the appendages continue to regress until they are no longer present (Figure 1.2) (174, 182).

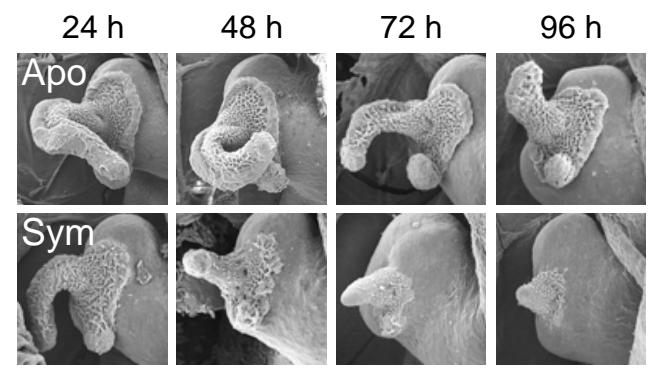


Figure 1.2. *E. scolopes* light organ morphogenesis. Scanning electron micrographs) show the progression of ciliated appendage regression over a time series. Only one side of each biolobed light organ is shown. The top series shows aposymbiotic animals (apo) while the bottom series shows animals infected with the wild type *V. fischeri* strain ES114 (sym). Scanning electron micrographs courtesy of Eric Stabb

Another dramatic event that coincides with the loss of the ciliated epithelial appendages is an increase in the number of macrophage-like cells in the ciliated appendages and in the light organ crypts (142, 193). As early as 2 hours after initial exposure to V. fischeri, hemocytes began to infiltrate sinuses in the ciliated appendages at a rate 3-4 times higher than in aposymbiotic animals. The signal from V. fischeri triggering hemocyte trafficking occurs very early, as curing the symbionts after 8 hours does not stop hemocyte infiltration but does prevent regression (142). Hemocytes within symbiotic animals contain a proteasome, a regulated enzyme complex responsible for the majority of cellular protein degradation in animal cells (138, 142); however, animal hemocytes do not produce proteasome when only transiently exposed to V. fischeri (142). Hemocytes with proteasome can be found in the ventate of adult E. scolopes and can contain partially degraded bacteria in them (193). Within the crypt, V. fischeri have been visualized surrounded by hemocytes without being phagocytosed, suggesting that the bacteria found within expelled hemocytes may be rogue bacteria and not V. fischeri (283). The macrophage-like hemocytes are presumably part of the innate immune response of the squid, and E. scolopes possesses components of the NF-κB pathway, a known modulator for these types of cellular responses (100). Despite this descriptive understanding of the events that initiate symbiosis, the mechanisms underlying these events have not been fully elucidated.

On the other side of the symbiosis, the bacterium has numerous traits that enable it to survive and develop within the *E. scolopes* light organ. As stated previously, motility, luminescence, and potentially chemotaxis are important for initial colonization and persistence in the light organ (60, 101, 177, 195). However, other factors have been determined as significant for colonization in the light organ, including siderophore production (103, 298), amino acid utilization (102), and a catalase (285). The apparent loss of flagella once colonization is initiated

may also play a part in colonization (223). Additionally, bacterial surface proteins appear to play a role in the colonization, as a trypsin-treated culture of *V. fischeri* showed that removal of superficial outer envelope peptides prevented colonization even though cells were viable and motile (118). Two putative surface proteins, OmpU and PilA, contribute modestly to the colonization, and others may have overlapping or redundant functions (3, 251). The ability of *V. fischeri* to create a biofilm may also be important for colonization as suggested by studies in the Visick lab with the <u>symbiosis polysaccharide</u> or *syp* cluster (306, 307). Mutations in *rscS*, which encodes the sensor kinase of a two-component response regulator for symbiotic colonization (287), was unable to form aggregrates suggesting that biofilm production is important in the early initiation phase of the colonization (306). Moreover, several mutants with altered LPS have been found to colonize at lower levels (59, 297).

Signals in the symbiosis

Since the first investigations of the *V. fischeri - E. scolopes* symbiosis, it has been suggested that a signal or multiple signals must be involved in the initial colonization and the triggering of morphogenesis in the squid's light organ (174). Many factors were explored, but the two that have proven to be most important for triggering apoptosis and regression of the ciliated appendages are lipopolysaccharide (LPS) and peptidoglycan/peptidoglycan monomers (PG/PG monomers). These factors are important in pathogenic relationships, but their roles in symbiotic relationships are less well understood.

Foster *et al.* found that the LPS of *V. fischeri* stimulated apoptosis of cells in the ciliated appendages; however, LPS did not induce regression. *H. influenzae* LPS also stimulated apoptosis, but this effect was attenuated when the lipid A moiety of LPS lacked secondary

acylations, which were known to affect the toxicity of the LPS to mammalian cells (75). This suggested that LPS, specifically lipid A, could be important for the initial light organ colonization by *V. fischeri*, much as it is in pathogenic infections.

PG monomers act as a morphogen that induces full regression of the light organ ciliated appendages (141). Exogeneous PG and PG monomers induced regression in synergy with LPS, triggering apoptosis similar to the effects seen with symbionts (141). PG fragments from Staphylococcus aureus and whole V. fischeri and V. parahaemolyticus cells also caused significant infiltration of hemocytes into the appendages suggesting that hemocytes are responding specifically to a signal for epithelial regression, and that this signal is PG (142). PG monomers that are structurally identical to those produced by V. fischeri are also released by Bordetella pertussis (53, 221) and Neisseria gonorrhoeae (220, 242). The PG monomers released from N. gonorrhoeae, called PGCT for peptidoglycan-derived cytotoxin, induce the sloughing of ciliated fallopian tube cells that can occur during a gonococcal infection (175). The PG monomers released by B. pertussis (221), named TCT for tracheal cytotoxin, are responsible for the epithelial damage to the ciliated respiratory epithelial cells during infection (52, 94), contributing to the whooping cough that is characteristic of a pertussis infection. Ν. gonorrhoeae, B. pertussis, and V. fischeri, each affect ciliated epithelial cells in their respective hosts (52, 141, 175), suggesting a conserved mechanistic role of PG monomers in pathogenic and mutualistic interactions.

Because of their apparent role in signaling in the *V. fischeri - E. scolopes* symbiosis, my research has focused on *V. fischeri* LPS and PG. In the next sections, I will discuss the general nature of LPS and PG and their interactions with the innate immune system. I will then discuss what is known about these molecules in other symbioses before describing my research goals.

LPS biosynthesis

The first line of defense for Gram-negative bacteria against antimicrobial and environmental stresses is LPS. LPS constitutes the major structural component of the outer membrane of Gram-negative bacteria and was originally called endotoxin because it was a heat-stable, non-proteinaceous, non-secreted toxin closely attached to, and an integral part of, *V. cholerae* (35). It provides a permeability barrier for hydrophobic and negatively charged molecules and also contributes to the structural integrity of the outer membrane. The three different components of LPS are O-antigen, core polysaccharide, and lipid A (Figure 1.3). These components differ structurally between and within bacterial species, and may change in a given bacterium in response to its environment, for example upon entering a host. Of these LPS components, lipid A is the most conserved and O-antigen is the most variable.

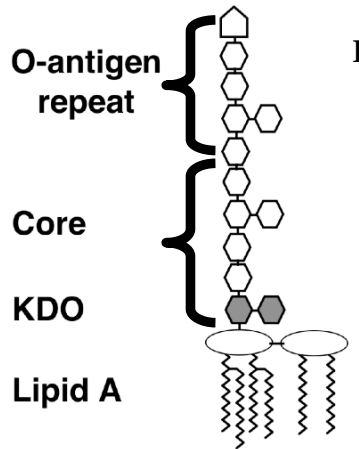


Figure 1.3. Simplified illustration of major LPS components.

The hydrophilic LPS O-antigen extends outward from the core into the environment. The O-antigen consists of repeating oligosaccharide subunits that contain anywhere from three to five sugars. Each monosaccharide may be one of more than twenty different types of sugars including some unique dideoxyhexoses. The hydrophilic domains of repeating O-antigen subunits varies in number but may contain 40 - 100 repeat linked units (186). Some genera, including *Neisseria*

and *Haemophilus*, do not produce an O-antigen but rather have an extended core region that lacks multiple repeating units. This absence of the O-antigen led researchers to alter the name of this structure to lipooligosaccharide, or LOS, to allow for differentiation between these structurally different endotoxins.

The LPS core consists of short chains of sugars that connect the O-antigen to lipid A. The core can be divided into the inner and the outer core. The outer core is attached to the O-antigen and is termed the hexose region due to a predominance of hexose sugars. The inner core is proximal to lipid A and typically contains three to six monosaccharides as well as a characteristic and unusual monosaccharide, 2-keto-3-deoxyoctonoic acid (Kdo). Kdo is often decorated with phosphate or sulfate groups and ethanolamine. In both *E. coli* and *S. typhimurium* the addition of 5 mM Ca⁺² induces the transferase EptB to incorporate a phosphoethanolamine onto Kdo (Figure 1.4) (134, 213). This addition may increase the stability of the outer membrane. The Kdo couples lipid A to the rest of the core with an acid-labile ketosidic linkage.

Lipid A contains the hydrophobic, membrane-anchoring region of LPS. It is the bioactive portion of the LPS that is often associated with toxic effects of Gram-negative infections in animals. Lipid A is recognized by lipid binding protein and Toll-like receptors (204, 267, 268), and induces an innate immune response by activating the NFκB pathway, which in turn transcriptionally activates responses to control bacterial invasion, such as nitric oxide and reactive oxygen species (6, 230). Lipid A is highly conserved and consists of a disaccharide of D-glucosamine that is acylated at positions 2, 3, 2' and 3'. In *E. coli*, these primary acylations, are made up of C_{14:0} groups and have secondary acylations of both C_{14:0} and C_{12:0}. Although highly conserved, lipid A can be altered with positively charged amine groups such as

phosphoethanolamine (83, 148), aminoarabinose (106, 107, 115, 272, 311), hydroxyl groups (83, 85, 107), phosphate (270), and the loss or addition of acylations including palmitate (19, 30, 36, 108) (Figure 1.4) thus affecting the overall charge and hydrophobicity. These alterations may enable the bacteria to cope with environmental stress or to modulate host innate immune responses.

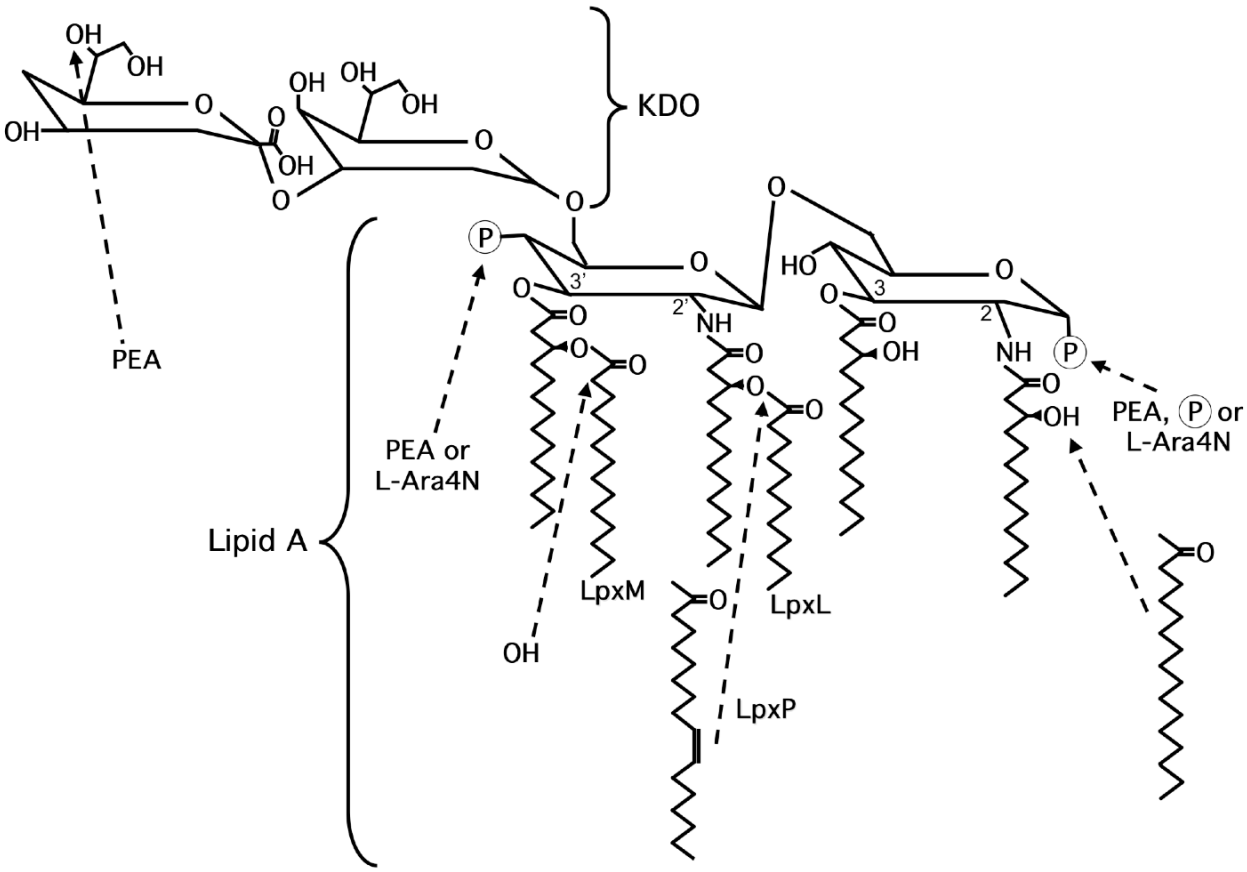


Figure 1.4. Modifications to the Kdo₂-lipid A in *E. coli* K12 and *Salmonella*. Known modifications to the Kdo₂-lipid A are indicated by arrows. Lipid A species with two phosphoethanolamine and two aminoarabinose moieties may occur. PEA, phosphoethanolamine; L-Ara4N, aminoarabinose; circled P, phosphate group.

The steps involved in synthesizing lipid A are best understood in $E.\ coli\ (208)$. In the cytoplasm, LpxA acylates UDP-GlcNAc with $C_{14:0}$ (5). LpxC removes an acetate (309) allowing LpxD to add a second $C_{14:0}$ (136), producing one monosaccharide subunit of lipid A. LpxH

removes the UDP from the monosaccharide, attaching a phosphate (11, 12). LpxB (206, 212) and LpxK (80, 81) complete the lipid A backbone by attaching two monosaccharides together, forming the disaccharide and adding a phosphate, respectively. Two Kdo residues are added by WaaA (KdtA) (17, 46); however, it has been shown in *V. cholerae*, *B. pertussis* and *H. influenzae* that a special kinase, KdkA, is required to add a phosphate to the single Kdo residue before the second Kdo residue is added (299, 300). Secondary acylations are added by the incorporation of a C_{12:0} by LpxL (HtrB) and a C_{14:0} by LpxM (MsbB) (31, 45, 47, 290). The Lipid A-Kdo structure serves as the acceptor for the core in the cytoplasm and the final lipid A structure with Kdo and core is then transported to the periplasm via MsbA (62, 63, 312). The addition of O-antigen occurs in the periplasm and is attached by the WaaL (RfaL) ligase (140). The completed LPS must then be moved from the periplasm, past the peptidoglycan layer, to the outer membrane through an as yet unknown mechanism.

Importance of LPS in innate immunity

Innate immune systems, which appear to be present in almost all multicellular organisms, are able to detect bacteria and allow a rapid first line of host defense (122). The recognition of microbe-associated molecular patterns (MAMPs), such as LPS, by signal transduction systems, like the Toll pathway, has been studied extensively in vertebrates and insects (1, 71, 135, 241). In vertebrates, dissociated LPS is recognized by the pattern-recognition receptor TLR4 (Toll-like receptor 4) that is present on macrophages and dendritic cells (1, 204). Lipid A is sensed initially by the serum LPS-binding protein, which delivers the macromolecule to CD14 (304, 305). TLR and LPS-binding protein have been found in almost all studied vertebrate genomes (217). CD14 is soluble or bound to the host cell and presents LPS to TLR4

(42). Only the lipid A domain is required to trigger an immune response (78, 215), and the important determinants of the lipid A structure in promoting TLR4 activities include the phosphate groups and the length and number of fatty acyl chains (95, 156, 201, 215). *E. coli* lipid A (Figure 1.3) is a potent activator of the innate immune system (95, 156, 215). Host responses to lipid A can include production of cytokines and other stimulatory molecules, antimicrobial peptides, and macrophage trafficking.

Although the Toll/NFκ-B pathway has been studied extensively in vertebrates and insects, less is known about this system in the Lophotrochozoa, the branch of the animal kingdom containing *E. scolopes*. Evidence exists for components of the pathway in the Pacific oyster (104, 180, 181) and more recently work by Goodson *et al.* has shown that *E. scolopes* has components of the NFκ-B pathway (100). Notably, there is a TLR4 homolog similar to *Drosophila melanogaster* TLR4 which functions in recognition of LPS specifically (100). A LPS-binding protein of *E. scolopes* was also found in a 3' expressed sequence tag library, although a full transcript was not isolated (100). Subsequent research has isolated 3 transcripts of a LPS-binding protein of which there are 2 full sequences and an incomplete sequence of a third (Josh Troll, personal communication).

PG biosynthesis and recycling

The rigidity and shape of a bacterial cell is usually dependent upon PG, which is composed of β -1,4 linked *N*-acetylglucosamine and *N*-acetylmuramic acid, combined with a small number of amino acids including D-alanine, D-glutamic acid, L-alanine, and diaminopimelic acid. The overall PG structure is a repeat of this polysaccharide with each unit linked to the next by a peptide interbridge. The PG layer, also known as the murein sacculus, of

E. coli consists of approximately 3.5 million repeating units (301). In Gram-negative bacteria, the PG structure is covalently linked to LPS via Braun's lipoproteins (28). Damage to PG layer can result in lysis of the cell. However, the PG layer must accommodate proteins that span the inner and outer membranes, and PG must grow, expand, and be separated into two daughter cells for division. Therefore, there must be a controlled process that allows incorporation of new subunits and clearing of preexisting PG.

The controlled growth and remodeling of PG is the result of combined *de novo* PG synthesis and recycling of liberated PG fragments as illustrated in Figure 1.5. *De novo* PG synthesis has been studied and reviewed extensively elsewhere (13, 26, 232, 288), but two aspects evident in Figure 1.5 are especially relevant to this thesis. First *de novo* PG synthesis begins in the cytoplasm prior to PG assembly in the periplasm. Second the bioactive 921 Da PG monomer released by *N. gonorrhoeae* (PGCT), *B. pertussis* (TCT), and *V. fischeri* is not generated in the periplasm via *de novo* PG synthesis. Rather, this PG monomer is found in the periplasm due to activities related to PG remodeling and recycling. Because this 921 Da PG monomer is our main subject of interest and its release from the cell presumably requires prior generation in the periplasm, I will focus on the processes involved in PG remodeling and recycling.

As PG is remodeled, new glycan strands of PG are incorporated while "old" strands must be removed (Figure 1.5). Specific hydrolases exist for almost every covalent bond in the PG of *E. coli* (240). *E. coli* has five *N*-acetylmuramyl-L-alanine amidases, six membrane bound lytic transglycosylases, and 3 endopeptidases, each of which have some contribution to not only septation of daughter cells (113, 114) but also to the recycling of PG components during cell growth (98). Lytic transglycosylases, which cleave the PG monomers with the concomitant

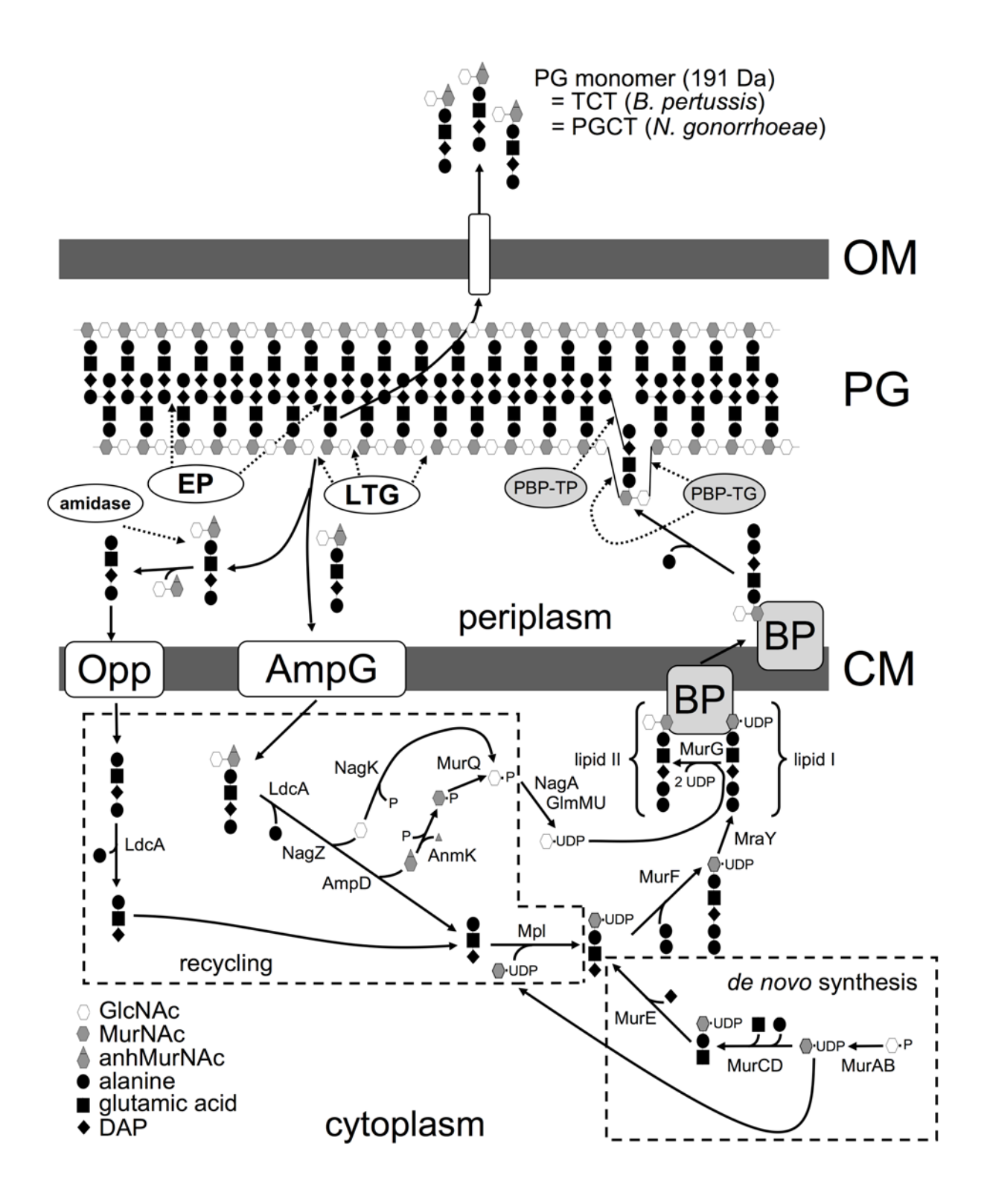


Figure 1.5. Schematic illustration of peptidoglycan synthesis and recycling. Abbreviations; uridine 5' phosphate, UDP; *N*-acetylglucosaminyl, GlcNAc; *N*-acetylmuramic acid, MurNAc; anhydrous MurNAc, anhMurNAc; *meso*-diaminopimelic acid, DAP; bactroprenol, BP; penicillin binding protein – transglycosylase, PBP-TG; penicllin binding protein – transpeptidase, PBP-TP; lytic transglycosylases, LTG; endopeptidases, EP; and oligo peptide permease, Opp.

formation of 1,6-anhydro ring on the MurNAc residue (124), and endopeptidases, which cleave the peptide bond between the monomers, allow for creation of PG tetrapeptide monomers, tripeptide monomers or tripeptides without disaccharides (289). All three breakdown products can then be recycled from the "old" PG into the cell.

About 50% of the PG layer in Gram-negative cells is hydrolyzed each generation and is recycled to form new PG precursors (Figure 1.5) (96). PG monomers removed from the Gramnegative PG layer are brought into the cytoplasm for recycling via Opp and AmpG. Opp, oligopeptide permease, is a high-affinity system required for the uptake of the tripeptide and tetrapeptide (97). PG monomers are subjected to an N-acetylmuramyl-L-alanine amidase which cleaves the peptide stem of the disaccharide allowing the tetrapeptide to be recycled by Opp (200, 276, 277); however, this amidase gene has not been isolated (113). AmpG, a permease that depends upon the proton motive force (38), is important for the recycling of PG monomers, including the GlcNAc-anhMurNAc-tetrapeptide (129) although the peptide stem length is not important (41). GlcNAc-anhMurNAc-tetrapeptide (referred to above as PGCT, TCT, or the 921 Da PG monomer), enters through AmpG, and the terminal alanine is removed by LdcA (262), resulting in GlcNAc-anhMurNAc-tripeptide, which is then hydrolyzed by AmpD and NagZ to produce the tripeptide, GlcNAc, and anhMurNAc (40, 291). These compounds are then fed back into the construction of lipid II of PG biosynthesis (Figure 1.5). Every component of the recycled PG monomer is salvaged and reused.

The PG monomer released by *V. fischeri* is the GlcNAc-anhMurNAc-tetrapeptide which should be cleaved from peptidoglycan by lytic transglycosylases and then brought into the cytoplasm by AmpG. The identification of proteins that are responsible for the cleavage and

subsequent release or recycling of the GlcNAc-anhMurNAc-tetrapeptide may allow for a better understanding of why this PG monomer is released by some bacteria and not by others.

Importance of PG in innate immunity

The role of PG recognition in innate immunity is less well understood relative to the role of LPS. Exposure to partially purified PG from Gram-positive bacterial cell walls or soluble muramyl peptides induced pro-inflammatory cytokines (130); however, research stalled in trying to purify PG away from associated macromolecules, and the sensors for the detection of PG within the host were not identified (90). More recently though, as described below, research on Nods and PG-recognition proteins (PGRP), both of which are sensors of PG in mammals, *Drosophila*, and invertebrates, suggests that the contributions of PG to the innate immune response might be more significant that previously appreciated.

PGRPs were originally isolated from the silkworm and later homologs were found in *Drosophila*, mammals and even in *E. scolopes* (70, 100). These proteins trigger the activation of innate immunity through the Toll system, although the actual mechanism for how the activation occurs is not understood. *Drosophila* PGRPs are able to distinguish between Gram-positive and Gram-negative PG, specifically differentiating between the third position of PG amino acid stem where Gram-positive bacteria have a lysine and Gram-negative bacteria have *meso*-diaminopimelic acid. This distinction affects the induction of different antimicrobial peptides (153). The human genome contains four PGRPs, each binding to PG with high affinity. Two of the PGRPs have unknown function. The limited data available for the two others suggest that PGRP-L it is a PG lytic enzyme (82, 292) while more thoroughly studied PGRP-S binds Gram-positive PG resulting in bacteriostatic activity (155). In *E. scolopes*, the expressed sequence tag

library and subsequent rapid amplification of cDNA ends by PCR yielded four distinct PGRP transcripts all of which encode the residues predicted to compose the PG binding pocket (100).

The cytoplasmic Nod proteins function in innate immune defense through pathways that are likely independent of TLR signaling. Nod1 is an upstream activator of the NF-κB pathway (127) and appears to be triggered by PG monomers released by Gram-negative cells (88). Nod2, a close homolog to Nod1, recognizes muramyl dipeptides and is thus a general sensor for both Gram-positive and Gram-negative bacteria (89, 128). However, Nod2, is not able to recognize the Gram-negative tripeptide with diaminopimelic acid (91). No Nod proteins or corresponding mRNAs have yet been detected from *E. scolopes*.

LPS and PG as signaling molecules in other symbioses

As may be evident from the discussion above, most of what is known about host responses to LPS and PG has been examined in terms of immune responses to pathogens. However, a growing body of research has found that many plant- and animal-microbe interactions are either benign or actually beneficial to the host. Beneficial bacterial partners have many roles including providing nutritional benefits to the host, preventing pathogen colonization, deterring predation by other microorganisms, and initiating normal development of the animal or plant host (29, 86, 87, 295). Normal development in the host can be triggered through a variety of mechanisms; however, two compounds of particular interest are LPS and PG. Because my research specifically concerns LPS and PG in a beneficial symbiosis, in the following sections I will review what is known about these molecules in other host-bacteria mutualisms.

Rhizobium – legume symbiosis and the role LPS and PG in the symbiosis

One of the best studied bacteria – host interactions is the relationship between Rhizobia and legumes. This relationship involves two-way signaling and the formation of N₂-fixing symbiotic nodules on the roots. Root infection is a multistep process beginning when roots of legumes exude amino acids, dicarboxylic acids, and flavonoids, enticing Rhizobium spp. to chemotax toward sites on the roots. Following attachment to root hairs, plant-produced flavonoids stimulate the rhizobia to release lipochito-oligosaccharides known as Nod factors (246). On the appropriate host, these Nod factors stimulate the root hair to branch, deform and curl, eventually leading to an infection thread through which the bacteria gain access to the plant cells within the root. In an interesting exception to Nod-factor dependent nodulation, two recently sequenced photosynthetic Bradyrhizobia (92) apparently produce a molecule that is similar to, or a precursor of, plant cytokinin hormones to help initiate nodulation (66). In either Nod factor-dependent or -independent infection, rhizobia gain access into the plant cell cytoplasm, the bacterial cells differentiate into bacteroids, and enlarged "nodules" of plant growth form on the roots. These nodules provide an anoxic, carbon-rich environment that allows the symbiont to reduce atmospheric N₂ to NH₃, providing a nitrogen source for the plant. Although, the Nod factors, or cytokinin-like molecules, released from the symbiont are the main component bacterial signal for establishing this productive symbiosis, other components are being uncovered, including LPS and lipid A.

The lipid A of *Rhizobium legumninosarum* contains a 27-hydroxyoctacosanoic acid (27OHC_{28:0}) that is added by the acyl carrier protein AcpXL (278, 280). The loss of this acylation in lipid A delayed nodule formation; however, the lack of the 27OHC_{28:0} did not prevent nitrogen fixation (280). The delay in nodulation was overcome nine days post-

inoculation although nitrogenase amounts remained lower than the parent strain (278). The mutant lacking 27OHC_{28:0} produced irregularly shaped and enlarged bacteroids in the nodules (278). With a slower growth phenotype and increased sensitivity to acidic conditions and salt concentrations (280), it was surprising that the mutant was not deficient in symbiosis. This mutant was reisolated from the nodules and the delayed onset and adaptation to form nodulation is due to an alternative host-induced mechanism to attach 27OHC_{28:0} to almost 50% of the lipid A isolated from within the nodule, as well as a considerable increase in the levels of C_{18:0} and C_{16:0} (279). A similar study with *Sinorhizobium meliloti* showed that 27OHC_{28:0} was replaced by $C_{18:0}$ in the same position on the lipid A (74). After mutating not only the acyl carrier protein but also the acyltransferase for the 27OHC_{28:0}/C_{18:0}, the mutant strain was still able to form nitrogenfixing nodules in a delayed manner (74). This suggests that there is an alternative mechanism for addition of the acylation to lipid A in S. meliloti as there is in R. leguinosarum, although there has been no analysis of the lipid A from nodules formed by the mutant S. meliloti. These data suggest the addition of this long chain fatty acid is important for symbiotic colonization by the bacteria.

LPS from symbiotic bacteria affects the response of the plant in a manner different than that of the LPS from plant pathogens. LPS from *R. leguminosarum* bv. *trifolii* strains when applied with Nod factor to white clover roots promotes the Nod-factor-initiated development of infection threads (58). LPS from other rhizobia or non-symbiotic enteric bacteria did not promote the development of infection threads, suggesting that LPS specific to its colonizing bacteria is needed (58). LPS from *Azorhizobium caulinodans* is the secondary signal after Nod factors to trigger the onset of the nodulation and colonization with the host *Sesbania rostrata*. LPS was needed to proceed with symbiosis and form a mature N₂-fixing nodule (166).

Rhizobia LPS plays an additional role in suppressing the host defenses to allow symbiosis. *Sinorhizobium meliloti* lipid A suppressed the production of reactive oxygen species in the host alfalfa plant, *Medicago sativa*, and the model legume *Medicago truncatula*; however, a *S. meliloti* lipid A lacking 270HC_{28:0} (239) still reduced the reactive nitrogen species suggesting that another feature of lipid A is important for the suppression in this system (234, 239). Recent evidence from a microarray analysis of *M. truncatula* has shown that LPS from *S. meliloti* suppresses the oxidative burst as well as transcription of innate immunity pathways while LPS of the phytopathogen *Xanthomonas campestris* pv *campestris* does not (261).

PG may also play a role in the *Rhizobium*-legume symbiosis. Host derived lectins, carbohydrate-binding proteins, or glycoproteins that are highly specific for their sugar moieties they bind, are able to interact with the muramic acid, *N*-acetylmraumic acid, *N*-acetylglucosamine, and muramyl dipeptides found in PG (9, 10). These lectins allow the bacteria to bind to the rhizobia on an emerging root hair, facilitating aggregation and promoting engulfment of bacteria to begin infection thread development. Recently, a receptor kinase gene encoding LysM domains was found in *Lotus japonicus* and appeared to be involved in *L. japonicus* reception of the Nod-factor rhizobial signal (162). LysM domains are known PG-binding proteins as well as chitinases. Though the major Nod-factor of *Mesorhizobium loti* is pentameric *N*-acetylglucosamine (189), it is possible that PG may play a part in the signaling to the host.

Complex gut microbiota symbioses and the role of LPS in maintenance of the microbial community

Studies of gut microbial consortia have numerous challenges, including the complex community structure. Attempts to tease apart the relationships of these bacteria with each other and the host have been difficult. Another constraint is that the loss of gut microbiota in "germ-free" mice, zebrafish and other animals can make the host highly susceptible to outside infections, compromise host health due to lack of nutrients, and affect the development of key parts of the intestinal tract. Despite these difficulties, research with "germ-free" animals has proven useful and interesting. Recently the work with "germ-free" zebrafish (211) and mice has uncovered conserved molecular foundations of symbioses between host and bacteria in the vertebrate digestive tract. Similar genes are expressed in the gut of both zebrafish and mice upon initial exposure to the native flora, and a subset of these responses appear to have microbial specificity (211). This conservation of responses might reflect a role for conserved MAMPs in host-microbiota signaling.

Signaling between zebrafish and its microbiota is illustrated by the observation that the microbiota induces alterations in the intestinal tract. A germ-free zebrafish gut epithelium is arrested in its differentiation of cell borders (15), due in part to a decrease in phosphatase activity in the brush border of the intestinal wall. By adding LPS alone, the phosphatase activity was up-regulated, suggesting that the gut epithelial maturation is mediated at least in part by LPS-mediated stimulation (15). Zebrafish possess an alkaline phosphatase that is able to detoxify LPS dephosphorylating lipid A, thereby preventing inflammation in the zebrafish gut due to exposure to the LPS (14). Research with whole blood cells has shown that the loss of one of the

phosphate groups of a synthetically constructed lipid A results in a less toxic lipid A (236). Thus, this may be one way a large population of Gram-negative bacteria can be maintained in the intestine of vertebrates without the risk of the quantity of LPS causing a toxic effect.

Future aims of research with PG and LPS

As research delves deeper into the relationships between hosts and their symbionts, our current foundation of knowledge will direct and inform investigations of specific components such as PG and LPS involved in beneficial microbial symbioses. Current research suggests that gut communities are assembled in a predictable way, and that the environment interacts with the host and microbial population to determine the final composition of the community (210). Some have speculated that vertebrates have a memory-based immune system to allow them to deal with highly complex beneficial microbial consortia living within the gut, whereas the microbiota of invertebrates tends to be simpler (and often intracellular) allowing these hosts to depend on MAMP detection and innate immunity, along with physical barriers to control their microbiota (169). Probing these topics more deeply will be facilitated by the development of model systems such as the *V. fischeri – E. scolopes* symbiosis.

Rationale and Objectives of this Study

To explore the recognition and signaling in the *V. fischeri/E. scolopes* system, I begin in Chapter 2 discussing the importance of lipid A in this symbiosis. Lipid A is an important signal in many pathogenic infections and based on the previously published work by Foster *et al.* (75) I hypothesized that mutations affecting the lipid A secondary acylations would have an effect on colonization. I demonstrate in Chapter 2 that *V. fischeri* contains at least three genes for the

incorporation of secondary acylations to *V. fischeri*'s lipid A. Mutations of two of these genes, *htrB2* and *msbB*, cause numerous pleiotropic effects in culture, but do not apparently affect host colonization; however, a third secondary acylation directed by *htrB1* has no substantial effects on growth in culture, but the *htrB1* mutant was delayed in the initiation of colonization, suggesting recognition of the symbiont by the host may be perturbed by this mutation. Mutations incorporating double and triple mutants in the genes resulted in increasingly more substantial pleiotropic effects, with the triple mutant being essentially non-motile, less luminescent, and significantly impaired in the presence of certain antimicrobials.

In Chapter 3, I focus on PG monomers and the proteins that are responsible for their release from V. fischeri. I show that the permease that brings PG monomers into the cell's cytoplasm, AmpG, is functional in V. fischeri, because a mutation in ampG results in a 100-fold increase in PG monomer release. However, the cleavage of the PG into these monomers is the responsibility of at least three lytic transglycosylases, LtgA1, LtgA2 and LtgD. A triple mutant lacking the genes encoding these proteins displayed significantly less release of PG monomers. In symbiotic infections, animals colonized by the ampG mutant did not display faster regression of the ciliated light-organ appendages, suggesting that the wild type releases sufficient PG monomer to trigger these effects. Interestingly, I show that a *flaJ ampG* double mutant was able to induce regression in the ciliated light-organ appendages, unlike the flaJ and other non-motile mutants. This demonstrates that crypt infection, which requires motility, is not necessary for PG-mediated signaling to the host. The triple lytic transglycosylase mutant still stimulated regression of the ciliated light-organ appendages, suggesting that potentially another lytic transglycosylase may be involved in the release of PG monomer in the squid or that other PG fragments may play a role in regression. Although morphogenesis was induced with the triple

lytic transglycosylase mutant, I saw a subtle attenuation of this strain's ability to stimulate regression of the host's light organ ciliated appendages. A more dramatic effect was apparent in the greater susceptibility of animals infected with the triple lytic transglycosylase mutant to a secondary *V. fischeri* colonist after regression of the infection-promoting ciliated appendages had begun. This implies that a small difference in regression of the ciliated appendages may have a large functional significance with regard to promoting or blocking further infection by other strains.

My next goal was to find regulators of ampG by using a lacZ reporter. I isolated mutants in an ampG-lacZ background with increased ability to cleave 5-bromo-4-chloro-3-indolyl- β -D-galactoside (X-gal); however, this was independent of the lacZ introduced downstream of ampG. Further experimentation revealed that such mutants derepress the celCBGKAI gene cluster, which enables V. fischeri to grow on cellobiose and also encodes a cryptic β -galactosidase activity. Chapter 4 describes this serendipitous discovery of a gene cluster for the catabolism of cellobiose in V. fischeri. The results in Chapter 4 have important implications for the use of lacZ as a reporter in V. fischeri and shed light on the evolution of a trait (cellobiose utilization) that is often used to distinguish Vibrio species.

CHAPTER 2

CHARACTERIZATION OF HTRB AND MSBB MUTANTS OF THE LIGHT ORGAN SYMBIONT VIBRIO FISCHERI 1

D.B., Stabb, E.V. 2008. Applied and Environmental Microbiology. 74: 633-644.

Reprinted here with permission of publisher.

¹ Adin, D.M., Phillips, N.J., Gibson, B.W., Apicella, M.A., Ruby, E.G., McFall-Ngai, M.J., Hall,

Abstract

Bacterial lipid A is an important mediator of bacteria-host interactions, and secondary acylations added by HtrB and MsbB can be critical for colonization and virulence in pathogenic infections. In contrast, Vibrio fischeri lipid A stimulates normal developmental processes in this bacterium's mutualistic host Euprymna scolopes, although the importance of lipid A structure in this symbiosis is unknown. To further examine V. fischeri lipid A and its symbiotic function, we identified two paralogs of htrB (designated htrB1 and htrB2) and an msbB gene in V. fischeri ES114 and demonstrated that these genes encode lipid A secondary acyltransferases. htrB2 and msbB are found on the Vibrio "housekeeping" chromosome 1 and are conserved in other Vibrio species. Mutations in htrB2 and msbB did not impair symbiotic colonization but resulted in phenotypic alterations in culture, including reduced motility and increased luminescence. These mutations also affected sensitivity to SDS, kanamycin, and polymyxin, consistent with changes in membrane permeability. Conversely, htrB1 is located on the smaller more variable vibrio chromosome 2, and an htrB1 mutant was wild-type-like in culture but appeared attenuated in initiating the symbiosis and was outcompeted 2.7-fold during colonization when mixed with the parent. These data suggest that htrB2 and msbB play conserved general roles in vibrio biology, whereas htrB1 plays a more symbiosis-specific role in V. fischeri.

Introduction

Vibrio fischeri is a bioluminescent bacterium that forms a mutualistic symbiosis with Euprymna scolopes, the Hawaiian bobtail squid. E. scolopes supports the growth and bioluminescence of V. fischeri in a specialized light organ (223), and the bacterial luminescence is apparently used by the squid in a camouflaging behavior (132). V. fischeri is more abundant in E. scolopes habitats, reinforcing the belief that the relationship is beneficial for both partners (151). Among the hundreds of bacterial species present in Hawaiian waters, only V. fischeri is able to colonize the E. scolopes light organ. This specific colonization triggers developmental changes in light organ tissue, and it is clear that E. scolopes identifies and responds to signals from V. fischeri (182). Although the mechanisms underlying the specificity, signaling, and persistence of this symbiosis are not entirely clear, previous studies suggested that a key molecule in some of these symbiotic processes is V. fischeri's lipopolysaccharide (LPS) (75).

LPS comprises 70% of the outer membrane of Gram-negative bacteria and has three main components: i) O-antigen, which is a variable hydrophilic polysaccharide that projects into the environment, ii) a relatively conserved central core of sugars, and iii) lipid A, which anchors LPS into the outer membrane. The innate immune systems of many animals recognize lipid A through LPS-binding protein and Toll-like receptors (117, 121), which stimulate inflammation to attract more host immune cells to clear pathogenic infections (56, 188). Indeed, the strong, sometimes overreactive, immune response to lipid A has earned LPS its alternate name "endotoxin". Interestingly, LPS-responsive elements of the innate immune system are conserved in *E. scolopes* (100), and *V. fischeri* LPS elicits host responses that typify normal development of this mutualistic symbiosis. For example, *V. fischeri* LPS or lipid A stimulates apoptosis in a specific field of ciliated

cells on the light organ (75) and LPS acts synergistically with peptidoglycan to induce light-organ morphogenesis (141).

Changes in lipid A structure, in particular the elimination or exchange of certain secondary acylations, affect the virulence of pathogens and the bioactivity of LPS. Accordingly, some pathogens regulate their lipid A structure and acylation patterns in adapting to a host environment (105, 218). Mutant analyses have been useful in unraveling the relationship between lipid A structure and its function in such infections. For example, mutations in genes that encode secondary acyltransferases, such as *htrB* (*lpxL*) or *msbB* (*lpxM*), can affect lipid A structure, its bioactivity, and pathogen virulence (55, 131, 245, 256, 275).

The relationship between lipid A structure and its function in non-pathogenic animal-bacterium interactions remains largely unknown. Citing precedent in pathogenic interactions and experiments with foreign LPS, Foster *et al.* suggested a relationship between *V. fischeri* lipid A acylation patterns and bioactivity in its symbiosis with *E. scolopes* (75). Our goal in this study was to determine how secondary acylation of lipid A affects the biology of *V. fischeri*, particularly its symbiotic phenotypes. We identified three lipid A secondary acyltransferases in *V. fischeri*, mutated the respective genes singly and in combination, and characterized these mutants in culture and in the host. Some of these mutants had deleterious phenotypes in culture; however, one mutant displayed a symbiosis-specific defect.

Materials and Methods

Bacterial strains and culture conditions. The strains used in this study are listed in Table 2.1. When added to LB medium (176) or a supplemented phosphate-buffered minimal Kozak medium (290) for selection of *Escherichia coli*, chloramphenicol (Cm), kanamycin (Kn) and

trimethoprin (Tp) were used at concentrations 20, 40, and 10 µg ml⁻¹, respectively. For selection of *E. coli* with erythromycin (Em), 150 µg ml⁻¹ was added to BHI medium (Difco, Sparks, MD). Unless otherwise noted, *E. coli* was incubated at 37°C except MKV15 (290), which was incubated at 28°C. *V. fischeri* was grown in LBS medium (250) or SWT medium (20) made with Instant Ocean (Aquarium Systems, Mentor OH). When added for selection of *V. fischeri*, Cm, Kn, Em, and Tp were used at concentrations of 2, 100, 5, and 10 µg ml⁻¹ respectively. *V. fischeri* was grown at 28°C or 24°C. Agar was added to a final concentration of 1.5% for solid media.

Molecular genetics. Plasmids (Table 2.1) were generated using standard cloning methods, and were isolated using QIAprep spin miniprep kit (Qiagen, Valencia, CA). Restriction and modification enzymes were obtained from New England Biolabs (Beverly, MA). The Zero Blunt TOPO PCR Cloning Kit (Invitrogen, Carlsbad, CA) was used to clone PCR products into pCR-BluntII-TOPO. DNA fragments were purified using either the Wizard DNA Cleanup Kit (Promega Corp., Madison, WI) or the DNA Clean & Concentrator-5 Kit (Zymo Research, Orange, CA). PCR was performed using an iCycler (BioRad Laboratories, Hercules, CA), with *Pfu*-Turbo (Stratagene, La Jolla, CA) to amplify *dfr1* or with KOD HiFi DNA Polymerase (Novagen, Madison, WI) for other PCR-based cloning. DNA sequencing was conducted on an ABI automated DNA sequencer at the University of Georgia Integrated Biotech Laboratories, and oligonucleotides were obtained from either the University of Georgia Integrated Biotech Laboratories or Integrated DNA Technologies (Coralville, IA).

Mutant alleles were generated as delineated in Table 2.1. In most instances, the target gene was amplified from *V. fischeri* ES114 with ~1.5 kb flanking DNA on either side, using the

genome sequence to guide primer design. PCR products were cloned into pCR-BluntII-TOPO and subcloned into the mobilizable suicide plasmid pEVS118. A second round of PCR outward from the target gene amplified sequences flanking the target as well as the vector. BglII (or StuI) sites were placed on the ends of the primers for this secondary PCR, and the PCR amplicon was digested with BglII (or StuI) and self-ligated to generate a Δtarget allele. These constructs were sequenced to ensure no unintended changes were incorporated. An Em-resistance (erm) cassette was inserted into the BglII (or StuI) site to generate $\Delta target::erm$ alleles, each plasmid was transferred into V. fischeri ES114 by triparental mating (252), and single and double recombinants were selected and screened as previously described (250). The Δtarget::erm alleles were exchanged onto the chromosome first, and then replaced by unmarked Δtarget alleles using Em-sensitivity as a screen. Exchange of each mutation onto the genome was confirmed by PCR analysis. In the lone exception to this approach, the htrB1 gene was cloned before the V. fischeri genome was sequenced by using PCR amplification with primers EVS69 and EVS72, which target conserved htrB sequences, to identify an htrB1-containing clone in increasingly smaller clone pools of an ES114 genomic library (285). Subsequent subcloning resulted in pEVS97, which contains htrB1 centered on a 4.2 kb fragment of ES114 DNA and interrupted by insertion of *erm* at a unique *Bsa*BI site.

Plasmids for complementation were generated by amplifying each gene with ~500 bp upstream sequence, and cloning the fragments first into pCR-BluntII-TOPO and then subcloning into pVSV105 for complementation of *V. fischeri* mutants. Each gene was also subcloned into pDMA5 and a Tp-resistance cassette was added to allow selection in MKV15.

Table 2.1 Bacterial strains, plasmids, and oligonucleotides

Strain, plasmid, or	Relevant characteristics*	Source or reference
oliogonucleotide		
Bacterial strains		
E. coli		
DH5α	F Φ80dlacZΔ(lacZYA-argF)U169 deoR supE44 hsdR17 recA1 endA1 gyrA96 thi-1 relA1	(109)
DH5α-λ <i>pir</i>	DH5 α lysogenized with λpir	(68)
MKV15	W3110 $lpxP$:: $kan lpxM$:: $\Omega cam lpxL$::Tn10	(290)
TOP10	F mcrA Δ (mrr-hsdRMS-mcrBC) Φ 80lacZ Δ M15 Δ lacX74	Invitrogen
TOP10	$recA1 \ ara\Delta 139 \ \Delta (ara-leu)7697 \ galU \ galK \ rpsL \ (StR) \ endA1 \ nupG$	mvinogen
W3110	F rph-1 IN(rrnD-rrnE)1 λ	(290)
V. fischeri	1 Tph 1 II (Thib Thib) 1 N	(2)0)
AO340	htrB1::erm allele from pEVS97 in DMA333 (htrB1::erm, ΔhtrB2, ΔmsbB)	this study
DMA310	ΔhtrB2::erm allele from pDMA24 in ES114 (ΔhtrB2::erm)	this study
DMA311	$\Delta htrB2$ allele from pDMA22 in DMA310 ($\Delta htrB2$)	this study
DMA321	$\Delta msbB$ allele from pHKG2 in HG320 ($\Delta msbB$)	this study
DMA330	htrB1::erm allele from pEVS97 in DMA311 (ΔhtrB1::erm, ΔhtrB2)	this study
DMA331	htrB1::erm allele from pEVS97 in DMA321 (ΔhtrB1::erm, ΔmsbB)	this study
DMA332	ΔmsbB::erm allele from pHKG4 in DMA311 (ΔmsbB::erm, ΔhtrB2)	this study
DMA333	$\Delta msbB$ allele from pHKG2 in DMA332 ($\Delta htrB2$, $\Delta msbB$)	this study
ES114	Wild-type E. scolopes isolate	(20)
EVS300	htrB1::erm allele from pEVS97 in ES114 (htrB1::erm)	this study
HG320	ΔmsbB::erm allele from pHKG4 in ES114 (ΔmsbB::erm)	this study
Plasmids		
pCR-BluntII- TOPO	Topo PCR-cloning vector; KnR	Invitrogen
pDMA5	$oriV_{p15A}$ $oriT_{RP4}$ $lacZ\alpha$ CmR	(68)
pDMA7	htrB1 (1.4 Kb) BglII-digested PCR product (primers dma19 and dma20, ES114 template) BamH1-digested pDMA5	this study
pDMA8	msbB (1.5 Kb) PCR product (primers dma7 and dma8, ES114 template) in pCR-BluntII-TOPO	this study
pDMA9	pDMA8 SpeI/XhoI msbB fragment in SpeI/XhoI-digested pDMA5	this study
pDMA10	htrB2 (3.8 Kb) PCR product (primers dma15 and dma16, ES114 template) in pCR-BluntII-TOPO	this study

pDMA11	htrB2 (1.5 Kb) PCR product (primers dma13 and dma14, ES114 template) in pCR-BluntII-TOPO	this study
pDMA12	htrB1 (3.8 Kb) PCR product (primers dma3 and dma4, ES114 template) in pCR-BluntII-TOPO	this study
pDMA13	msbB (4.0 Kb) PCR product (primers dma9 and dma10, ES114 template) in pCR-BluntII-TOPO	this study
pDMA15	pDMA12 BamHI/ApaI htrB1 fragment in BglII/ApaI-digested pEVS118	this study
pDMA19	htrB1 in-frame deletion; PCR product (primers dma5 and dma6, pDMA15 template) BglII digested, self-ligated	this study
pDMA20	pDMA10 <i>Bam</i> HI/ <i>Eco</i> RV <i>htrB2</i> fragment in <i>Bgl</i> II/ <i>Asc</i> I-digested and Klenow filled pEVS118	this study
pDMA22	htrB2 in-frame deletion; PCR product (primers dma17 and dma18, pDMA20 template) BglII-digested, self-ligated	this study
pDMA23	pDMA11 <i>SpeI/XhoI htrB2</i> fragment in <i>SpeI/XhoI</i> -digested pDMA5	this study
pDMA24	pEVS122 BamHI/BglII EmR fragment in pDMA22 BglII site	this study
pDMA25	pJLB2 <i>Eco</i> RV/ <i>Spe</i> I <i>dfrI</i> fragment, Klenow filled, in pDMA7 <i>Eco</i> RV site	this study
pDMA27	pJLB2 <i>Eco</i> RV/ <i>Spe</i> I <i>dfrI</i> fragment, Klenow filled, in pDMA23 <i>Eco</i> RV site	this study
pDMA28	pJLB2 <i>Eco</i> RV/ <i>Spe</i> I <i>dfrI</i> fragment, Klenow filled, in pDMA5 <i>Eco</i> RV site	this study
pDMA34	pDMA7 <i>Hin</i> CII/ <i>Spe</i> I <i>htrB1</i> fragment in <i>Hin</i> CII/ <i>Spe</i> I-digested pVSV105	this study
pDMA42	pDMA8 SpeI/XbaI msbB fragment in XbaI-digested pVSV105	this study
pDMA43	pDMA11 SpeI/XbaI htrB2 fragment in XbaI-digested pVSV105	this study
pDMA114	pJLB2 <i>Eco</i> RI <i>dfrI</i> fragment, Klenow filled, in <i>Eco</i> RV-digested pDMA8	this study
pDFR1	V. salmonicida dfrI (Genbank AJ277063) in pUC19; ApR TpR	H. Sørum
pEVS79	$oriV_{ m ColE1}$ $oriT_{ m RP4}$ CmR	(252)
pEVS94	$oriV_{ m R6K_{Y}}oriT_{ m RP4}$, EmR	(252)
pEVS96	oriV _{ColE1} oriT _{RP4} CmR EcoRI-HinDIII htrB1 fragment from ES114 in pEVS79	this study
pEVS97	pEVS94 <i>Eco</i> RV EmR-fragment into <i>Bsa</i> BI site in <i>htrB1</i> on pEVS96	this study
pEVS104	$oriV_{R6K_{\gamma}}$ $oriT_{RP4}$ KnR RP4-derived conjugal helper plasmid	(252)
pEVS118	$oriV_{ m R6K_{Y}}oriT_{ m RP4}$ CmR	(68)
pEVS122	$oriV_{ m R6K_{Y}}oriT_{ m RP4}$ $lacZlpha$ EmR	(68)
pHKG1	pDMA13 BamHI/ApaI msbB fragment in BglII/ApaI-digested pEVS118	this study

pHKG2	msbB in-frame deletion; PCR product (primers dma11 and dma12, pHKG1 template) StuI digested, self-ligated	this study
pHKG4	pEVS122 <i>Eco</i> RV EmR fragment in <i>Stu</i> I-digested pHKG2	this study
pJLB2	dfr1 PCR product (primers JB1 and JB2, pDFR1 template) in	this study
	pCR-BluntII-TOPO; KnR, TpR	Ĵ
pVSV103	oriT _{RP4} oriV _{pES213} KnR lacZ	(69)
pVSV105	$oriV_{ m R6K_{\gamma}}oriT_{ m RP4}$ $oriV_{ m pES213}$ CmR $lacZlpha$	(69)
<u>Oligonucleotides</u>		
dma3	5' TACCCAAGGCTTAATGAGCCGCCCC 3'	this study
dma4	5' CGCCTAAACGCTTTGAAGCTTACGGCTGGC 3'	this study
dma5	5' CGGAGATCTCATCAAAACTAAGACACC 3'	this study
dma6	5' GGCAGATCTTAACAATTCTTTTGCCGTG 3'	this study
dma7	5' GGCTTAGTGTTAGTAAGTAAAAGGCAG 3'	this study
dma8	5' CCCGCAGAACTGTGTAATTCTACGGG 3'	this study
dma9	5' GGTAATTTTTGCGGAGAGTATCAGTTCG 3'	this study
dma10	5' CCTAAAGCTTGAGCAATAAACGTTGCGCC 3'	this study
dma11	5' GCCAGGCCTCATGAATTGCTTCACTGTCTCATTATTATAAG 3'	this study
dma12	5' GGCAGGCCTTAACTTTTTTGTTATTCGGCTCTTATTTGAAACC 3'	this study
dma13	5' GCGTTATATCGCCATTTCCCAAGC 3'	this study
dma14	5' GCGATCACCAAGGCTAGCCGCCC 3'	this study
dma15	5' GCGGTCTAGAGCGGGCCCCAACTCGTGAAGCC 3'	this study
dma16	5' CGCCTCTAGAGCGTAATGCCATAATGATTGGCG 3'	this study
dma17	5' GCGGAGATCTCATCGTGAGCCTATTTTATCTAATTAATTA	this study
dma18	5' GCGGAGATCTTAGGGCGTGTCAGGATAAATAATGAAAACC 3'	this study
dma19	5' GGCAGATCTCAGATGGTTTGATTAATATTGAATCAGG 3'	this study
dma20	5' CGGAGATCTCGTAGGTTTCGGTGGCAAGATCATCGGC 3'	this study
EVS69	5' GAAACTGGTATTACTTGGTTTTGG 3'	this study
EVS72	5' TACTGCAAAAAAAGGAACAAAAAC 3'	this study
JB1	5' GCGCTTCGAACTCTGAGGAAGAATTGTG 3'	(68)
JB2	5' GCGCCCTAGGTTAGTTAGCTTAGCCAGA 3'	(68)

^{*} Abbreviations used: Ap^R, ampicillin resistance; Cm^R, chloramphenicol resistance; Em^R, erythromycin resistance; Kn^R, kanamycin resistance; Tp^R, trimethoprim resistance; St^R, streptomycin resistance. Oligonucleotides sequences are provided in the 5'-3' orientation.

LPS and lipid A purification and analysis. LPS was purified from *E. coli* or *V. fischeri* strains as described previously (205). Lipid A from *E. coli* W3110, MKV15 or MKV15 carrying plasmids with *V. fischeri htrB1*, *htrB2*, *msbB*, or no insert, was obtained from the LPS by mild acid hydrolysis (1% acetic acid, 2 hours, 100°C) followed by centrifugation and washing (202).

Lipid A pellets were partitioned in $CHCl_3/MeOH/H_2O$ (10:5:6), and the bottom organic layers plus interfaces were saved and evaporated to dryness under a stream of N_2 .

Lipid A samples were analyzed by matrix-assisted laser desorption ionization-time-of-flight mass spectrometry (MALDI-TOF MS) on a Voyager DESTR Plus (Applied Biosystems, Framingham, MA) equipped with a 337 nm nitrogen laser. All samples were run in the negative-ion linear or reflectron mode with delayed extraction and 20 kV extraction voltage. Prior to analysis, lipid A samples were dissolved in CHCl₃/MeOH (3:1) and desalted with cation exchange resin (Dowex 50W-X8, NH₄⁺ form; Bio-Rad, Hercules, CA). Samples were then mixed with an equal volume of matrix solution, saturated 6-chloro-2-mercapto-benzothiazole in CHCl₃/MeOH (3:1), spotted onto a stainless steel target, and air dried. ~200 laser shots were acquired for each sample, and the spectra were baseline corrected and smoothed with a 5-point Gaussian function. Spectra were calibrated externally with angiotensin II, renin substrate tetradecapeptide, and insulin chain B (oxidized) (all from Sigma, St Louis, MO). Ions measured by reflectron MALDI-TOF are reported as monoisotopic masses of the ¹²C-containing component.

GC/MS analysis of fatty acids derived from lipid A. Approximately 100 µg of the *E. coli* or *V. fischeri* lipid A samples were treated with 0.5 ml of 10% (wt/wt) BF₃-methanol (Supelco, Inc., Bellefonte, PA) and heated at 100°C for 6 h. After cooling to room temperature, the samples were partitioned between saturated NaCl and HPLC grade hexanes (Aldrich, St. Louis, MO), extracted, and evaporated to dryness under a stream of N₂ (202). The fatty acid methyl esters (FAMEs) were redissolved in hexanes and analyzed by gas chromatography/mass spectrometry (GC/MS) in the electron impact (EI) mode using a Varian Saturn 2100T ion trap MS/MS

interfaced with a Varian 3900 GC (Varian, Inc., Walnut Creek, CA). Injections were made with a 1:20 or a 1:50 split, with the injector temperature set at 200°C and the ion trap temperature at 195°C. FAMEs were separated on a 30-m x 0.25-mm BPX70 column with a 0.25-μm film thickness (SGE, Inc., Austin, TX) using helium as the carrier gas (constant column flow, 1.0 ml/min). The initial oven temperature was 90°C for 3.5 min, followed by a temperature gradient from 90°C to 220°C at 4°C min⁻¹. A mixture of bacterial acid methyl esters (Matreya, LLC, Pleasant Gap, PA) was used as a GC/MS standard solution.

Antimicrobial Assays. To assess growth inhibition by sodium dodecyl sulfate (SDS), polymyxin B, or Kn, these were serially diluted in water in \leq two-fold steps, 100 μ l of each dilution were added to 900 μ l of SWT in a 10 mm test tube, 10 μ l of mid-log phase cultures were added, cultures were grown at 24°C until the control tubes lacking the test substance reached an OD₅₉₅ between 0.5 and 0.9, and then the OD₅₉₅ of the culture in each tube was determined. The inhibitory concentration yielding 50% of the OD₅₉₅ in the antimicrobial-free control (IC₅₀) was determined by plotting OD₅₉₅ from three independent trials, each with three replicates/dilution of the substrate, versus the log of the dose. The IC₅₀ was calculated using a model fitted to all nine trials with the non-linear mixed effects function in the software S-PLUS (203).

Motility Assays. Motility was assessed as described previously (60, 302). Cultures were grown to mid-log phase (OD_{595} 0.5) at 24°C, 5 μ l of the culture was spotted onto a quadrant of an SWT soft (0.25%) agar plate and diameter measurements of the movement away from the point of inoculation were taken every hour. For each spot, a slope estimate was obtained from a simple linear regression of diameter versus time to quantify the velocity of spread, or motility rate. The

resulting six slopes per strain were then analyzed using a one-way analysis of variance (ANOVA) to test for equal mean motility rates across strains, and Tukey's Studentized Range Test was used to perform pair-wise comparisons among the strains at a simultaneous significance level of alpha=0.001. The ANOVA model was fit using weighted least squares, weighted by the precision (inverse estimated variance) of each slope estimate. All analyses were performed using the statistical program SAS (SAS Institute Inc, Cary, NC).

Microscopy. 100 μl of mid-log phase cultures were fixed in Parducz solution [3:3:1 4% OsO₄: 2% saline: saturated HgCl₂] (197) for 1 h. Each sample was pelleted, washed twice with 2% saline, dehydrated with sequential washes of 25, 30, 50, 70, 85, 90 and 100% ethanol for 10 min each, and applied with a 5-ml syringe to a 13 mm diameter Millipore 0.2 mm filter. Samples were dried in a Samdri-780A critical point drying apparatus with liquid CO₂, coated with gold until approximately 76.5 Å thick using a SPI-Module Sputter Coater, and examined with a LEO 982 FE-SEM running at 5 kV.

Luminescence Assays. Luminescence of cells cultured in SWT at 24°C was determined using a TD 20/20 Luminometer (Turner Designs, Sunnyvale, CA). Symbiotic luminescence of individual animals was measured using a LS6500 Scintillation Counter (Beckman-Coulter, CA).

Competition in mixed cultures. Mutants were competed against the wild type in mixed cultures with one of the strains marked by pVSV3, which expresses *lacZ* allowing blue/white screening of strain ratios on LBS plates supplemented with 50 or 100 μg ml⁻¹ 5-bromo-4-chloro-3-indolyl-β-D-galactoside (X-gal). To ensure that plasmid loss or bias in blue/white scoring did

not skew results, each mutant's competitiveness was calculated by averaging the results of mutant/pVSV3 mixed with ES114 (wild type) and mutant mixed with ES114/pVSV3. Individual strains were grown to mid-log phase, mixed ~1:1, and the culture was dilution plated to determine the starting strain ratio. The mixed culture was then subcultured 2¹⁰-fold, regrown to the starting OD₅₉₅, and plated on LBS containing X-gal to determine the strain ratio after ten generations. The process of subculturing, regrowth, and plating was repeated for later generations. The relative competitiveness index (RCI) of mutants was calculated by dividing the ratio of mutant to wild type by the starting ratio. An RCI <1 indicates the mutant strain was outcompeted, an RCI >1 indicates the wild-type strain was outcompeted, and an RCI=1 indicates no competitive difference between strains.

Squid colonization assays. For infection with individual *V. fischeri* strains, *E. scolopes* juveniles were inoculated within 4 h of hatching as previously described (223). Briefly, between nine and thirty hatchlings were placed in 100 ml of filter-sterilized seawater to which the strain of interest was added, left in this inoculum for 3 h, and then transferred to 5 ml of bacteria-free seawater in a 20-ml glass vial. After assaying luminescence (see above), squid were homogenized, and the homogenates were serially diluted and plated to determine the CFU per squid. To determine a mutant's competitiveness relative to ES114, juvenile squid were exposed to a ~1:1 mix of the strains for 14 h and then moved to bacteria-free water. After 48 h the squid were homogenized and dilution plated to determine the ratio of mutant to wild type. The RCI was determined as described above by dividing the mutant to wild type ratio in each individual squid by the ratio in the inoculum. Average RCI and statistical significance was calculated using log-transformed data.

Results

Analysis of putative lipid A secondary acyltransferase genes in *V. fischeri*. To begin addressing the relationship between *V. fischeri* lipid A structure and its symbiotic function, we identified homologs of lipid A secondary acyltransferase genes *htrB* and *msbB* in *V. fischeri* ES114, an isolate from the *E. scolopes* light organ (20). Initially, we used PCR-based approaches with primers targeting conserved regions of these genes to identify two *htrB* homologs, designated *htrB1* and *htrB2*, and one *msbB* homolog, and to clone the full-length *htrB1* gene from an extant library. Subsequent sequencing of the ES114 genome (226) confirmed the presence of these genes and no other *htrB* or *msbB* homologs, and enabled us to clone *htrB2* and *msbB*. The *V. fischeri htrB1* (VFA0687), *htrB2* (VF0122), and *msbB* (VF1799) genes encode proteins that are at least 36% identical and 53% similar to their respective homologs in *E. coli*. Interestingly, the two *V. fischeri htrB* genes are significantly diverged from each other, with only 48% and 53% identity in nucleotide and amino acid comparisons, respectively.

The genomic context of *htrB1*, *htrB2*, and *msbB* provided insight into their roles. Notably, the *htrB2* and *msbB* genes are located on the relatively large conserved vibrio "housekeeping" chromosome 1, whereas *htrB1* is on the more variable and species-specific chromosome 2. We also compared these genes to the putative lipid A secondary acyltransferase genes present in fully-sequenced genomes of four other vibrios; *Vibrio cholerae* O1 biovar eltor str. N16961 (112), *Vibrio parahaemolyticus* RIMD 2210633 (163), *Vibrio vulnificus* CMCP6 (137) and *Vibrio vulnificus* YJ016 (39). As in *V. fischeri* ES114, each of these four vibrios has one *msbB* homologue located on chromosome 1. Each of these strains also has an *htrB* gene on chromosome 1 immediately downstream of a gene encoding a putative *tetR*-family regulator, an organization conserved in *V. fischeri htrB2* (Fig. 2.1). In addition to this conserved organization, the translated sequences of these

four other *Vibrio htrB* genes are also the closest four matches to *V. fischeri* HtrB2. Only *V. parahaemolyticus* RIMD2210633 has additional *htrB* genes, two of them, but neither shared the genetic context and localization to chromsome II of *V. fischeri htrB1*. These bioinformatic data suggest that *V. fischeri htrB2* and *msbB* are evolutionarily conserved in the *Vibrionaceae*, whereas *htrB1* may be performing a more niche-specific activity for *V. fischeri*.

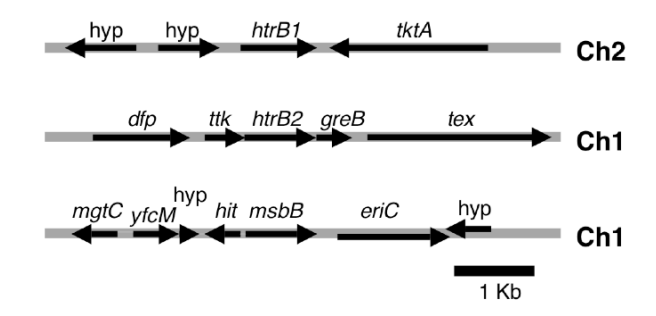


FIG. 2.1. Chromosomal location and orientation of *htrB1*, *htrB2*, and *msbB* in *V. fischeri* ES114. Open reading frames encoding hypothetical proteins are designated "hyp". BLAST-P searches of the National Center for Biotechnology Information database were used to determine homologies (e<10⁻¹⁵) and assign names for genes flanking *htrB1*, *htrB2*, or *msbB*. Arrows indicate gene orientation. Ch1 and Ch2 indicate localization to chromosomes one or two, respectively.

Lipid A acyltransferase activity *of V. fischeri htrB1*, *htrB2*, and *msbB*. To test whether *V. fischeri htrB1*, *htrB2*, and *msbB* encoded lipid A acyltransferases, we placed these genes on plasmids in *E. coli* mutant MKV15 (*htrB*::Tn10, *msbB*::*cam*, *lpxP*::*kan*), which lacks secondary acylations on lipid A (290). Lipid A samples were prepared from these and control strains by mild acid hydrolysis of the LPS, partially purified, and analyzed by mass spectrometry. Figure 2.2 shows a stack plot of the MALDI spectra of these lipid A samples. The major lipid A components obtained from wild-type *E. coli* are a diphosphorylated lipid A (DPLA) and a monophosphorylated lipid A (MPLA) each containing four 3-hydroxymyristic acids (C14:0(3-OH)), one myristic acid (C14:0), and one lauric acid (C12:0), yielding (M-H)⁻ ions for DPLA and MPLA at m/z 1796.1 and 1716.1, respectively. As previously reported (290), MKV15 lipid A lacks both of the secondary acyl chains (C12:0 and C14:0), yielding DPLA and MPLA with

(M-H)⁻ ions at m/z 1403.9 and 1323.9, respectively (Fig. 2.2). This was unaffected by either of the insertless plasmids, pDMA28 or pJLB2 (Fig. 2.2), although in some samples these negative controls contained small amounts of lipid A that were 238 Da larger, consistent with the addition of a C16:0 moiety.

Each of the *V. fischeri htrB1*, *htrB2*, and *msbB* genes directed acylation of MKV15 lipid A, although their acyl-chain substrates differed from those of their *E. coli* homologues. When MKV15 was transformed with plasmids carrying *V. fischeri htrB1* or *htrB2*, a 226 Da moiety was added to lipid A (Fig. 2.2), suggesting the addition of a hydroxylated C14:0 fatty acid. This result suggests that *htrB1* and *htrB2* encode enzymes with different substrate specificity than *E. coli* HtrB, which adds a lauric acid (C12:0) to the *E. coli* lipid A. Similarly, MKV15 complemented with *V. fischeri msbB* added a 182 Da moiety (C12:0 fatty acid) to the lipid A (Fig. 2.2), whereas *E. coli* MsbB adds a myristic acid (C14:0). FAME analyses of lipid A from the strains shown in Figure 2 were consistent with our interpretation of these strains' lipid A mass profiles and confirmed that *V. fischeri msbB* directed addition of C12:0 to MKV15 lipid A while *htrB1* and *htrB2* were responsible for addition of C14:O(3-OH) (data not shown). These results demonstrate that the *V. fischeri htrB1*, *htrB2* and *msbB* gene products have lipid A acylase activity and suggest that their substrate specificity differs from that of their respective homologs in *E. coli*.

We further investigated the activities of *htrB1*, *htrB2*, and *msbB* by generating *V. fischeri* mutants lacking these genes and examining their lipid A. FAME analyses of partially purified LPS from ES114 and mutant strains are shown in Table 2.2. These data must be interpreted cautiously, because the structure of *V. fischeri* lipid A is unknown and appears to contain unusual

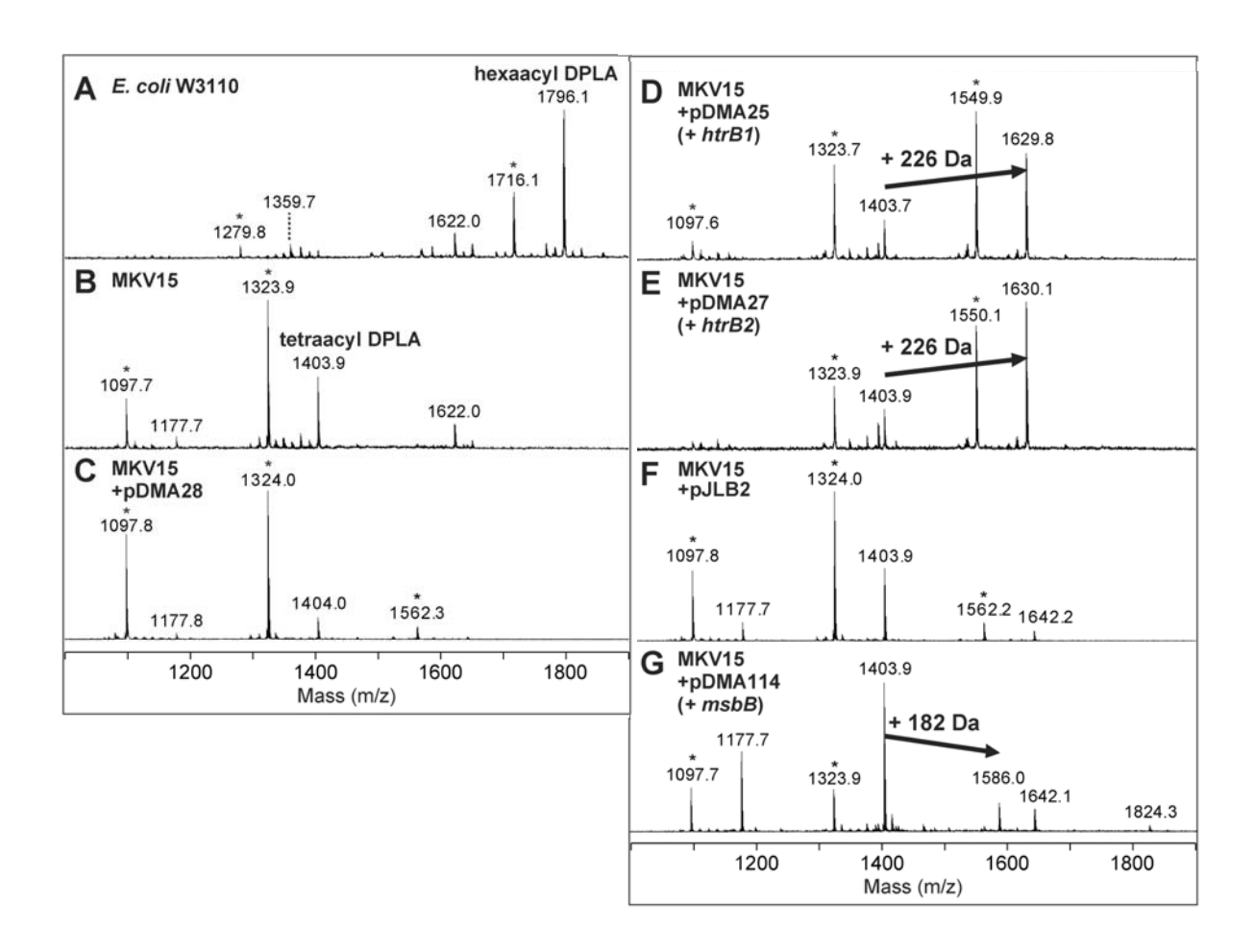


FIG. 2.2. Complementation of *E. coli* MKV15 with putative lipid A secondary acyltransferase genes from *V. fischeri*. Lipid A was obtained from LPS preparations of *E. coli* strains grown in minimal media at 30°C, including W3110 (parent-panel A), MKV15 (mutant lacking lipid A secondary acylations-panel B), and MKV15 carrying plasmids with either no insert (pDMA28-panel C or pJLB2-panel F) or with inserts of *htrB1*, *htrB2*, or *msbB* from *V. fischeri* (panels D, E, and G, respectively). pDMA28 serves as the isogenic insert-free control for pDMA25 and pDMA27, whereas pJLB2 serves this purpose for pDMA114. Samples were analyzed by negative-ion MALDI-TOF mass spectrometry in the reflectron mode. The (M-H) ion at m/z 1796.1 (panel A) arises from the *E. coli* hexaacylated diphosphorylated lipid A (DPLA). Strain MKV15 produces a tetraacylated DPLA with a (M-H) ion at m/z 1403.9 (panel B), which is also seen in MKV15 with the control plasmids (panels C and F). Arrows in panels D, E, and G indicate the molecular weight shifts caused by complementation. Peaks marked with asterisks are monophosphorylated lipid A forms. The small peak at m/z 1622.0 (seen in panels A and B) is an unidentified impurity. The minor addition of a C16:0 fatty acid (+238 Da) occasionally occurred even in the negative controls (seen in panels C, F and G).

msbB has a reduced C_{12:0} composition (Table 2.2), consistent with the apparent activity of *V. fischeri msbB* in transgenic *E. coli* (Fig. 2.2). Also, each of the mutants lacking *htrB2* had a reduction in C_{14:0}, although no difference in the 3-OH C_{14:0} content was detectable. The *htrB1* mutant showed no clearly significant differences from the wild type, although strains lacking *htrB1* tended to have relatively low 3-OH C_{14:0} content. A more dramatic effect of *htrB1* was evident upon comparing the *htrB1 htrB2* mutant to the *htrB2* mutant, which revealed a decrease in C_{12:0} associated with the mutant *htrB1* allele (Table 2.2). This is consistent with other phenotypes measured in culture (reported below) in that effects of mutating *htrB1* were only evident in other mutant backgrounds. Taken together these data further indicate that HtrB1, HtrB2, and MsbB direct the modification of lipid A in *V. fischeri*, although the activity of HtrB1 may be insignificant in wild type when grown in culture.

Table 2.2. Percent fatty acid composition of partially purified lipid A from *V. fischeri* ES114 and mutants derivatives

	$C_{12:0}$	$C_{14:0}$	$C_{16:0}$	$C_{16:1}$	$C_{16:1}$	$C_{12:0}$	$C_{18:0}$	$C_{18:1}$	$C_{18:1}$	C _{14:0}	C _{14:1}
Strain				a	b	3-OH		a	b	3-OH	3-OH
ES114 (wild type)	5.2	10.6	14.6	3.7	15.6	20.0	4.4	0.9	1.2	15.5	8.4
EVS300 (htrB1 ⁻)	4.2	12.4	17.8	3.9	15.3	19.2	5.0	1.3	1.6	12.9	6.5
DMA310 (htrB2 ⁻)	4.1	4.8	16.2	4.0	17.2	20.4	4.6	1.1	1.7	18.1	7.7
HG320 (<i>msbB</i> ⁻)	1.0	10.4	22.6	3.0	17.8	16.4	9.5	1.6	1.7	11.8	4.4
DMA330											
(htrB1 ⁻ , htrB2 ⁻)	1.3	4.4	19.9	3.2	21.5	20.6	7.2	0.8	3.3	11.3	6.5
DMA331											
$(htrB1^-, msbB^-)$	0.8	11.4	21.2	3.5	17.1	16.2	8.9	1.7	1.5	12.1	5.5
DMA332											
$(htrB2^{-}, msbB^{-})$	1.0	5.2	20.1	2.5	18.8	16.8	7.5	1.4	1.8	18.9	6.0
AO340											
(htrB1 ⁻ , htrB2 ⁻ , msbB ⁻)	0.9	6.0	17.5	4.2	24.8	17.6	8.8	1.5	2.3	10.8	5.6

Sensitivity of mutants to SDS, kanamycin and polymyxin B. Changes to the acylation pattern of lipid A can affect outer membrane stability and the resistance of bacteria to detergents, antibiotics and host-derived antimicrobial peptides (108). Therefore, antimicrobial sensitivity assays provide a direct test of the barrier function of LPS and an indirect test for alterations in LPS structure. Notably, the activity of the antimicrobial peptide polymyxin B is thought to involve direct binding to lipid A, and alterations in lipid A structure can influence polymyxin B resistance. We determined the concentrations of SDS, kanamycin and polymyxin B yielding a 50% reduction in growth (IC₅₀) of the wild type ES114 and each of the htrB1, htrB2 and msbB mutants (Table 2.3). The htrB1 mutant EVS300 was essentially like wild type with respect to antimicrobial sensitivity. In contrast, htrB2 mutant DMA310 and msbB mutant HG320 were each more sensitive to kanamycin and more resistant to polymyxin B, with DMA310 also displaying significantly increased sensitivity to SDS (Table 2.3). Combining mutations often resulted in more pronounced effects on antimicrobial sensitivity. Moreover, statistical analyses revealed significant allelic interactions leading to IC₅₀'s that were not simply additive effects. This is illustrated by the influence of the presence or absence of htrB2 on the effect htrB1 has on SDS sensitivity. Mutating htrB1 in the wild type had little or no effect on growth in SDS, but in an htrB2 mutant background mutating htrB1 caused a dramatic increase in SDS sensitivity. Thus, the data in Table 3 are consistent with htrB2 and msbB affecting lipid A structure, whereas the effect of htrB1 is negligible for wild type growing in culture and is only evident in other mutant backgrounds.

Table 2.3. Effects of *htrB* and *msbB* mutations on *V. fischeri* sensitivity to SDS, polymyxin B, and kanamycin

		$\mathrm{IC}_{50}{}^{\mathrm{a}}$				
Strain	genotype	% SDS	μg ml ⁻¹ Kanamycin	μg ml ⁻¹ Polymyxin B		
		10 (0 0 11)	104 (06 112)	0.72 (0.66.0.70)		
ES114	wild type	10 (8.8-11)	104 (96-113)	0.73 (0.66-0.79)		
EVS300	htrB1::erm	9.5 (8.3-10.7)	106 (98-115)	0.58 (0.54-0.62)		
DMA310	ΔhtrB2::erm	3.5 (3.2-4.0) *	74 (68-80) *	1.1 (1.0-1.2) *		
HG320	∆msbB::erm	7.1 (6.4-8.0)	66 (61-71) *	1.6 (1.4-1.8) *		
DMA330	htrB1::erm ∆htrB2	0.031 (0.029-0.035) *	35 (32-38) *	1.7 (1.5-1.9) *		
DMA331	htrB1::erm ∆msbB	7.0 (6.2-7.9)	59 (54-64) *	1.5 (1.3-1.6) *		
DMA332	ΔmsbB::erm ΔhtrB2	2.0 (1.8-2.2) *	47 (44-51) *	4.7 (4.3-5.1) *		
AO340	htrB1::erm ΔhtrB2	0.024 (0.022-0.026) *	35 (32-38) *	2.6 (2.1-3.18) *		
	$\Delta msbB$					

^a The IC₅₀ is the concentration at which growth yield is half-maximal (see Methods). Data represent combined results of three independent assays, and the 95% confidence interval is given in parentheses. Values marked with an asterisk indicate IC₅₀'s that were significantly (p<0.01) different from that of wild type in each of the three independent assays.

Growth, luminescence and motility of *V. fischeri* lipid A mutants in culture. One goal of this study was to examine the symbiotic competence of the *htrB1*, *htrB2* and *msbB* mutants; however, we considered the possibility that these mutations might cause pleiotropic effects on cells making it difficult to interpret whether any deficiencies in host colonization reflected symbiosis-specific defects. In particular, to fully colonize the *E. scolopes* light organ, *V. fischeri* must be able to swim (101), grow rapidly (223), and bioluminesce (282), and we therefore examined these phenotypes in culture before examining the mutants' symbiotic competence.

We first assessed the ability of the *htrB1*, *htrB2*, and *msbB* mutants to swim through soft agar (Fig. 2.3A). The *htrB1* mutant EVS300 had no detectable difference in swimming rate relative to the wild-type parent ES114. In contrast, DMA310 (*htrB2*⁻) and HG320 (*msbB*⁻) displayed significant (p<0.001) attenuation of motility (Fig. 2.3A), and this could be complemented *in trans* by restoring the *htrB2* or *msbB* gene, respectively (Fig. 2.3B). Combining mutations in the same strain caused more severe attenuation in swimming, particularly in strains lacking *htrB2* (Fig. 2.3A).

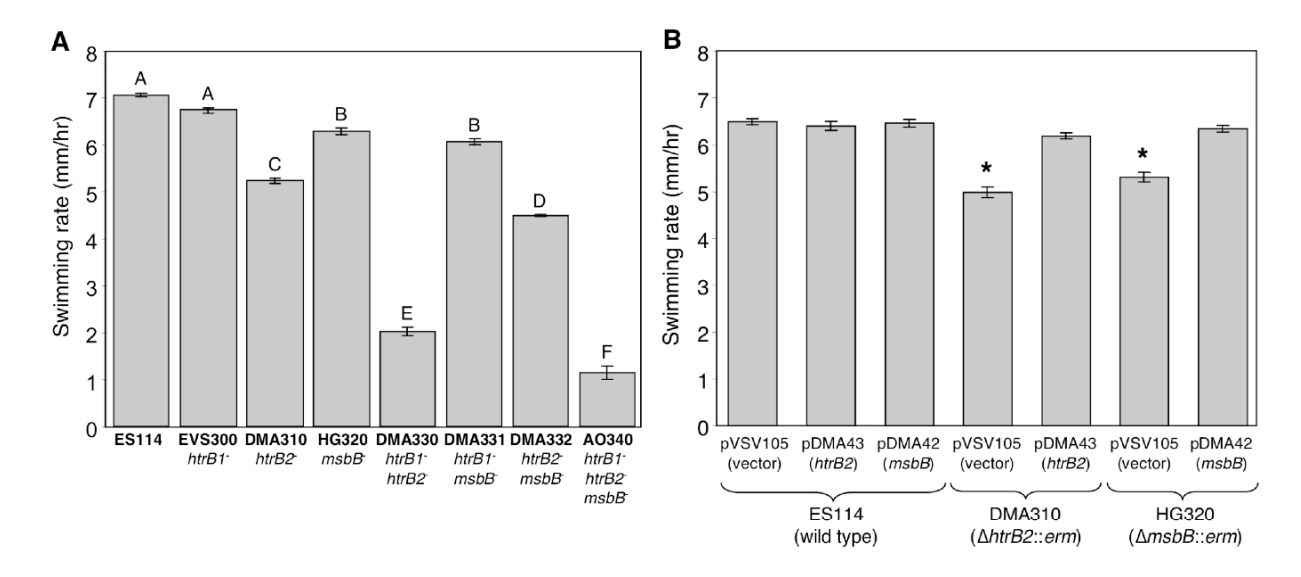


FIG. 2.3. Motility of *V. fischeri htrB1*, *htrB2*, and *msbB* mutants. Both panels report average rate of movement through 0.25% agar plates and show representative data from one experiment of at least three. Standard error (n=6) is shown. **A.** Motility of ES114 and mutants. Bars labeled with the same capital letter do not differ significantly (p<0.001) as determined by analysis of variance. **B.** Motility of ES114, DMA310 (*htrB2*) and HG320 (*msbB*) with pVSV105, pDMA43 (pVSV105+*htrB2*), or pDMA42 (pVSV105+*msbB*). Asterisks represent significant difference (p<0.01) from wild type carrying the same vector.

Microscopic observations provided a possible mechanistic explanation for these motility defects (Fig. 2.4). Unlike ES114 (Fig. 4A) and *htrB1* mutant EVS300 (not shown), mutants DMA310 (*htrB2*⁻), DMA330 (*htrB1*⁻ *htrB2*⁻), and DMA332 (*htrB2*⁻ *msbB*⁻), formed chains of cells (e.g. Figs. 2.4B and C). These mutant cells appeared septated but still linked together (e.g. Fig. 2.4B). Nonmotile mutant AO340 (*htrB1*⁻ *htrB2*⁻ *msbB*⁻) formed large groups of cells that adhered together, as well as unusually shaped, large and possibly unseptated cells (Fig. 2.4D). *V. fischeri* normally swims using polar flagella, and it seems plausible that multiple cells linked end to end would not be as motile as free individual cells.

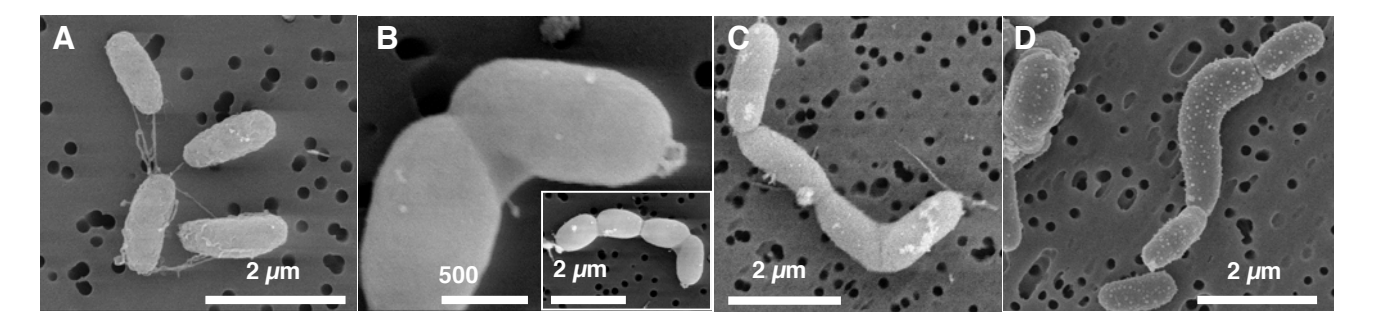


FIG. 2.4. Morphology of *htrB2* mutants. SEM images of (A) ES114 (wildtype) (B) DMA310 (*htrB2*⁻), (C) DMA330 (*htrB1*⁻ *htrB2*⁻) and (D) AO340 (*htrB1*⁻ *htrB2*⁻ *msbB*⁻).

We next tested the growth rates of the *htrB1*, *htrB2*, and *msbB* mutants in broth cultures. EVS300 (*htrB1*⁻), DMA310 (*htrB2*⁻), HG320 (*msbB*⁻), DMA331 (*htrB1*⁻ *msbB*⁻), and DMA332 (*htrB2*⁻ *msbB*⁻) had no discernable difference in growth rate relative to their wild-type parent ES114. AO340 (*htrB1*⁻ *htrB2*⁻ *msbB*⁻) and DMA330 (*htrB1*⁻ *htrB2*⁻) grew extremely poorly in LBS medium; however, addition of 55 mM MgCl₂ and 8 mM CaCl₂ to LBS restored growth to both strains indicating that divalent cations are important for growth when both *htrB1* and *htrB2* are absent (data not shown). In SWT, which contains divalent cations, AO340 (*htrB1*⁻ *htrB2*⁻ *msbB*⁻) and DMA330 (*htrB1*⁻ *htrB2*⁻) grew at a rate similar to wild type; however, when culture optical density (OD₅₉₅) was ~0.5, AO340 cells clumped, and growth rate could no longer be determined by measuring OD₅₉₅ or by enumerating CFUs.

We also assayed each mutant's bioluminescence. EVS300 (*htrB1*⁻) and DMA310 (*htrB2*⁻) displayed wild-type-like luminescence; however, we found that DMA330 (*htrB1*⁻ *htrB2*⁻) and AO340 (*htrB1*⁻ *htrB2*⁻ *msbB*⁻), each had decreased luminescence compared to ES114 (Fig. 2.5). HG320 (*msbB*⁻), DMA331 (*htrB1*⁻ *msbB*⁻) and DMA332 (*htrB2*⁻ *msbB*⁻) each displayed at least a 2-fold increase in specific luminescence relative to ES114 (Fig. 2.5), and this was complemented in HG320 by providing *msbB* in *trans* or by replacing the mutant deletion with the wild-type allele on the chromosome (data not shown). A potentially limiting substrate for the light-generating luciferase

in *V. fischeri* is the aliphatic aldehyde that is (re)generated by LuxC and LuxE from the corresponding long-chain fatty acid, which is provided in part by LuxD (27, 249, 274). We speculated that eliminating MsbB might increase the substrate pool for luciferase thereby resulting in the observed enhancement of luminescence. To test this we added 10 µM myristic acid to the media and found that the luminescence of both the wild type and HG320 (*msbB*⁻) increased to the same level (data not shown), supporting the idea that MsbB and bioluminescence compete for a limited supply of long-chain fatty acids.

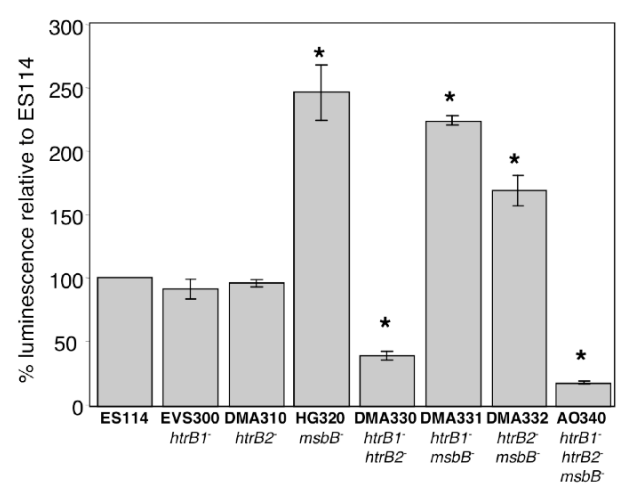


FIG. 2.5. Effects of htrB1, htrB2, and msbB mutations on bioluminescence. Maximal luminescence per OD_{595} of mutant strains grown in SWT at 24°C is expressed as a percentage of that emitted by ES114. Error bars indicate standard error (n=3) and asterisks indicate a significant difference from ES114 (p<0.05). One representative experiment of three is shown.

Taken together, the in-culture phenotypic characterization described above indicated that some, but not all, of the mutants were appropriate for symbiotic infection studies. EVS300 (htrB1) was indistinguishable from ES114 in culture, and therefore any attenuation during colonization of *E. scolopes* could be considered symbiosis-specific, at least insofar as this mutant is not generally attenuated in growth. DMA310 (htrB2), HG320 (msbB), and DMA331 (htrB1) msbB) were also chosen for symbiotic characterization, because their differences from wild type

were moderate. Other mutant strains were not included in symbiotic studies because of their low motility, decreased luminescence, odd cell morphology, and growth requirements.

Symbiotic colonization of *E. scolopes* by lipid A mutants. Despite their phenotypic differences from ES114 in culture (e.g. see Tables 2.1 and 2.2, Figures 2.3, 2.4 and 2.5), neither DMA310 (*htrB2*) nor HG320 (*msbB*) had an apparent defect in colonization of *E. scolopes* over 48 h following inoculation (data not shown). On the other hand, EVS300 (*htrB1*) and DMA331 (*htrB1 msbB*) appeared similarly attenuated relative to ES114 in their ability to initiate this symbiosis. For example, inoculation with EVS300 resulted in a reduced onset of symbiotic bioluminescence during initial colonization relative to animals inoculated with ES114 (Fig. 2.6A). This difference in symbiotic luminescence was subtle, and during initial colonization ES114-infected animals became between 1.5- and 4-fold brighter than animals infected by EVS300. Moreover, this difference was reproduced in natural seawater, but in one experiment using Instant Ocean no difference was seen between mutant and wild type. Interestingly, we found that infections with wild type or EVS300 were indistinguishable after the first light-triggered diurnal venting of symbionts (Fig. 2.6A).

Luminescence is a good indirect indicator of colonization levels in squid assays, and EVS300 produced luminescence indistinguishable from that of ES114 in culture (Fig. 2.5); however, we considered the possibility that differences in luminescence levels in EVS300- and ES114-infected animals did not reflect colonization levels. In a separate experiment, juvenile squid were infected with either ES114 or the *htrB1* mutant, and after luminescence of the two sets of animals diverged, (Fig. 2.6B) we homogenized and plated the animals to determine CFU. EVS300-infected animals had fewer cfu than ES114-infected animals, confirming that lower luminescence corresponded to fewer bacteria in the light organ in this experiment (Fig. 2.6C).

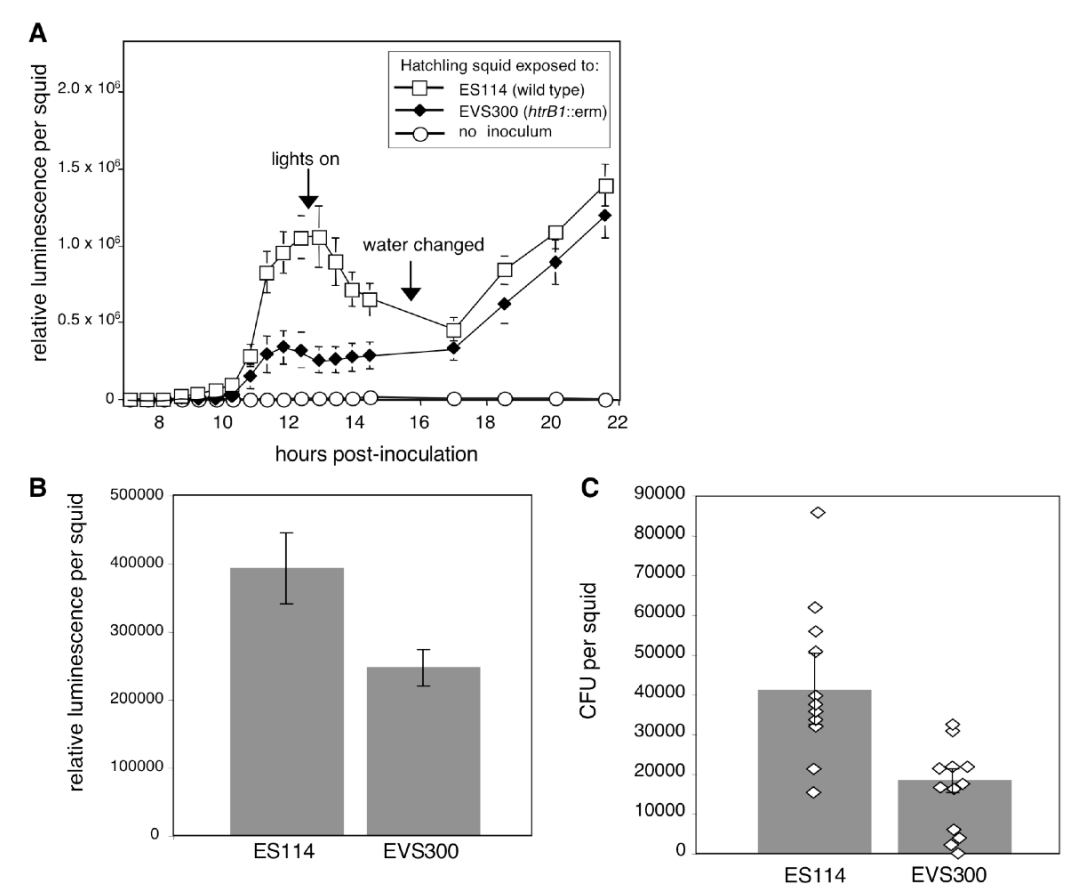


FIG. 2.6. Symbiotic luminescence and colonization for *V. fischeri* wild type and an *htrB1* mutant. **A.** Animal luminescence during the initial stages of *E. scolopes* colonization by strains ES114 (wild type) and *htrB1* mutant EVS300. The luminescence pattern indicates the initial onset of colonization (0-12.5 h) followed by a changing level of light emission that reflects the diurnal venting behavior of the animal and regrowth of symbionts (22). Mean values of 21 animals were calculated and standard errors of the mean are indicated. **B.** In a separate experiment from (A), luminescence of hatchling squid inoculated with wild type (ES114) or *htrB* mutant (EVS300) at 16 h post inoculation. Each bar represents the average of 11 or 12 animals with the standard error. **C.** Colonization levels of *V. fischeri* from the same animals presented in panel B. Each bar represents the average of 11 or 12 animals with the standard error. Diamonds represent the CFU's present in individual animals.

These experiments were technically challenging due to the light-triggered venting of the animal's symbionts and the lack of a discernable difference between animals infected with wild type or *htrB1* mutants after the first venting. To obtain data like those in Figure 2.6C, animal luminescence was monitored using a scintillation counter, and after the onset of luminescence animals were plated while keeping the room as dark as possible to prevent triggering the animals'

venting behavior. We attempted to alleviate this problem using competition experiments wherein animals were exposed to a 1:1 mixture of mutant and wild-type cells and the ratio of the two strains in the squid was determined at some time after infection. We reasoned that even if the mutant had a defect only in a narrow window of time during early infection, this might still be reflected in the populations later on, after venting. Another advantage of competition experiments is that variability between animals is less of a complicating factor, because both strains are exposed to the same set of animals. Importantly, such competition experiments have been used in the past in studies of this symbiosis, and sometimes reveal colonization defects that are not immediately apparent in singlestrain inoculations (149, 251, 285). To ensure that any competitive defect we might find would not simply reflect a generally attenuated mutant, we first competed ES114 and the htrB1 mutant EVS300 in culture and found no competitive defect for the mutant under these conditions (Fig. 2.7A). However, when squid were co-inoculated with these strains we found that the wild type outcompeted the htrB1 mutant EVS300 by 2.7-fold (Fig. 2.7B). This is a similar magnitude of attenuation relative to the wild type as we saw during early infection in experiments with clonal inocula (e.g., Fig. 2.6A); however, these results were more reproducible and robust, and more animals could be analyzed because they did not have to be kept in the dark and plated during a narrow window of time. In contrast to this competitive defect of the htrB1 mutant evident in the host and not in culture, the msbB mutant was not outcompeted by ES114 either in the symbiosis or in culture, and the htrB2 mutant was outcompeted to a similar extent under both symbiotic and culture conditions (data not shown).

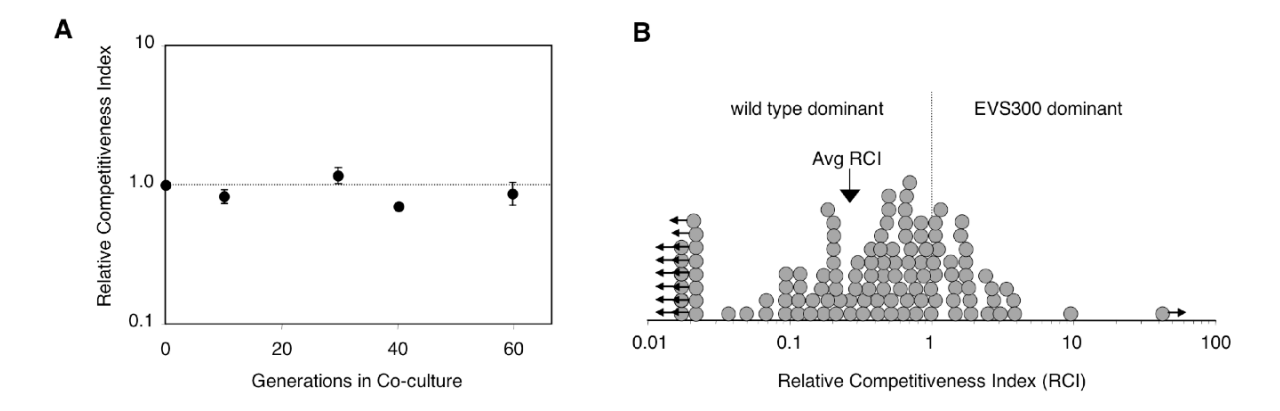


FIG. 2.7. Competition between ES114 and its *htrB1* mutant EVS300 in culture and in squid. **A.** Relative competitiveness of *htrB1* co-cultured with ES114 in LBS. In parallel cultures, one strain or the other was tagged with *lacZ* to facilitate determination of strain ratios by blue/white screening (see Methods). Error bars represent standard error (n=3). **B.** Relative competitiveness of *htrB1* mutant during colonization of *E. scolopes*. Juvenile squid were exposed to a mixed inoculum of wild type and *htrB1* mutant EVS300 at a total concentration of ~2,500 CFU/ml, and the relative competitiveness was determined after 48 h. Circles represent the RCI determined from the infection in each of 118 individual animals. Circles with arrows represent animals that were clonally infected. Data represent combined results of four similar experiments.

Discussion

Despite intense interest regarding how lipid A structure affects pathogenic animal-bacteria interactions, little is known about how lipid A functions in a mutualism, such as the *V. fischeri–E. scolopes* symbiosis. *V. fischeri* is uniquely able to colonize and induce the morphogenesis in *E. scolopes* light organ, and previous evidence suggested that lipid A plays an important role in these processes (75, 141). In this study we examined *htrB* and *msbB* genes, which encode lipid A secondary acyltransferases, to investigate their effects on the *V. fischeri–E. scolopes* mutualism and on the general biology of *V. fischeri*. Our results suggest that *htrB2* and *msbB* are conserved in other vibrios and that in *V. fischeri* they are active outside the symbiosis. This is illustrated by the observation that *htrB2* and *msbB* mutants displayed several phenotypic differences relative to wild type in culture (e.g., see Tables 2.2 and 2.3, Figs. 2.3, 2.4 and 2.5). In contrast, the *htrB1* gene, found on the more variable chromosome 2, appears distinctive to *V.*

fischeri, and the *htrB1* mutant displayed a slight symbiosis-specific defect (Figs. 2.6 and 2.7), but was indistinguishable from wild type in culture.

The symbiotic attenuation of the htrB1 mutant was evident early in colonization (Fig. 2.6), possibly suggesting that HtrB1 modifies lipid A in a way that is important for symbiont recognition or other initial events in the infection. Indirect evidence for a role of lipid A and HtrB in signaling in this symbiosis came from Foster et al. (75), who found that LPS from a H. influenzae htrB mutant caused an attenuated apoptotic response in E. scolopes relative to LPS derived from the wild-type H. influenzae. However, using a similar approach to that of Foster et al. (75), we did not detect a reduction in the apoptotic response in E. scolopes treated with LPS from the V. fischeri htrB1 mutant relative to treatment with LPS from the wild-type strain (data not shown). If released LPS does act as a signal early in infection, one might expect that the wild type would compensate for the htrB1 mutant when the strains are mixed; however, in mixed-strain competition experiments the htrB1 mutant was outcompeted by wild type (Fig. 2.7). This may indicate that HtrB1 plays some role other than in signaling. On the other hand, significant segregation of strains occurs once cells colonize the light-organ crypts during mixed infections (69), leaving open the possibility that a signaling defect of mutant cells in the crypt spaces cannot be compensated for by the wild type due to spatial separation. If so, it is possible that a signal conferred by HtrB1 is important in the early establishment of the symbiosis within the crypts rather than in the initial aggregation and migration of the bacteria on the surface of the light organ (195).

V. fischeri mutants lacking htrB2, msbB, or a combination of lipid A acyltransferase genes, had unpredicted phenotypes, including motility defects, altered cell morphology and enhanced bioluminescence (Figs. 2.3, 2.4 and 2.5). These observations should be considered

when examining the roles of htrB and msbB in host-bacteria interactions. Numerous studies in pathogenic organisms, including $Salmonella\ typhimurium$ and $E.\ coli$, show that htrB or msbB mutants colonize their animal hosts poorly or are less able to evade the immune system, suggesting a direct link between lipid A structure and virulence (131, 171, 244). However, motility contributes to colonization and virulence in these and other bacteria (145, 254), and motility was not reported in these studies of msbB and htrB mutants. We have now shown that htrB2 and msbB mutants have attenuated motility at least in $V.\ fischeri$ (Fig. 2.3). Similarly, a recent study found that mutations in htrB or msbB in $E.\ coli$ could have pleiotropic effects by affecting expression of the alternative sigma factor σ^E (258). Therefore, mutating htrB and msbB in pathogens could affect virulence indirectly in unexpected ways, and thorough analyses of htrB and msbB mutants in culture is important to determine whether decreased virulence reflects a general attenuation of the mutant, an indirect effect through another virulence determinant, or a defect specific to a direct role of LPS in the pathogen-host interaction.

The structure of *V. fischeri* lipid A has been difficult to solve and may include novel decorations. However, we have gained insight into the biochemical roles of *htrB1*, *htrB2*, and *msbB* by expressing these genes in an *E. coli* strain lacking secondary acylations on lipid A (Fig. 2.2) and by examining the fatty acid profiles of lipid A from *V. fischeri* mutants (Table 2.2). Interestingly, both approaches indicated that the *V. fischeri* MsbB adds a C_{12:0} fatty acid to lipid A, in contrast to the C_{14:0} acylation added by *E. coli*'s MsbB. This suggests that comparisons of *E. coli* and *V. fischeri* MsbB could offer a powerful approach toward determining the acyl-chain substrate specificity of MsbB enzymes. The C_{12:0} content of lipid A was also decreased in an *htrB1 htrB2* double mutant (Table 2.2). Given the lack of evidence that either HtrB1 or HtrB2

uses $C_{12:0}$ as a substrate, these data could indicate that V. *fischeri* MsbB works most efficiently on lipid A that has already been decorated by the activity of HtrB, as is the case in E. coli (45, 47).

The direct activities of V. fischeri HtrB1 and HtrB2 are less clear, although they also seem to differ from their namesake in E. coli, which directs addition of a C_{12:0} moiety to lipid A. For example, the V. fischeri htrB1 and htrB2 genes each directed addition of 3-OH C_{14:0} to lipid A in transgenic E. coli (Fig. 2.2). Hydroxylated secondary acylations of lipid A are unusual but not unprecedented, and they have been observed on lipid A in Bordetella hinzii 2-OH C_{14:0}, Bordetella trematum 2-OH C_{14:0}, and Rhizobium etli 27-OH C_{28:0} (34, 280). Consistent with the results in transgenic E. coli, V. fischeri strains lacking htrB1 apparently tended to have a lower 3-OH C_{14:0} content in their lipid A (Table 2.2), although this subtle trend in our data may not reflect a real effect. In contrast, there was no indication that htrB2 mutants had decreased 3-OH C_{14:0} in their lipid A. If anything, lipid A from htrB2 mutant strains had slightly elevated levels of this fatty acid (Table 2.2). Instead, the htrB2 mutant had a decrease in the C_{14:0} component of lipid A (Table 2.2). This discrepancy between the apparent roles of htrB2 in transgenic E. coli and V. fischeri could reflect different substrate structure and availability in these organisms. Ongoing attempts to elucidate the structure of V. fischeri LPS may help resolve the activities of HtrB1 and HtrB2.

Future studies of lipid A and LPS in *V. fischeri* should consider the possibility that factors other than lipid A are important in the signaling between *V. fischeri* and *E. scolopes*, and that the signaling effects of lipid A may be co-dependent on other signaling molecules. Koropatnick *et al.* (141) found that *V. fischeri* releases peptidoglycan (PG) monomers that are structurally identical to those released by *Bordetella pertussis*, which kills ciliated tracheal cells leading to the symptoms of whooping cough. In *V. fischeri*, released PG monomer triggers regression of *E.*

scolopes ciliated appendages, and PG monomer acts synergistically in combination with LPS to stimulate morphogenesis similar to that seen in an infection with symbiotic *V. fischeri* (141). Given this relationship between LPS and the PG monomer, it would be interesting to place the lipid acyltransferase mutations described here in a *V. fischeri* strain that also has a reduction in release of the PG monomer and assess signaling-related phenotypes such as apoptosis and morphogenesis as well as colonization. This multivariant approach may give more insight on the effects of the lipid A mutants in colonization when the PG monomer is not present and perhaps show a more dramatic symbiotic effect. As has been suggested before, it seems increasingly likely that signaling in this bacteria-animal mutualism will involve multiple signals and complex interactions similar to the recognition of pathogens by animal hosts (75, 141, 171).

Acknowledgements

We would like to thank Mel Sunshine, Hannah Gehman, Andrew O'Carroll, Mark Farmer and John Shields for technical assistance. We would also like to thank Anne Dunn and Jeffrey Bose for their insightful comments. This work was supported by grants from the National Institutes of Health (R01 AI50661 and R01 RR12294) and from the National Science Foundation (MCB-0347317 and IBN-0139083), and by a University of Georgia Research Fellowship to DMA.

CHAPTER 3

MUTATIONS IN AMPG AND LYTIC TRANSGLYCOSYLASE GENES AFFECT THE NET RELEASE OF PEPTIDOGLYCAN MONOMERS FROM $\it ViBRIO$ $\it Fischeri$ 2

² Adin, D.M., Engle, J. T., Goldman, W. E., McFall-Ngai, M. J. Stabb, E.V. To be submitted to the *Journal of Bacteriology*.

Abstract

The light-organ symbiont Vibrio fischeri releases N-acetylglucosaminyl-1,6-anhydro-Nacetylmuramylalanyl-γ-glutamyldiaminopimelylalanine, a disaccharide-tetrapeptide component of peptidoglycan (PG), referred to here as "PG monomer", that in most other Gram-negative bacteria is recycled and not released. This molecule can stimulate normal light-organ morphogenesis in the squid Euprymna scolopes, resulting in regression of ciliated appendages similar to that triggered by infection with its symbiont V. fischeri. We examined whether the net release of PG monomers by V. fischeri resulted from lytic transglycosylase activity or from defects in AmpG, the permease through which PG monomers enter the cytoplasm for recycling. An ampG mutant displayed a 100-fold increase in net PG monomer release, indicating that AmpG is functional. The ampG mutation also conferred the uncharacteristic ability to induce light-organ morphogenesis even when placed in a non-motile flaJ mutant that cannot infect the light-organ crypts. We next targeted five lytic transglycosylase genes singly and in specific combinations to assess their role in PG monomer release. We found that combinations of mutations in ltgA1, ltgA2 and ltgD decreased net PG monomer release, and that a triple mutant lacking all three of these genes had little to no accumulation of PG monomers in culture supernatants. This mutant colonized the host as well as the wild type; however, the mutantinfected squid were more prone to later superinfection by a second V. fischeri strain. We propose that lack of PG monomer release by this mutant results in less regression of the infection-promoting ciliated appendages leading to this propensity for superinfection.

Introduction

Microbe associated molecular patterns (MAMPs) are recognized by hosts in a variety of pathogenic and symbiotic relationships. MAMP is an umbrella term for a variety of semiconserved bacterial molecules, including lipopolysaccharide, lipoproteins, flagella, and peptidoglycan (PG), that are sensed by conserved host surveillance mechanisms (e.g., the innate immune system) triggering context-dependent reactions to bacterial colonization. Mounting evidence shows that PG-derived MAMPs play important and previously underappreciated roles in host-bacteria interactions (50).

The PG layer of Gram-negative bacteria is a rigid network in the periplasm that protects against osmotic lysis and helps to determine cell size and shape, while still allowing diffusion of molecules into the cell (61). In PG, repeated subunits of *N*-acetylglucosamine and *N*-acetylmuramic acid are connected to a short pentapeptide side chain of L-alanyl-D-γ-glutamyl-meso-diaminopimelyl-D-alanyl-D-alanine (ala-glu-DAP-ala-ala). Adjacent peptides are crosslinked through ala-DAP or DAP-DAP peptide bonds, and side-chains are converted to tetra-, tri-, and dipeptides through the action of carboxypeptidases in the periplasm (93, 187).

Despite its mechanical stability, PG is a dynamic structure that undergoes remodeling and recycling. Murein hydrolases, including lytic transglycosylases, hydrolyze PG to allow the insertion of new material as the cell grows or to accommodate structures that span the periplasm (235, 289). Lytic transglycosylases cleave the *N*-acetylmuramic acid-\(\beta\)-1,4-*N*-acetylglucosamine linkage in peptidoglycan and catalyze the formation of a 1,6-anhydro bond on the *N*-acetylmuramic acid (124). After cleavage, PG monomers enter the cytoplasm through the permease AmpG (129), and are recycled and ultimately reincorporated into PG (96). Murein hydrolase activity and the recycling of PG monomers presumably allow for growth and cell

expansion; however, *Escherichia coli* mutants lacking *ampG* or several lytic transglycosylases were not affected in growth or cell division (114, 154).

Only a few bacteria are known to release PG monomers during growth, presumably because PG monomers are usually efficiently recycled. These include *Neisseria gonorrhoeae* (242) and *Bordetella pertussis* (221), which cause gonorrhea and whooping cough, respectively. These pathogens each release *N*-acetylglucosaminyl-1,6-anhydro-*N*-acetylmuramylalanyl-γ-glutamyldiaminopimelylalanine (referred to herein as "PG monomer"), which triggers the death of ciliated host cells (52, 164, 175); but the basis for their shedding of PG monomers differs. *B. pertussis* release of PG monomer, or "tracheal cytotoxin" (TCT), apparently is due to disruption of *ampG* expression by the insertion of an IS481 element 90 bp upstream of this gene (160), and artificially expressing *ampG* in *B. pertussis* decreased PG monomer release (160). However, in *N. gonorrhoeae* the activities of two lytic transglycosylases, LtgA (49) and LtgD (48), appear to be responsible for the release of the PG monomer, or "PG cytotoxin" (PGCT). An *ampG* mutant in *N. gonorrhoeae* showed a seven-fold increase in PG monomer release suggesting a functional AmpG and PG recycling pathway (79). Unfortunately, humans are the host for *N. gonorrhoeae* and *B. pertussis* hindering examination of the effects of PG monomer during natural infections.

Recently the bioluminescent marine bacterium *Vibrio fischeri* was found to release the same PG monomer as *N. gonorrhoeae* and *B. pertussis* (141). *V. fischeri* is a light-organ symbiont of the Hawaiian bobtail squid, *Euprymna scolopes*, and this host-bacterium association can be reconstituted in the laboratory. *E. scolopes* hatchlings contain ciliated appendages that increase water flow across the light organ and help facilitate infection (170, 174, 183). During initial colonization, *V. fischeri* triggers regression of these ciliated fields (64, 182), and this can be mimicked by adding PG monomers to the seawater (141). In this study, we constructed and

analyzed mutants to determine the contributions of lytic transglycosylases and AmpG to PG monomer release in *V. fischeri*. We also determined the abilities of the mutants to colonize and stimulate morphogenesis of the squid host.

Materials and Methods

Bacterial strains, plasmids and growth conditions. The strains used in this study are listed in Table 3.1. *E. coli* was incubated at 37°C in LB medium (176), BHI medium (Difco, Sparks, MD), or, for PG monomer analysis, in M9 minimal medium (231) with 30 μM glucose. When added to LB medium (176) for selection of *E. coli*, chloramphenicol (Cm) and kanamycin were used at concentrations 20 and 40 μg ml⁻¹, respectively. For selection of *E. coli* with erythromycin (Em), 150 μg ml⁻¹ was added to BHI medium. *V. fischeri* was grown at 28°C in LBS (250), at 24°C in SWT and SWTO (24), or minimal salts medium (0.340 mM NaPO₄ pH 7.5, 0.05 M Tris pH 7.5, 0.3 M NaCl, 0.05 M MgSO₄-7H₂O, 0.01 M CaCl₂-2H₂O, 0.01 M NH₄Cl, 0.01 M KCl, 0.01 mM FeSO₄-7H₂O and 30 mM glucose). When added to LBS for selection of *V. fischeri*, Cm, kanamycin, and Em, were used at concentrations of 2, 100, and 5 μg ml⁻¹ respectively. Agar was added to a final concentration of 1.5% for solid media.

DNA and plasmid manipulations. Standard methods were used to manipulate plasmids and DNA fragments. Restriction enzymes and T4-DNA Ligase were obtained from New England Biolabs (Ipswich, MA). Chromosomal DNA was purified using the Easy-DNA kit (Invitrogen, Carlsbad, CA). Plasmids were isolated using QIAprep spin miniprep kit (Qiagen, Valencia, CA) or GenElute Plasmid Miniprep kit (Sigma, St. Louis, MO). Zero Blunt TOPO PCR Cloning Kit (Invitrogen, Carlsbad, CA) was used to clone PCR products into pCR-BluntII-TOPO. DNA

fragments were purified using DNA Clean & Concentrator-5 Kit (Zymo Research, Orange, CA). PCR was performed using KOD HiFi DNA Polymerase (Novagen, Madison, WI) by following manufacturers' recommendations for cycle programs based on predicted product size. Annealing temperature for each primer was usually determined by subtracting 5°C from the lower calculated primer melting temperature. PCR was performed using an iCycler (BioRad Laboratories, Hercules, CA). DNA sequencing was conducted on an ABI automated DNA sequencer at the University of Michigan DNA Sequencing Core, and sequences were analyzed using Sequencher 4.6 (Gene Codes, Ann Arbor, MI). Oligonucleotides (Table 3.1) were obtained from Integrated DNA Technologies (Coralville, IA).

Mutant construction. Descriptions of select plasmids and the primers used in their construction are provided in Table 3.1. Construction of mutant strains and alleles is outlined in Table 3.1, and a summary follows. To generate plasmid insertion mutants, an internal fragment of each targeted gene was PCR amplified and either cloned directly into pEVS122 (a vector that does not replicate in V. fischeri) or cloned into pCR-BluntII-TOPO and subsequently subcloned into pEVS122. The resulting plasmids were mobilized into V. fischeri, and plating on LBS-Em selected for transconjugants that had undergone homologous recombination between the genome and the internal gene fragment, enabling us to isolate vector integration mutants. In this way, plasmids pDMA48, pDMA89, pDMA90, pDMA91, pDMA108, and pDMA109 were used to generate mutations in ampG, ltgA1, ltgA2, ltgD, lysM2, and lysM1, respectively. In-frame $\Delta ampG$, $\Delta ltgA1$, and $\Delta ltgD$ deletion alleles were constructed in plasmids pDMA110, pDMA187, and pDMA199, respectively, such that the region between the start and stop codon of each target

Table 3.1. Bacterial strains, plasmids, and oligonucleotides

Strain, plasmid,	Relevant characteristics ^a	Source or
or		reference
oligonucleotide		
Bacterial strains		
E. coli		
CC118-λpir	Δ (ara-leu) araD Δ lac74 galE galK phoA20 thi-1 rpsE rpsB	(119)
	argE(Am) recA λpir	` ′
DH5α	$F^{-}\Phi 80dlacZ\Delta (lacZYA-argF)U169 deoR supE44 hsdR17 recA1$	(109)
	endA1 gyrA96 thi-1 relA1	, í
DH5α-λ <i>pir</i>	DH5 α lysogenized with λpir	(68)
MG1655	$F^{-}\lambda^{-}ilvG \ rfb50 \ rph1$	C. Gross
	F $mcrA \Delta(mrr-hsdRMS-mcrBC) \Phi 80lacZ\Delta M15 \Delta lacX74$	
TOP10	recA1 araΔ139 Δ(ara-leu)7697 galU galK rpsL (StrR)	Invitrogen
	endA1 nupG	
V. fischeri		
AKD200	ES114 mini-Tn7 insertion; CmR	A. Dunn
DM131	ES114 flaJ::aph; KnR	D. Millikan
DMA350	ES114 ampG::pDMA48; EmR	This study
DMA352	ES114 $\triangle ampG$ (allele exchanged from pDMA110 into ES114)	This study
DMA354	DM131 $\Delta ampG$ (allele exchanged from pDMA110 into	This study
	ES114); KnR	•
DMA360	ES114 ltgA1::pDMA89; EmR	This study
DMA361	ES114 ltgA2::pDMA90; EmR	This study
DMA362	ES114 ltgD::pDMA91; EmR	This study
DMA363	ES114 $\Delta ltgA1$ (allele exchanged from pDMA187 into ES114)	This study
DMA368	ES114 $\Delta ltgD$ (allele exchanged from pDMA199 into ES114)	This study
DMA369	ES114 Δ <i>ltgA1</i> Δ <i>ltgD</i> (allele exchanged from pDMA199 into DMA363)	This study
DMA380	ES114 lysM1::pDMA109; EmR	This study
DMA385	ES114 lysM2::pDMA108; EmR	This study
DMA386	ES114 $\Delta ltgA1$ $ltgA2$::pDMA90; EmR	This study
DMA387	ES114 Δ <i>ltgD ltgA</i> 2::pDMA90; EmR	This study
DMA388	ES114 $\Delta ltgA1 \Delta ltgD ltgA2$::pDMA90; EmR	This study This study
ES114	Wild-type isolate from <i>E. scolopes</i>	(20)
Plasmids	white-type isolate from <i>E. scolopes</i>	(20)
pCR-BluntII TOPO	TOPO PCR-cloning vector; KnR	Invitrogen
pDMA46	internal <i>ampG</i> fragment (PCR product; primers dma30 and dma31, ES114 template) in pCR-BluntII TOPO; KnR	This study
pDMA48	pDMA46 BamHI fragment in BamHI-digested pEVS122; internal $ampG$ fragment $oriV_{R6K_{\gamma}}$ $oriT_{RP4}$ EmR	This study

pDMA74	internal <i>ltgA1</i> fragment (PCR product; primers dma58 and dma59, ES114 template) in pCR-BluntII TOPO; KnR	This study
pDMA75	internal <i>ltgA2</i> fragment (PCR product; primers dma60 and dma61, ES114 template) in pCR-BluntII TOPO; KnR	This study
pDMA76	internal <i>ltgD</i> fragment (PCR product; primers dma62 and dma63, ES114 template) in pCR-BluntII TOPO; KnR	This study
pDMA77	ampG complementing fragment (PCR product; primers dma52 and dma53, ES114 template) in pCR-BluntII TOPO; KnR	This study
pDMA89	pDMA74 <i>Bgl</i> II fragment in <i>Bam</i> HI-digested pEVS122; internal <i>ltgA1</i> fragment; <i>oriV</i> _{R6Kγ} <i>oriT</i> _{RP4} EmR	This study
pDMA90	pDMA75 <i>Bgl</i> II fragment in <i>Bam</i> HI-digested pEVS122; internal <i>ltgA2</i> fragment; <i>oriV</i> _{R6Kγ} <i>oriT</i> _{RP4} EmR	This study
pDMA91	pDMA76 $BglII$ fragment in $BamHI$ -digested pEVS122; internal $ltgD$ fragment; $oriV_{R6K_{\gamma}}$ $oriT_{RP4}$ EmR	This study
pDMA96	~1.5 Kb fragment downstream of <i>ampG</i> stop (PCR product; primers 55 and dma57, ES114 template) in <i>Sma</i> I digested pEVS79; <i>oriV</i> _{ColE1} <i>oriT</i> _{RP4} CmR	This study
pDMA100	~1.5 Kb fragment upstream of <i>ampG</i> start (PCR product; primers dma54 and dma56, ES114 template) in <i>Hpa</i> I-digested pJLB103; <i>oriV</i> _{R6Ky} KnR	This study
pDMA104	internal <i>lysM2</i> fragment (PCR product; primers dma76 and dma77, ES114 template) in pCR-BluntII TOPO; KnR	This study
pDMA105	pDMA96 SmaI-digested fused to SmaI-digested pDMA100; $oriV_{ColE1} oriV_{R6K_{Y}} oriT_{RP4}$ KnR CmR	This study
pDMA106	pDMA77 SpeI-XbaI fragment in SpeI-XbaI-digested pEVS79; $oriV_{ColE1}$ ori T_{RP4} CmR	This study
pDMA108	pDMA104 <i>Bgl</i> III fragment in <i>Bam</i> HI-digested pEVS122; internal <i>lysM2</i> fragment; <i>oriV</i> _{R6Kγ} <i>oriT</i> _{RP4} EmR	This study
pDMA109	internal <i>lysM1</i> fragment (PCR product; primers dma78 and dma79) <i>Bam</i> HI-digested in <i>Bam</i> HI-digested pEVS122; <i>oriV</i> _{R6Ky} <i>oriT</i> _{RP4} EmR	This study
pDMA110	pDMA105 $AvrII$ - $SpeI$ digested and self-ligated; $\Delta ampG$ allele; $oriV_{ColE1}$ $oriT_{RP4}$ CmR	This study
pDMA115	pDMA106 SpeI-XbaI fragment in AvrII-digested pVSV104; V. fischeri ampG in shuttle vector pVSV104; $oriV_{R6K_{\gamma}}$ $oriT_{RP4}$ $oriV_{pES213}$ KnR	This study
pDMA176	~1.5 Kb fragment upstream of <i>ltgA1</i> start (PCR product; primers dma95 and dma99, ES114 template) in pCR-BluntII TOPO; KnR	This study
pDMA185	~1.5 Kb fragment downstream of <i>ltgA1</i> stop (PCR product; primers dma96 and dma100, ES114 template) in pCR-BluntII TOPO; KnR	This study

pDMA186	pDMA182 <i>Xho</i> I-digested and self-ligated; $oriV_{R6K_{\gamma}}$ $oriT_{RP4}$ CmR	This study
pDMA187	pDMA185 <i>Sma</i> I fragment in <i>Sma</i> I-digested pDMA186; $\Delta ltgAI$ allele; $oriV_{R6K_{\gamma}}$ $oriV_{ColE1}$ $oriT_{RP4}$ CmR	This study
pDMA191	~1.5 Kb fragment downstream of <i>ltgD</i> stop (PCR product; primers dma102 and dma106, ES114 template) in pCR-BluntII TOPO; KnR	This study
pDMA197	~1.5 Kb fragment upstream of $ltgD$ start (PCR product; primers dma105 and dma115, ES114 template) in $SmaI$ -digested pEVS122; $oriV_{R6K_{\gamma}}oriT_{RP4}$ EmR	This study
pDMA198	pDMA191 <i>Kpn</i> I- <i>Xba</i> I fragment in <i>Kpn</i> I- <i>Xba</i> I-digested pEVS79; <i>oriV</i> _{ColE1} <i>oriT</i> _{RP4} CmR	This study
pDMA199	pDMA198 Sma I-digested fused to Sma I-digested pDMA197; $\Delta ltgD$ allele; $oriV_{ColE1}$ $oriV_{R6K_{\gamma}}$ $oriT_{RP4}$ CmR EmR	This study
pEVS79	$oriV_{\text{ColE1}}$ $oriT_{\text{RP4}}$ CmR	(252)
pEVS104	$oriV_{R6K_{\gamma}}$ $oriT_{RP4}$ KnR RP4-derived conjugal helper plasmid	(252)
pEVS118	$oriV_{ m R6K_{\gamma}}$ $oriT_{ m RP4}$ CmR	(68)
pEVS122	$oriV_{ m R6K_{\gamma}}$ $oriT_{ m RP4}$ EmR $lacZlpha$	(68)
pJLB103	pVSV104 BamHI-digested and self-ligated; $oriV_{R6K_{\gamma}}$ KnR $lacZ\alpha$	This study
pVSV102	oriV _{R6Ky} oriT _{RP4} oriV _{pES213} KnR gfp	(69)
pVSV104	$oriV_{R6Ky}$ $oriT_{RP4}$ $oriV_{pES213}$ KnR $lacZ\alpha$	(69)
<u>Oligonucleotides</u>	1 2	` /
dma30	5' GCC <u>AGATCT</u> GTCATTGGTTGGTGGACAGGCTAT 3'	This study
dma31	5' CGG <u>AGATCT</u> CCCAGCCGATCAGTTTAGAGTA 3'	This study
dma52	5' CTTCATGGCTCAAGGTGGTGGTTT 3'	This study
dma53	5' GGCCTCCTAGATTAGGAGGCTTTG 3'	This study
dma54	5' GGTTGTGGCAATGGAGTACTCAGTG 3'	This study
dma55	5' TTCTGGGTTCCAATCGACACTTGG 3'	This study
dma56	5' CCG <u>CCCGGG</u> CATGAAACGCTCCTTGTTATTTGTTC 3'	This study
dma57	5' GCC <u>CCCGGG</u> TAAGTTCTTATACGTAACAACTGTGCTAC 3'	This study
dma58	5' GGC <u>AGATCT</u> GGGCTGAAGCTGGGAAACTCAGTGATGATT 3'	This study
dma59	5' CGG <u>AGATCT</u> TGCACGAATAGCAACACGAATTCGGCG 3'	This study
dma60	5' CGG <u>AGATCT</u> CGTCAGCCTGAAAAGTTTACCGTGG 3'	This study
dma61	5' CGG <u>AGATCT</u> CCGCACTCTTGGCTTGATTCTCTTT 3'	This study
dma62	5' GGC <u>AGATCT</u> CGAATTGGTGAAGAGTATGGCGTTCAAC 3'	This study
dma63	5' CGG <u>AGATCT</u> CCTAGCTCTTGCCATTGTGCTAACG 3'	This study
dma76	5' GGC <u>AGATCT</u> CCTTAGAATCAACGGTAAGTACGCTAGAGTC 3'	This study
dma77	5' CCG <u>AGATCT</u> GCTCAACTTGTTGTTGTTGCTG 3'	This study
dma78	5' GCCGGATCCGCAACAACCGCAGCCTTAGATTACATG 3'	This study
dma79	5' GCC <u>GGATCC</u> GCAATGGCAAGATCTAACTGCTGCTT 3'	This study
dma95	5' GCGTCTTTCAATCATTAGGCTACT 3'	This study
dma96	5' CCGCGAAACCTGTTCGA 3'	This study
dma99	5' CGG <u>CCCGGG</u> CATTGATTTCTTTAACACCTAAACTTTCCAA 3'	This study

dma100	5' GCC <u>CCCGGG</u> TGATAAGTTTAAATTCTAATAGCAATTGGTATTAAGC 3'	This study
dma102	5' GGCAAGAATATGACCAGCGTCGTTTTG 3'	This study
dma105	5' CGG <u>CCCGGG</u> CATATAATTAATTCTCTTCTCTTGCTGCTTTATCT 3'	This study
dma106	5' CGC <u>CCCGGG</u> TAACAGAGCAGGGTTCAGATCGCTTC 3'	This study
dma115	5' TGGCTTTTTCTGTGGTCTAAAAAA 3'	This study

^a Abbreviations used: CmR, chloramphenicol resistance; EmR, erythromycin resistance; KnR, kanamycin resistance; StrR, streptomycin resistance; Kb, kilobase.

gene was replaced by a 6-bp restriction enzyme recognition site. These in-frame deletion mutations were placed in ES114 or in mutant backgrounds by allelic exchange. All mutants were confirmed by PCR. Constructs were generated in *E. coli* and transferred to *V. fischeri* by triparental mating using pEVS104 as a conjugative helper plasmid (252).

Bioinformatic analyses. Protein sequence comparisons to Genbank entries were generated using BLAST-P (4) and the BLOSUM62 scoring matrix (116). Genomes with similar regions surrounding the lytic transglycosylase ORFs were found using the SEED pinned region search (196). To assess genetic context within the *Vibrionaceae* family, we compared local gene arrangement in *V. fischeri* ES114 (226) to that in the genomes of *V. alginolyticus* 12G01, *V. angustum* S14, *V. campbellii* AND4, *V. cholerae* O1 biovar eltor str. N16961 (112), *V. harveyi* ATCC BAA-1116, *V. parahaemolyticus* RIMD 2210633 (163), *V. vulnificus* CMCP6 (39), and *Photobacterium profundum* SS9 (281). Sequence alignments were performed with MEGA 4.0 using the default settings (260). The similarity and identity between homologs that is reported was determined with MatGAT using the default settings (33).

PG monomer detection and quantification. Culture supernatants were subject to solid phase extraction and reverse-phase HPLC as described previously (52). Briefly, cultures were grown

^b Underlined sequences indicate restriction enzyme recognition sites added to primers (BgIII; A/GATCT, BamHI; G/GATCC or SmaI; CCC/GGG).

in minimal medium supplemented with 30 mM glucose at 24°C until reaching an OD_{595} of ~ 0.8-1.0 (mid- to late-log growth). Cultures were centrifuged in either 15-ml Falcon tubes (two spins at 4,500 x g for 10 min each at 4°C) or sequential spins in a 250-ml centrifuge bottle at 4,500 x g and then in a 30-ml centrifuge bottle at 8,500 x g, each for 10 min at 4°C, to pellet cells. Culture supernatants were adjusted to 1% trifluoracetic acid (TFA) with 100% TFA and filtered through a 0.22 µm mixed cellulose membrane filter units (Fisher Scientific, Hanover Park, IL). Samples were desalted using a C₁₈ Plus Sep-Pak cartridge (Waters Corporation, Milford, MA) that was prepared prior to receiving the sample with 100% methanol and two washes with 0.1% TFA in water. Samples were then loaded and allowed to flow by gravity through the column. After complete loading, the column was washed twice with 10 ml of 0.1% TFA in water. Materials retained in the column were eluted with 4-ml of 100% methanol and concentrated to dryness under a vacuum with a SpeedVac Plus (ThermoSavant, Holbrook, NY). 200 µl of drying reagent (2 H_2O : 2 MeOH: 1 triethylamine acetate (TEA)) was added to the dried C_{18} fraction, vortexed, and dried under vacuum in a SpedVac Plus. 30 µl of phenylisothiocyanate (PITC) (Pierce, Rockford, IL) reagent (10% H₂O, 75% methanol, 10% TEA and 5% PITC) was added to derivitize each sample, and the samples were then dried.

Reversed-phase HPLC was employed to separate the PITC-derivitized PG monomers from the extract. Buffer A consisted of 150 mM sodium acetate and 0.05% TEA brought to pH 6.35 with glacial acetic acid, and Buffer B consisted of a 60:40 mix of acetonitrile and water. Samples were resuspended in a 92:8 solution of Buffer A:Buffer B such that it was 100-fold more concentrated than culture supernatant. Each sample was vortexed, and 200 µl was injected into the HPLC. A Brownlee Spheri-5, RP-8 C8 4.6 x 220 mm column with a 4.6 x 30 mm guard column of the same matrix was used for all chromatographic separations (Perkin Elmer,

Waltham, MA). Column temperature was maintained at 35°C with a flow rate of 1 ml/min. The gradient (Buffer A: Buffer B) was as follows: 0 min 92:8, 13 min 65:35, 15 min 0:100, 35 min 0:100, 36 min 92:8 with reinjection at 45 min. Absorption at 254 nm was detected using a Spetraflow 757 variable- λ UV detector. Peak areas and retention times were recorded using Dynamic MacIntegration, version 1.4.1 and version 1.4.3 software. PG monomer retention time was approximately 13.2 minutes. A PG monomer standard (*B. pertussis* TCT) was also PITC-derivitized and run to compute pmoles of PG monomer in each sample based on comparisons of peak areas. For experiments assessing PG monomer released by mutant strains, PG monomer release from wild type *V. fischeri* ES114 and *E. coli* MG1655 were run as controls. Over 14 different experiments, *V. fischeri* ES114 samples averaged 21.2 \pm 3.9 (standard error) nM PG monomer per OD₅₉₅. As a negative control, *E. coli* MG1655 was included in six experiments and averaged 2.9 \pm 1.6 (standard error) nM PG monomer per OD₅₉₅ with PG monomer below the limit of detection (~1.5 nM per OD₅₉₅) in three of these experiments.

Luminescence and motility assays. Motility and luminescence were assessed as described previously (2). Luminescence of cells cultured in SWTO (23) at 24°C was determined using a TD 20/20 Luminometer (Turner Designs, Sunnyvale, CA). For motility assays, cultures were grown to mid-log phase (OD₅₉₅ 0.5) at 24°C, 5 μl of the culture was spotted onto a quadrant of an SWT soft (0.25%) agar plate and diameter measurements of the movement away from the point of inoculation were taken every hour. For each spot, a slope estimate was obtained from a simple linear regression of diameter versus time to quantify the velocity of spread, defined as the motility rate.

Squid colonization assays. For infection with individual *V. fischeri* strains, *E. scolopes* juveniles were inoculated within 4 h of hatching as previously described (223). *E. scolopes* were maintained in Instant Ocean (Aquarium Systems, Mentor, OH) mixed to ~36 ppt, and cultures for inoculation were grown as previously described (69). Hatchlings were exposed to inocula for up to 14 h before being rinsed in *V. fischeri*-free Instant Ocean. To study infection kinetics, hatchlings were placed in 5 ml of inoculant in 20-ml glass vials and luminescence was monitored using a LS6500 scintillation counter (Beckman Coulter, Fullerton, CA). To determine whether a mutant had a competitive disadvantage in the symbiosis relative to wild type, animals were exposed to a ~1:1 mix of the wild-type and mutant strains for 14 h and then moved to *V. fischeri*-free Instant Ocean. Individiual squid were homogenized and plated after 48 or 96 h, and 50 colonies were patched on to LBS Em to determine the ratio of mutant to wild type. The relative competitive index (RCI) was determined by dividing the mutant to wild type ratio in each individual squid by the ratio in the inoculum. Log transformed data were used to calculate the average RCI and to determine statistical significance.

Assessment of how effectively juvenile squids colonized with one strain could be secondarily infected with another strain was performed as previously described (149, 297). Newly hatched animals were infected with wild type or DMA388 as described above. At 72 h post-infection, approximately 2.5 x 10⁴ CFU/ml of the secondary inoculant AKD200 (mini-Tn7 CmR) was added for 14 h. 120 h after the initial inoculation began, animals were homogenized and plated on LBS to determine total CFU and on LBS-Cm to estimate the proportion of symbionts from the secondary infection. Mini-Tn7 CmR inserts at a single intergenic *att* site in *V. fischeri*, and this does not affect colonization competitiveness (168), making AKD200 an appropriate marked strain for this purpose.

Squid morphogenesis assays. Animals were infected with strains as described above. At certain times after inoculation, infected and aposymbiotic animals were stained with both Cell Tracker Orange and Tubulin Tracker Green (Invitrogen, Carlsbad, CA) for approximately 1 h. After staining, animals were anesthetized by adding an equal volume of 0.37 M MgCl₂ and dissected to expose the light organ on the ventral side. Stage of regression was determined by fluorescence microscopy using a Nikon (Melville, NY) Eclipse E600 microscope and a 51004 V2 FITC/TRITC dual label filter set (Chroma Technology Corp, Rockingham, VT). Regression stage (stages 1-4) was scored blind, as set forth by Doino et al. (64).

Results

Bioinformatic analysis of PG synthesis and recycling in *V. fischeri*. Before the 921 Da PG monomer known as TCT (53, 221) or PGCT (220, 242) can be released from Gram-negative bacteria, it must first be generated intracellularly, and this occurs even in bacteria such as *E. coli* that do not shed PG monomers. Based on our understanding of *E. coli*, this PG monomer apparently is not generated during *de novo* PG synthesis but rather is produced during PG remodeling and consumed by recycling pathways (198). To examine whether *de novo* PG synthesis or PG recycling might be substantively different in *V. fischeri*, we examined its genome and found homologs of the *E. coli* PG synthesis and recycling pathways (Table 3.2). Only minor deviations from the *E. coli* PG processing systems were evident. *V. fischeri* possesses only one homolog (AmiB) of the four amidases that may process PG monomer in the periplasm of *E. coli* (113, 273), but it seems reasonable that one such amidase might be insufficient. *V. fischeri* also lacks a clear homolog of LdcA, an L,D-carboxypeptidase found in

the *E. coli* PG monomer recycling pathway (262); however, it does appear to encode distinct peptidases not found in *E. coli*, including a putative PG-targeting peptidase (encoded by ORF VF2017). Moreover, all of the functions downstream of LdcA in the recycling pathway appear intact. Based on these results, we speculated that *V. fischeri*'s net release of PG monomer might parallel either the poor *ampG* expression of *B. pertussis* or the high activity of lytic transglycosylases of *N. gonorrhoeae*, and we investigated these possibilities further.

Table 3.2. PG biosynthesis and recycling protein homologs in *V. fischeri*

Protein in E. coli	Function	ORF in V. fischeri
Biosynthesis		
MurA	UDP- <i>N</i> -acetylglucosamine enolpyruvyl transferase	VF0401
MurB	UDP- <i>N</i> -acetylenolpyruvylglucosamine reductase	VF2426
MurC	L-alanine ligase	VF2200
MurD	D-glutamic acid ligase	VF2203
MurE	meso-diaminopimelic acid ligase	VF2205
MurF	D-alanyl-D-alanine ligase	VF2206
MurG	glycosyltransferase	VF2201
MraY	undecaprenyl-phosphate phospho-N-acetylmuramoyl-	VF2204
	pentapeptide transferase/translocase	
Bactroprenol/UppS	undecaprenyl phosphate (C ₅₅ -P)	VF2245
Periplasmic Incorp	oration and Cleavage	
PBP1A	transpeptidase/transglycosylase	VF2298
PBP1B	transpeptidase/transglycosylase	VF2162
PBP1C	unknown	ND^a
PBP2	transpeptidase/elongase	VF0747
PBP3	transeptidase	VF2207
PBP4	endopeptidase	VF0474
PBP5	carboxypeptidase	VF0745
PBP6	carboxypeptidase	VF0724
PBP7	endopeptidase	ND^a
MepA	endopeptidase	ND ^a
MipA	scaffolding protein for murein synthesis	VF1632
AmiA	<i>N</i> -acetylmuramyl-L-alanine amidase	ND^a
AmiB	<i>N</i> -acetylmuramyl-L-alanine amidase	VF2326
AmiC	<i>N</i> -acetylmuramyl-L-alanine amidase	ND ^a
AmiD	N-acetylmuramyl-L-alanine amidase	ND ^a

Slt70/SltY	Soluble lytic murein transglycosylase	VF0558 ^b
		VF1329 ^c
MltA	membrane-bound lytic murein transglycosylase	VF0587
MltB	membrane-bound lytic murein transglycosyalse	VF1702 ^d
MltC	membrane-bound lytic murein transglycosylase	VF0419/420
		VF1368
MltD	membrane-bound lytic murein transglycosylase	VF1939 ^e
EmtA	lytic murein endotransglycosylase	ND ^a
YfhD	periplasmic binding protein/transglycosylase	VF0651
AtlA	N-acetylglucosamindase	ND ^a
Recycling		
AmpG	muropeptide permease	VF0720
Opp	oligopeptide permease	VF681-VF677
MppA	Murein tripeptide permease	VF1597
LdcA	L,D-carboxypeptidase	ND ^a
AmpD	N-acetylmuramyl-L-alanine amidase cytoplasmic	VF2183
NagA	GlcNAc-6-P deacetylase	VF0807
NagK	N-acetylglucosamine kinase	VF1408
NagZ	beta-N-acetylglucosaminidase	VFA0493
AnmK	anhydromuramic acid kinase	VFA0492
MurQ	<i>N</i> -acetylmuramic acid-6-phosphate etherase	VF1114
GlmM	phosphoglucosamine mutase	VF0481
GlmU	N-acetylglucosamine-1-PO ₄ uridyltransferase	VF2562
Mpl	UDP-N-acetylmuramate: L-alanyl-γ-D-glutamyl-	VF0265
_	meso-diaminopimelate ligase	

a ND indicates not detected; no significant homolog ($e > 1^{-10}$)

Analysis of AmpG in V. fischeri. The single AmpG homolog found in BLAST searches of the V. fischeri genome is encoded by ORF VF0720, which shares 26% identity and 49% similarity to E. coli AmpG. The V. fischeri AmpG amino acid sequence is shorter than that of E. coli at the C-terminus by 73 amino acids; however, N. gonorrhoeae AmpG is similarly shorter than E. coli AmpG by 77 amino acids, yet it has demonstrated functionality (79).

b Now designated *ltgA1* Now designated *ltgA2* d Now designated *ltgD*

^e Now designated *lysM1*

Mutation of ampG increases the net release of PG monomers. To test the functionality of V. fischeri AmpG in PG monomer recycling, we analyzed the amount of PG monomer released into the supernatant during log-phase growth of DMA350 (ampG::pDMA48) in comparison to that of the wild type using a HPLC-based method for PG monomer detection (52, 141). We saw an increase in net PG monomer release from DMA350 (ampG::pDMA48) of approximately 39-fold (data not shown). Next, we generated an in-frame deletion mutant of ampG, and found that DMA352 (ΔampG) had more than a 100-fold increase in net PG monomer release (Fig. 3.1). This phenotype could be complemented by the introduction of ampG on a stable plasmid (pDMA115), decreasing the extracellular levels of PG monomer accumulation back to wild-type amounts (Fig. 3.1). We occasionally saw a decrease in the amount of net PG monomer release when ampG was added in multicopy in trans to ES114; however, this result was not consistent from experiment to experiment, and in Figure 3.1 this apparent slight effect is not statistically significant (p>0.05). These data suggest that V. fischeri AmpG is functional, and unlike B. pertussis, lack of AmpG is probably not responsible for the extracellular accumulation of PG monomers in cultures of *V. fischeri*.

Analysis of lytic transglycosylases in *V. fischeri*. In *N. gonorrhoeae* the activity of lytic transglycosylases is responsible for the large amounts of PG monomer accumulated in culture supernatants. Therefore, we examined whether *V. fischeri* had homologs to the *N. gonorrhoeae* lytic transglycosylases, LtgA and LtgD, which are important for release of PG monomers during log-phase growth in *N. gonorrhoeae* (48, 49). Two homologs were found in *V. fischeri* to *N. gonorrhoeae* LtgA sequence, and these are encoded by VF0558 and VF1329 (Table 3.2). VF0558, now termed *ltgA1*, is well conserved in sequence and genetic context within the family

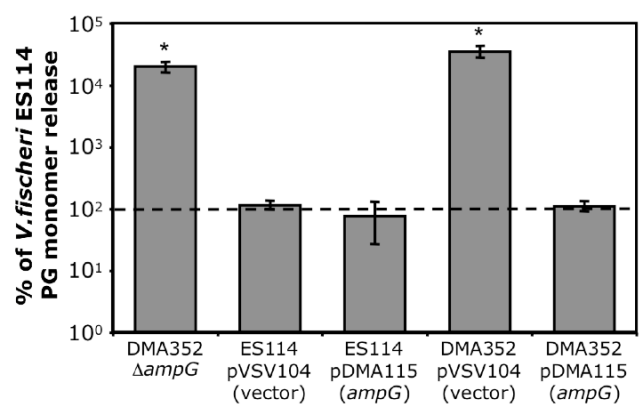


Figure 3.1. Mutation in V. fischeri ampG increases PG monomer release in log-phase cultures. PG monomer was measured in culture supernatants of ES114 (wild type) and DMA352 ($\Delta ampG$) along with both strains containing plasmids pVSV104 (control vector) and pDMA115 (ampG in pVSV104) grown in minimal media. To account for experiment to experiment variations, within each experiment each strain's calculated PG monomer release was expressed as a percent of ES114 (wild type) PG monomer release. Values shown are the averages of three different experiments. Dotted line represents ES114 PG monomer release, defined as 100% which averaged 20.4 nM per OD₅₉₅. Error bars are standard error. "*" indicates a significant difference (p<0.05) relative to ES114 as determined by a Student's T-test.

Vibrionaceae, and the predicted amino acid sequence for V. fischeri LtgA1 has 24% identity and 43% similarity to the N. gonorrhoeae LtgA. VF1329, termed ltgA2, is related to ltgA1 but was absent from the other members of the Vibrionaceae family that we examined. The predicted amino acid sequence of LtgA2 shares 34% identity and 55% similarity with LtgA1 and 24% identity and 42% similarity with N. gonorrhoeae LtgA. Only one homolog in V. fischeri was found to N. gonorrhoeae LtgD, and this is encoded by VF1702. This gene, now termed ltgD, has a conserved upstream genetic context within the Vibrionaceae family; however, the downstream genetic context is different. The predicted amino acid sequence of the V. fischeri LtgD had 30% identity and 48% similarity to the N. gonorrhoeae LtgD.

We also searched the ES114 genome for other genes potentially encoding lytic transglycosylases. Two ORFs, VF1939 and VF1247, were found to encode LysM domains that

are important in general peptidoglycan binding and have potential to be peptidoglycan hydrolases (32), and these ORFs were named *lysM1* and *lysM2*, respectively.

Mutations in lytic transglycosylase genes result in reduced release of PG monomers. To determine if any of these putative lytic transglycosylases were responsible for release of PG monomers by *V. fischeri*, we generated plasmid integration mutants yielding DMA360 (*ltgA1*::pDMA89), DMA361 (*ltgA2*::pDMA90), DMA362 (*ltgD*::pDMA91), DMA380 (*lysM1*::pDMA109) and DMA385 (*lysM2*::pDMA108). We then assayed the effects of the mutations on net PG monomer release as described above. DMA360 (*ltgA1*::pDMA89) had 3-fold less net PG monomer release than did the wild type (Fig. 3.2A). Similarly, DMA361 (*ltgA2*::pDMA90) and DMA362 (*ltgD*::pDMA91) each appeared to accumulate fewer PG monomers in culture supernatants than wild type, but these differences were not significant (p>0.05). Finally, both DMA380 (*lysM1*::pDMA109) and DMA385 (*lysM2*::pDMA108) appeared unaffected in net PG monomer release (Fig. 3.2A).

In *N. gonorrhoeae* multiple mutations in the lytic transglycosylase genes are necessary to drastically reduce the net amount of PG monomer released. To determine whether this might be the case in *V. fischeri*, we constructed in-frame deletions of ltgA1 and ltgD, resulting in DMA363 ($\Delta ltgA1$) and DMA368 ($\Delta ltgD$). These alleles were combined with the ltgA2::pDMA90 allele construct both in pairwise combinations and to generate a triple mutant. The $\Delta ltgA1$ allele combined with other mutations resulted in significantly less extracellular accumulation of PG monomer. This was true for DMA369 ($\Delta ltgA1$ $\Delta ltgD$), DMA386 ($\Delta ltgA1$ ltgA2::pDMA90), and DMA388 ($\Delta ltgA1$ $\Delta ltgD$ ltgA2::pDMA90), which has very low (2 ± 1 nM per OD₅₉₅) levels of PG monomer in culture supernatants (Fig. 3.2B). Strangely, extracellular PG monomer was not

decreased in DMA363 ($\Delta ltgA1$) to the same extent as the plasmid insertion mutant DMA360 (ltgA1::pDMA89) (Figure 3.2). This may be due to an effect of the ltgA1::pDMA89 allele on genes surrounding ltgA1, or it could indicate that the truncated LtgA1 encoded by DMA360 (ltgA1::pDMA89) inhibits the activity of other lytic transglycosylases. Alternatively, the apparent difference between DMA363 ($\Delta ltgA1$) and DMA360 (ltgA1::pDMA89) may to some extent reflect experiment to experiment variability in our HPLC assay and the relatively low values for wild type PG monomer in Figure 3.2B.

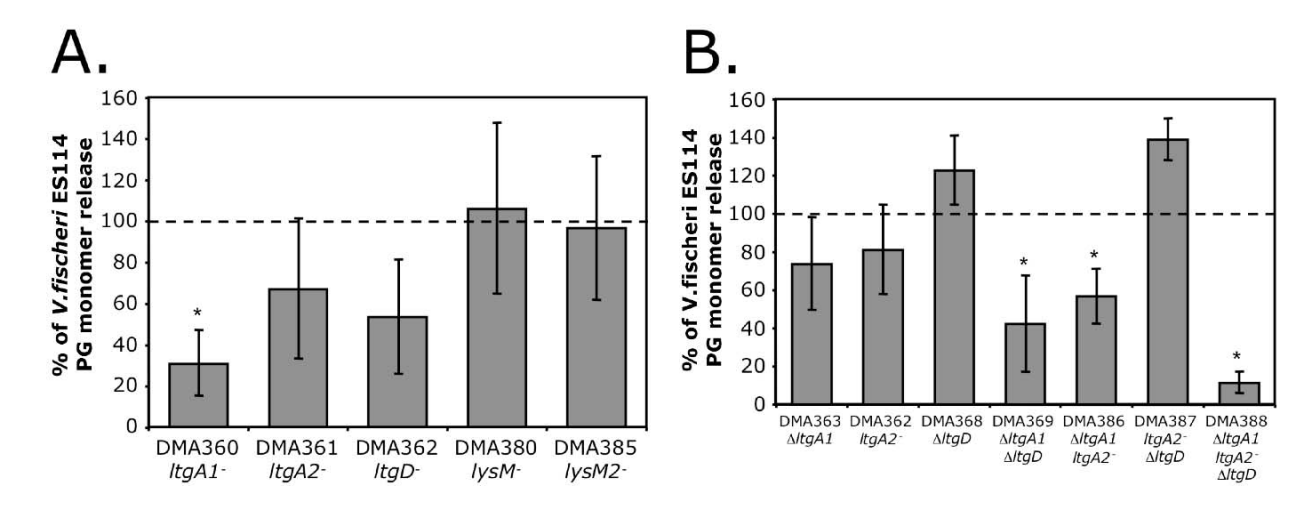


Figure 3.2. Mutations in V. fischeri lytic transglycosylases result in a decrease in PG monomer release in log-phase cultures. Strains in both panels were grown in minimal media and analyzed for PG monomer release. Values shown are the averages of three different experiments. Dotted line represents ES114 PG monomer release, defined as 100%. Error bars are standard error. "*" indicates a significant difference (p<0.05) relative to ES114 as determined by a Student's T-test. Panel A. Plasmid-insertion mutants with disruptions in ltgA1, ltgA2, ltgD, lysM1, and lysM2. Wild type averaged 28 nM per OD₅₉₅. Panel B. Comparison of mutants with combinations of in-frame deletion mutations $\Delta ltgA1$ and $\Delta ltgD$, and a plasmid-insertion mutation in ltgA2. Wild type for this experiment averaged 14 nM per OD₅₉₅.

Growth, motility, and luminescence of *ampG* and lytic transglycosylase mutants. Mutations affecting recycling and remodeling of PG could affect cell division, growth, motility and even metabolism. However, all mutants had wild-type-like growth, cell morphology, and bioluminescence (data not shown) indicating that these are not generally attenuated strains.

Mutants also had at least 80% to 99% motility relative to wild type (data not shown), and a previous study found that these swimming rates are sufficient to confer full symbiotic competence (2).

Symbiotic competence of DMA352 ($\Delta ampG$) and DMA388 ($\Delta ltgA1 \Delta ltgD ltgA2::pDMA90$). One of our goals was to examine the effect of altered extracellular PG monomer accumulation on symbiotic colonization. We therefore examined the symbiotic competence of the mutants with the greatest deviations in net PG monomer release; DMA352 ($\Delta ampG$) and DMA388 ($\Delta ltgA1 \Delta ltgD ltgA2::pDMA90$). In single-strain infections of squid, neither DMA352 nor DMA388 showed a difference from wild type (data not shown). Competition experiments have been used previously as a measure of relative symbiotic proficiency, revealing colonization defects not apparent in single-strain inoculations (23, 125, 149, 157, 159, 179, 195, 251, 282, 284, 298, 306). However, there was no apparent competitive defect 48 h or 96 h post inoculation when either DMA352 ($\Delta ampG$) or DMA388 ($\Delta ltgA1 \Delta ltgD ltgA2::pDMA90$) was co-inoculated with wild type (data not shown).

Mutant effects on host light-organ morphogenesis. Because PG monomers act as a morphogen triggering regression of the ciliated appendages on the light organ (141), we were interested to see if mutations affecting the net amount of PG monomer released would alter this morphogenesis. Animals inoculated with DMA352 ($\Delta ampG$) and stained at 24 h intervals up to 120 h showed ciliated appendage regression similar to that in animals infected with the wild type. Thus the ~100-fold increase in net PG monomer release by the ampG mutant in culture did not appear to correlate with a more rapid rate of ciliated appendage regression.

We next examined whether the *ampG* mutation could trigger morphogenesis in a strain that could not colonize the light-organ crypts. Nonmotile *V. fischeri* strains do not enter the light organ crypts and do not induce regression (64), although they are able to induce mucus production from the ciliated fields and can form aggregates outside the pores of the light organ (195). We therefore tested whether a non-motile strain generating large amounts of extracellular PG monomer might be able to induce regression without colonizing the light-organ crypts, by constructing a *flaJ ampG* double mutant. We then compared morphogenesis in animals infected by wild type, DM131 (*flaJ::aph*), and DMA354 (Δ*ampG flaJ::aph*). To ensure that the non-motile *flaJ* mutants did not infect the light-organ crypts, each of the three strains used was labeled with the stable *gfp*-expressing plasmid pVSV102 (69), and epifluorescence microscopy confirmed that only wild-type cells could be visualized colonizing the crypts.

At 72 and 96 h post-inoculation, wild-type-infected animals all displayed regression of the ciliated epithelial appendages while animals infected with DM131 (*flaJ*::KnR) displayed no regression, consistent with previous reports comparing wild type to non-motile mutants (101, 178). However, approximately 40% of animals inoculated with DMA354 (Δ*ampG flaJ*::*aph*) showed some level of regression (Fig. 3.3) even though the *flaJ* mutation blocked invasion of the light-organ crypts. We considered the possibility that PG monomer already present in the inoculum might be inducing regression, as Koropatnick et al. observed with as little as 10 nM purified PG monomer (141); however, assuming PG monomer release is similar under the growth conditions used to prepare inocula as it was in minimal media, then carryover of PG monomer from the inoculum should have resulted in animals being exposed to only ~10 pM PG monomer in these experiments. Moreover, similar results were obtained when DMA354 (Δ*ampG flaJ*::*aph*) cells were washed in Instant Ocean before exposing them to hatchlings. This

suggests that the regression induced by DMA354 (Δ*ampG flaJ*::*aph*) is due to bacteria aggregating and shedding high levels of PG monomer *in situ*, on the light organ.

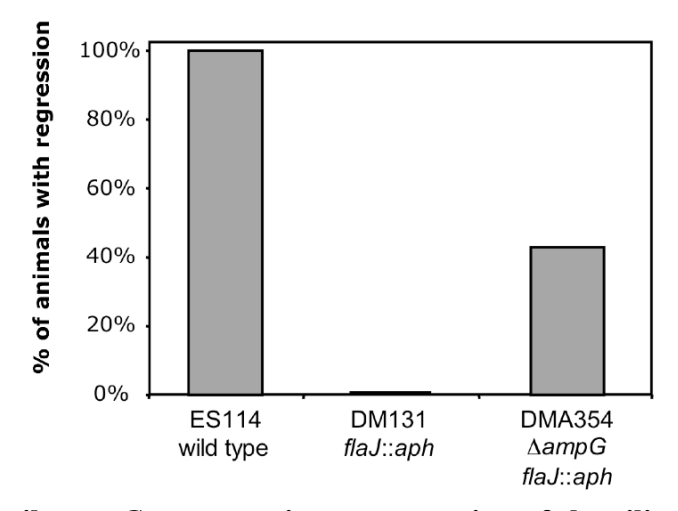


Figure 3.3. A non-motile *ampG* **mutant triggers regression of the ciliated appendages of the light organ.** Freshly hatched juvenile animals were inoculated with ~2500 CFU/ml of either ES114 (wild type), DM131 (*flaJ*::*aph*) or DMA354 (Δ*ampG flaJ*::*aph*), each of which were labeled with the *gfp*-expressing plasmid pVSV102 to confirm that the non-motile *flaJ* mutants did not infect the light-organ crypts. Animals were stained at 72 or 96 h post-inoculation and scored for regression using the stages 1-4 by Doino et al. (64). Animals infected with DM131 (*flaJ*::*aph*) had 0% of the animals with any regression of the ciliated appendages of the light organ.

Our next goal was to see if the low amount of net PG monomer release by the lytic transglycosylase mutant DMA388 ($\Delta ltgA1 \ \Delta ltgD \ ltgA2$::pDMA90) would reduce the stimulation of morphogenesis. It did appear that there was less regression of the ciliated appendages in animals infected with DMA388 ($\Delta ltgA1 \ \Delta ltgD \ ltgA2$::pDMA90), relative to animals infected with the wild type; however, using the semi-quantitative scoring of regression stages 1-4 defined previously (64), we did not see a consistent and statistically significant difference in these treatments. We also observed what appeared to be more dense and active fields of cilia on the appendages of DMA388-infected animals, but again we were unable to quantify and adequately test this supposition. We therefore sought another way to measure status of the ciliated appendages. We surmised that if some animals retain their infection-promoting ciliated

appendages longer, these animals might be more susceptible to a secondary infection with another bacterial strain presented well after initial infection. To address this experimentally, animals were inoculated following hatching with either the wild-type strain or DMA388 ($\Delta ltgA1$ $\Delta ltgD$ ltgA2::pDMA90), and at 72 h post-inoculation of the primary strain, animals were exposed to a secondary inoculant strain, AKD200 (mini-Tn7 CmR). At 120 h post-primary inoculation and 48 h post-secondary inoculation, animals were homogenized and plated on LBS to assess total colonization and plated on LBS-Cm to enumerate bacteria from the secondary infection.

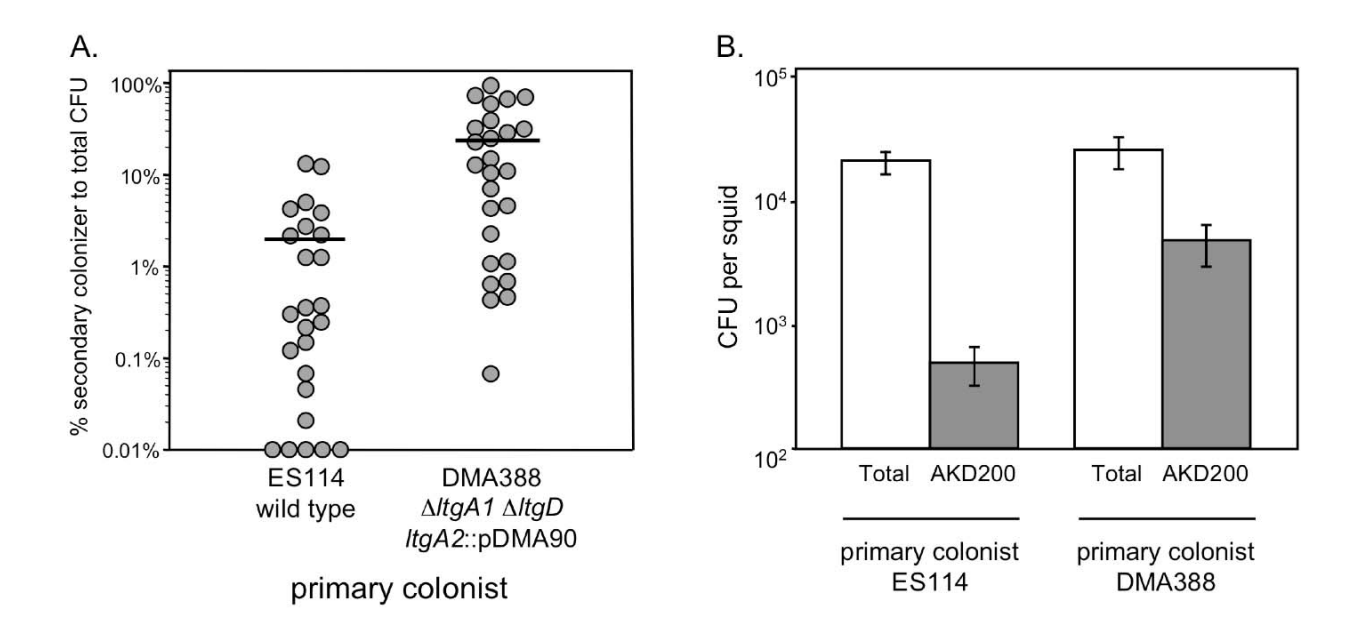


Figure 3.4. Animals infected with DMA388 (Δ*ltgA1* Δ*ltgD ltgA2*::pDMA90) are more susceptible to a secondary infection. Fresh hatchlings were inoculated with either ES114 or DMA388 (Δ*ltgA1* Δ*ltgD ltgA2*::pDMA90). After 72 h, animals were challenged with the secondary strain AKD200 (mini-Tn7 CmR). At 120 h, animals were homogenized and plated on LBS to determine total CFU and plated on LBS-Cm to enumerate the secondary colonizers. Values shown are the combined average of six independent experiments each of which yielded similar results (total n=25 for ES114 and n=26 for DMA388). Panel A. Percent of total infection comprised by the secondary colonist, AKD200. Each circle represents a single squid. Horizontal lines show the average of all animals within each treatment (2% in ES114-infected animals, and 24% in DMA388-infected animals). Panel B. Average of both total CFU (open bars) and CFU from secondary infection by AKD200 (shaded bars). Error bars are standard error. Secondary infection by AKD200 in DMA388-infected animals was significantly greater (p<0.01) than in ES114-infected animals as determined by a Student's T-test.

DMA388-infected animals had 10-fold more bacteria from the secondary AKD200 infection than did wild-type-infected animals (Fig. 3.4). Thus, DMA388-infected animals are more prone to secondary infection, consistent with our perception that the infection-promoting ciliated appendages were more intact in these animals.

Discussion

A specific 921 Da component of Gram-negative PG referred to here as PG monomer (and elsewhere as TCT or PGCT) is usually recycled by bacterial cells, but in instances where PG monomer is released it elicits dramatic effects on host epithelial tissues. When released by the pathogens *B. pertussis* or *N. gonorrhoeae*, PG monomer causes severe cytopathology in ciliated human epithelial cells (52, 175), but PG monomer is also released by the mutualistic symbiont *V. fischeri*, and purified PG monomer triggers the regression of ciliated epithelial appendages of the symbiotic light organ reminiscent of the normal developmental program induced in the symbiosis (141). In this study we generated mutants of *V. fischeri* that displayed either increased or decreased extracellular accumulation of PG monomer, providing insight into the basis for PG monomer shedding in this bacterium and the role of PG monomers in this model symbiotic infection.

We first examined the genetic determinants of PG monomer release in *V. fischeri*. In contrast to *B. pertussis*, where extracellular PG monomer accumulation is thought to be a result of poor *ampG* expression (160), *V. fischeri* AmpG functioned well in reducing net PG monomer release, as illustrated by the 100-fold increase in PG accumulated in the medium of an *ampG* mutant, and by the observation that overexpressing *ampG* from *V. fischeri* or *E. coli* did little to lessen PG monomer release (Fig. 3.1 and data not shown, respectively). *V. fischeri* apparently

also has a complete recycling pathway (Table 3.2) suggesting that *V. fischeri* recycles PG monomers like other Gram-negative bacteria. Apparently, the basis for *V. fischeri*'s extracellular accumulation of PG monomers is more similar to *N. gonorrhoeae* where the deletion of two lytic transglycosylases results in the reduced net release of PG monomers (48). In *V. fischeri*, mutation of multiple lytic transglycosylases similar to those in *N. gonorrhoeae* also reduced net PG monomer release (Fig. 3.2B).

The generation of mutants with more or less extracellular accumulation of PG monomer than wild type enabled us to evaluate the importance of this molecule in vivo during symbiotic infection. When squid were inoculated with DMA352 (ΔampG), which accumulates 100-fold more PG monomers in culture supernatants than wild type (Fig. 3.1), we did not see a faster progression of light-organ morphogenesis (data not shown). This is consistent with the idea that PG monomer elicits effects on the host as a triggering signal molecule, and that the wild type sheds sufficient PG monomer to trigger these effects. Interestingly, we did show that a flaJ ampG double mutant was able to induce regression of the ciliated light-organ appendages (Fig. 3.3), unlike the *flaJ* and other non-motile mutants. Non-motile mutants will aggregate around the light-organ pores, but are unable to colonize the light organ crypt spaces (101, 195). The inability of these mutants to stimulate morphogenesis has suggested a requirement for crypt infection in signal transduction (64), although it was subsequently shown that purified PG monomer added to seawater can stimulate morphogenesis (141). The flaJ ampG double mutant demonstrates that crypt infection is not necessary for PG-mediated signaling, and this strain should be a useful tool for separating PG monomer-mediated signaling from signaling that truly requires infection of the crypts. In the future, it also will be interesting to compare the effects of this mutant to the effects of purified PG-monomer, to explore possible PG-independent signaling factors that may be perceived by the host on the light-organ surfaces.

We also investigated DMA388 ($\Delta ltgA1 \Delta ltgD ltgA2$::pDMA90), which accumulates only low levels of PG monomer in culture (Fig. 3.2). We hypothesized that this strain would have reduced regression of the ciliated light-organ appendages; however, it still induced regression of the ciliated appendages. A reason for this could be that another lytic transglycosylase is induced only in the symbiosis, supplying a mechanism for PG monomer release that is not evident in culture. By creating *gfp*-based transcriptional reporters of each of the lytic transglycosylase genes listed in Table 3.2, we may be able to determine if any of the genes are transcriptionally activated within the squid. It is also possible that a small amount of PG monomer released by this strain is sufficient to stimulate morphogenesis or that other PG fragments could have an effect on regression besides the 921 Da fragment. A reduced version of the PG monomer is also released by *V. fischeri* (data not shown), and this or other PG fragments might have important morphogenic activity.

Despite the morphogenesis induced by DMA388 ($\Delta ltgA1 \Delta ltgD ltgA2$::pDMA90), we did perceive a subtle attenuation of this strain's ability to stimulate regression of the host's light organ ciliated appendages. A more dramatic or at least more easily quantifiable effect was evident in the greater susceptibility of DMA388-infected animals to a secondary V. fischeri colonist after regression of the infection-promoting ciliated appendages had begun (Fig. 3.4). This suggests that even an apparently small difference in the regression of the ciliated appendages may have large functional significance with regard to preventing or allowing further infection by environmental bacteria. In the future it will be interesting to more closely examine

the effects of DMA388 on specific infection-promoting characteristics of the ciliated appendages, such as water movement and mucus secretion.

The dramatic regression of the infection-promoting ciliated appendages on the E. scolopes light organ following successful infection with V. fischeri symbionts can be easily rationalized as an advantage for the host. This morphogenesis effectively deters further infection, and if these infection-promoting structures carry any risk of promoting detrimental pathogenic infections, then the risks associated with these structures may outweigh the advantages once mutualistic symbionts are obtained. Our results illustrate how V. fischeri may also have an evolutionary impetus for shedding PG monomers. By stimulating morphogenesis, PG monomers help V. fischeri to essentially close the door behind them after initial infection. A secondary infection with another strain would create competition within the light organ potentially causing the initial colonizer to lose some of the fitness advantage of colonizing the light organ. Initiating the regression of the ciliated epithelial appendages therefore enhances the initial colonizer's ability to maintain dominance in the light organ. Further use of secondaryinfection challenge assays should be valuable in the future. Mutants that lack the ability to prevent secondary infections could reveal genes important for stimulating regression of the ciliated appendages that may not be found using other screens.

Acknowledgements

We thank Josh Troll, Melissa Altura, and Amy Schaeffer for helpful discussions, Joseph Dillard for sharing data on *ltgD* before publication, William Swinehart for technical assistance and Debbie Millikan, Edward Ruby, and Anne Dunn for providing strains. This work was supported

by NIH Grant A150661 to M. McFall-Ngai and by the National Science Foundation under Grant CAREER MCB-0347317 to E.V.S.

CHAPTER 4

IDENTIFICATION OF A CELLOBIOSE UTILIZATION GENE CLUSTER WITH CRYPTIC $\beta\text{-}GALACTOSIDASE\ ACTIVITY\ IN\ \textit{VIBRIO\ FISCHERI}\ ^3$

³ Adin, D.M., Visick, K. L., Stabb, E.V. 2008. *Applied and Environmental Microbiology*. 74: 4059-4069. Reprinted here with permission of publisher.

Abstract

Cellobiose utilization is a variable trait that is often used to differentiate members of the Vibrionaceae. We investigated how Vibrio fischeri ES114 utilizes cellobiose and found a cluster of genes required for growth on this β -1,4-linked glucose disaccharide. This cluster includes genes annotated as a phosphotransferase system II (celA, celB, and celC), a glucokinase (celK) and a glucosidase (celG). Directly downstream of celCBGKA is cell, which encodes a LacIfamily regulator that represses *cel* transcription in the absence of cellobiose. When transferred to cellobiose-negative strains of Vibrio and Photobacterium, the celCBGKAI gene cluster conferred the ability to utilize cellobiose. Genomic analyses of naturally cellobiose-positive Vibrio species revealed that V. salmonicida has a homolog of the celCBGKAI cluster; however, V. vulnificus does not. Moreover, bioinformatic analyses revealed that CelG and CelK share the greatest homology with glucosidases and glucokinases in the Firmicutes. These observations suggest that distinct genes for cellobiose utilization have been acquired by different lineages within the Vibrionaceae. In addition, the loss of the cell regulator, but not the structural genes, attenuated the ability of V. fischeri to compete for colonization of its natural host, Euprymna scolopes, suggesting that repression of the *cel* gene cluster is important in this symbiosis. Finally, we show that the *V. fischeri* cellobioase (CelG) preferentially cleaves β-D-glucose linkages but also cleaves β-D-galactose-linked substrates such as 5-bromo-4-chloro-3-indolyl-β-D-galactoside (Xgal), a finding that has important implications for the use of lacZ as a marker or reporter gene in V. fischeri.

Introduction

The *Vibrionaceae* family encompasses a diverse collection of marine bacteria that are studied both for their direct significance to humankind and as models for a variety of basic biological phenomena (248). For example, our research groups and others study *Vibrio fischeri* as a model of bacterial bioluminescence, symbiotic host-bacteria interactions, and pheromone-mediated gene regulation (7, 194, 247, 253, 286). Other *Vibrio* species are investigated because of their pathogenicity toward humans or marine animals, their contributions to aquatic ecosystems and processes, or their genomic plasticity and remarkable adaptability (67, 72, 263, 265). Although there are exceptions, a hallmark of this family is the ability to grow rapidly in culture and to use a variety of nutrient sources. There is considerable interspecies variability in metabolic patterns, and such differences may reflect ecologically important traits for individual species. Nutrient utilization profiles have also been important in practice both for developing taxonomic schemes to identify *Vibrio* species and for growing and manipulating these bacteria in the laboratory.

Traditionally, carbon source utilization patterns have been among the criteria used to distinguish different species within the *Vibrionaceae* (16, 72), and this information has also guided the development of semi-selective media to enrich for specific species (65). For example, cellobiose utilization is among the variable traits used to describe and distinguish species within the *Vibrionaceae* (16), and cellobiose-based media have been used to enrich for certain species, particularly *Vibrio vulnificus* (37, 165). Molecular markers and DNA sequence analyses are becoming more widespread taxonomic tools with great value, but carbon source utilization phenotypes are still useful discriminators and have been tested through decades of research (16, 72). In the future, once the genetic basis for utilization of particular carbon sources is better

understood, it should be possible to generate molecular DNA-based techniques that draw directly on the wealth of phenotypic information available for identifying *Vibrio* species.

Understanding the genetic basis for various metabolisms in different *Vibrio* species will also help elucidate the evolutionary history of the *Vibrionaceae*. Despite interest in both the metabolic variability of this family and the mechanisms underlying its evolution, much remains to be learned about these subjects. For example, it is not known whether cellobiose utilization was an ancestral trait lost by some members of this family, or if it was a trait acquired by certain lineages more recently. Bioinformatic analyses of genome sequences in the *Vibrionaceae* (39, 112, 163, 226, 238, 281) promise to help answer such questions, but gene and pathway annotations can be ambiguous or incorrect. Therefore, continued experimental determination of metabolic pathways will be necessary to connect genomic and phenotypic variability.

In this study we describe a gene cluster that is both necessary for cellobiose utilization by *V. fischeri* and sufficient to confer cellobiose utilization on other *Vibrio* species. Based on our results and bioinformatic analyses, we propose a model for cellobiose utilization arising from the acquisition of distinct pathways by different lineages within the *Vibrionaceae*. We also show that this cellobiose utilization cluster in *V. fischeri* is responsible for an unexpected cryptic β-galactosidase activity. This observation has immediate practical significance, because the β-galactosidase gene *lacZ* from *Escherichia coli* has been used as both a marker (69, 125) and a transcriptional reporter (158, 287, 306, 307) in *V. fischeri*.

Materials and Methods

Bacterial strains, plasmids and growth conditions. Bacterial strains used in this study are described in Table 4.1. Plasmids were maintained in $E.\ coli$ strain DH5 α (109) except conjugative helper plasmid pEVS104 (252), which was maintained in CC118 λpir (119), pCR

Blunt-TOPO-derivatives, which were maintained in TOP-10 (Invitrogen, Carlsbad, CA), and other plasmids containing the R6Ky replication origin, which were maintained in DH5 $\alpha\lambda pir$ (68). E. coli was incubated at 37°C in LB medium (176) or BHI medium (Difco, Sparks, MD). For selection of E. coli, chloramphenicol (Cm), kanamycin (Kn) and trimethoprin (Tp) were used at concentrations 20, 40, and 10 µg ml⁻¹, respectively. For selection of E. coli with erythromycin (Em), 150 µg ml⁻¹ was added to BHI. V. fischeri and all other Vibrionaceae strains were grown at 28°C in LBS (250) or using a specific carbon source, as indicated, added to a minimal salts medium (0.340 mM NaPO₄ pH 7.5, 0.05 M Tris pH 7.5, 0.3 M NaCl, 0.05 M MgSO₄-7H₂O, 0.01 M CaCl₂-2H₂O, 0.01 M NH₄Cl, 0.01 M KCl, 0.01 mM FeSO₄-7H₂O, plus carbon source). When added to LBS or minimal media for selection of V. fischeri or other Vibrionaceae strains, Cm, Kn, Em, and Tp were used at concentrations of 2, 100, 5, and 10 µg ml⁻¹ respectively. Dcellobiose (Acros Organics, Geel, Belgium) was added to solid and liquid media at concentrations of 5 mM and 10 mM, respectively. Glucose was added to media at a concentration of 20 mM. Bromocresol purple sodium salt (BCP) (Eastman Kodak, Rochester, NY) and 5-bromo-4-chloro-3-indolyl-β-D-galactoside (X-gal) (Research Products International, Prospect, IL) were added to LBS at concentrations of 0.02 and 100 µg ml⁻¹, respectively. Agar was added to a final concentration of 1.5% for solid media.

DNA and plasmid manipulations. Standard methods were used to generate plasmids and to clone DNA fragments. Plasmids were mobilized from *E. coli* into recipients by triparental mating using pEVS104 as a conjugative helper, as described previously (252). Restriction enzymes, DNA ligase and Klenow fragment, were obtained from New England Biolabs (Ipswich, MA). Chromosomal DNA was purified using the Easy-DNA kit (Invitrogen, Carlsbad,

CA). Plasmids were isolated using QIAprep spin miniprep kit (Qiagen, Valencia, CA) or GenElute Plasmid Miniprep kit (Sigma, St. Louis, MO). The Zero Blunt TOPO PCR Cloning Kit (Invitrogen, Carlsbad, CA) was used to clone PCR products into pCR-BluntII-TOPO. DNA fragments were purified using DNA Clean & Concentrator-5 Kit (Zymo Research, Orange, CA). PCR was performed using KOD HiFi DNA Polymerase (Novagen, Madison, WI) following manufacturer's recommendations for cycle programs based on predicted DNA product size. Oligonucleotides (Table 4.1) were obtained from Integrated DNA Technologies (Coralville, IA). The annealing temperature for primer pair dma91 and dma92 was 55°C, and for dma93 and dma94 it was 47°C. PCR was performed using an iCycler (BioRad Laboratories, Hercules, CA). DNA sequencing was conducted on an ABI automated DNA sequencer at the University of Michigan DNA Sequencing Core, and sequences were analyzed using Sequencher 4.6 (Gene Codes, Ann Arbor, MI).

Construction of mutants and complementation plasmids. Descriptions of select plasmids and primers used in their construction are provided in Table 4.1. Details of plasmid construction follow. To generate a 2-bp insertion in *celG*, we first screened an existing library of *Xba*I-digested ES114 DNA cloned into pBluescript (Stratagene, La Jolla, CA) to isolate pKV150, which contains the *cel* gene cluster. pKV150 was digested with *BgI*II, and the *cel* gene cluster was subcloned into *BamH*I-digested pEVS79, yielding pKV153. pKV153 was digested with *Spe*I and self-ligated to roughly center *celG* within the insert, making pKV156. pKV156 was then digested with *Cla*I, the overhangs filled in with Klenow fragment, and the plasmid recircularized by self-ligation yielding pKV162, which has a frame-shifting 2-bp insertion in

celG. This mutation was placed on the chromosome of ES114 and DMA420 by allelic exchange, yielding strains KV1319 and DMA401, respectively.

The *celI* complementation plasmid pDMA171 was generated by first amplifying *celI* with ~500 bp of upstream sequence and incorporating *NheI* sites near the 5' end of each primer (dma91 and dma92). This PCR product was cleaned and digested with *NheI* before being cloned directly into *AvrII*-digested pVSV107. Plasmid pKV151 contains the active *cel* cluster and was isolated from a library of *BglII*-digested ES114 DNA cloned into pV08 (3).

To construct pDMA193, the P_{cel}-gfp reporter, the intergenic DNA upstream of celC was PCR amplified with NheI sites incorporated near the 5' ends of the primers (dma93 and dma94) and cloned into pCR-BluntII-TOPO (Invitrogen, Carlsbad, CA) yielding pDMA181. pDMA181 was digested with SpeI and XhoI, and the promoter fragment was subcloned into pEVS79 digested with the same enzymes, making pDMA184. pDMA184 was digested with NheI and the promoter was subcloned into AvrII-digested pVSV209, which contains a promoterless gfp, completing the construction of pDMA193.

Transposon mutagenesis was performed by conjugating the mini-Tn5 delivery plasmid pEVS170 (N. Lyell and E. Stabb, unpublished results) into wild-type *V. fischeri* strain ES114. After conjugation proceeded for more than 8 h, the conjugation mix was diluted and plated onto selective media. The mini-Tn5 mutagenesis was performed in three independent experiments for each screen, encompassing ~10,000 colonies per screen. In one screen, mutant colonies were isolated based on their blue color on LBS supplemented with Em and X-gal. In the other screen, mutant colonies were examined for yellowish-white color on LBS supplemented with cellobiose, Em and X-gal. The site of transposon insertion in each mutant strain was determined by cloning the transposon and flanking DNA and then sequencing across the transposon::chromosome

Table 4.1. Bacterial strains, select plasmids, and oligonucleotides

Strain, plasmid, or	Relevant characteristics	Source or
oligonucleotide		reference
Bacterial strains		
E. coli		
CC118-λpir	CC118- λ pir $\Delta(ara-leu)$ araD $\Delta lac74$ galE galK phoA20 thi-1 rpsE rpsE	
	$argE(Am) recA \lambda pir$	
DH5α	F Φ80dlacZΔ(lacZYA-argF)U169 deoR supE44 hsdR17	(109)
	recA1 endA1 gyrA96 thi-1 relA1	
DH5α-λ <i>pir</i>	DH5 α lysogenized with λpir	(68)
TOP10	· · · · · · · · · · · · · · · · · · ·	
	$recA1 \ ara\Delta 139 \ \Delta (ara-leu) 7697 \ galU \ galK \ rpsL \ (StrR)$	Invitrogen
	endA1 nupG	
Vibrionaceae		
ATCC33653	Vibrio mimicus	E. Lipp
ATCC33564	Vibrio hollisae	E. Lipp
ATCC17803	Vibrio parahaemolyticus	E. Lipp
DMA401	ES114 <i>celI</i> ::mini-Tn5-Em and 2-bp insertion in <i>celG</i>	This study
DMA420	ES114 <i>celI</i> ::mini-Tn5-Em (insertion at bp 914)	This study
DMA421	ES114 <i>celI</i> ::mini-Tn <i>5</i> -Em (insertion 53 bp before predicted	This study
	start of <i>cell</i>)	11110 00000
DMA422	ES114 <i>celK</i> ::mini-Tn5-Em (insertion at bp 548)	This study
DMA423	ES114 <i>celA</i> ::mini-Tn5-Em (insertion at bp 20)	This study
DMA424	ES114 ptsI::mini-Tn5-Em (insertion at bp 247)	This study
DMA425	ES114 <i>celG</i> ::mini-Tn5-Em (insertion at bp 502)	This study
DMA426	ES114 celC::mini-Tn5-Em (insertion at bp 1166)	This study
DMA427	ES114 <i>celB</i> ::mini-Tn5-Em (insertion at bp 39)	This study
DMA428	ES114 VF2408::mini-Tn5-Em (insertion at bp 614) and	
	11-bp deletion in <i>cell</i> (at bp 566)	This study
DMA429	ES114 VF0170::mini-Tn5-Em (insertion at bp 314) and	This study
	11-bp deletion at in <i>celI</i> (at bp 566)	,
ES114	Wild-type isolate from <i>E. scolopes</i>	(20)
KNH6	Photobacterium leiognathi	(252)
KV1319	ES114, 2-bp insertion in <i>celG</i>	This study
KV2801	ES114, <i>ptsI</i> ::pTMO151	(282)
VC4056	Vibrio cholerae	R. Colwell
VC4103	Vibrio cholerae	R. Colwell
Plasmids		
pDMA171	celI in pVSV107	This study
pDMA193	P_{cel} -gfp reporter in pVSV209;	This study
pEVS79	oriV _{ColE1} oriT _{RP4} CmR	(252)
pEVS170	mini-Tn5-Em, oriV _{R6Ky} oriT _{RP4} KnR	N. Lyell
pKV151	celCBGKAI plus 824 bp upstream of putative start in pVO8	This study

pKV162	2-bp insertion in <i>celG</i> and flanking sequences in pEVS79; source of <i>celG</i> allele in KV1319 and DMA401	This study
pVO8	$oriV_{P15A}$ $oriT_{RP4}$ CmR EmR $lacZlpha$	(285)
pVSV107	$oriV_{ m R6K_{\gamma}}oriT_{ m RP4}$ $oriV_{ m pES213}$ TpR $lacZlpha$	(69)
pVSV209	$oriV_{R6K_{\gamma}}oriT_{RP4}$ $oriV_{pES213}$ rfp KnR promoterless CmR- gfp	(69)
Oligonucleotides		
dma91	5' CGGCGCTAGCGGTGCACGCCCAAGATCATATTATGAC 3'	This study
dma92	5' CGCCGCTAGCCGCTGTAACAGCCAGAGCAACAGG 3'	This study
dma93	5' GCCGCTAGCTGTGACTTCCTATATTTCAGCTTT 3'	This study
dma94	5' GGCGCTAGCTGTTCACCCCTAATTAGAATTATAATTTA 3'	This study

^{*} Abbreviations used: Cm^R, chloramphenicol resistance; Em^R, erythromycin resistance; Kn^R, kanamycin resistance; Tp^R, trimethoprim resistance; St^R, streptomycin resistance.

junction using the M13 Forward primer. Insertions were cloned by digesting chromosomal DNA with *Hha*I, self-ligating the fragments, and recovering the transposon and flanking DNA as a plasmid, taking advantage of the origin of replication and Em-resistance gene contained within the transposon.

Carbon utilization assays. The ability to grow on glucose or cellobiose as a sole carbon source was tested by adding these sugars to a minimal medium and then streaking single colonies of each strain onto plates, which were incubated at 28°C for ~48 h and assessed for growth. To test for acid production by strains in the presence of glucose or cellobiose, single colonies were used to inoculate test tubes containing LBS with BCP and either cellobiose, glucose or no sugar added. Cultures were incubated at 28°C with shaking (200 rpm) for 24 h and acidification was scored as a change in the BCP from purple to yellow.

cel induction measurements in culture. Overnight cultures of *V. fischeri* carrying pDMA193 (P_{cel}-*gfp*) were grown in LBS with appropriate antibiotics and were diluted 1:500 into 30 ml of antibiotic-free LBS, with or without cellobiose or glucose, in 125-ml baffled flasks, and were

then incubated at 24° C with shaking (200 rpm). The reporter and control plasmids used are derived from a vector that is stable in *V. fischeri* and does not require selection for maintenance (69). 500-µl samples were removed at intervals and culture optical density (OD₅₉₅) was determined using a BioPhotometer (Brinkman Instruments, Westbury, NY). Fluorescence was measured using a TD-700 fluorometer (Turner Designs, Sunnyvale, CA) using excitation and emission filters of 486 nm and >510 nm, respectively. Fluorescence reported is the average of measurements taken when the OD₅₉₅ readings were approximately 2.5. Fluorescence of strains carrying the promoterless-*gfp* construct in pVSV209 was subtracted as background.

To examine the ability of various carbon sources to induce the *cel* operon, 15 μl of 100 mM stocks of cellobiose, raffinose, sucrose, maltose, lactose, N-acetyl-glucosamine, fructose, mannose, ribose, galactose, xylose, arabinose and glucose were spotted on filter disks placed on LBS plates supplemented with X-gal and spread plated with ES114. After 24 h of incubation, plates were examined for induction of the *cel* operon, which was scored as rings of blue in the lawn surrounding the sugar-impregnated disk. Parallel plates with *celG* mutant KV1319 served as negative controls and did not develop blue color.

Enzyme assays using *p*-Nitrophenyl Conjugated Substrates. Strains tested were grown to an OD₅₉₅ ~2.0, pelleted, lysed by freezing at -80°C for 20 min, and the pellets were resuspended in the original volume of a 500 mM sodium phosphate buffer, pH 7.0. 100 μl of this lysate were added to 400 μl of a 10 mM *p*-nitrophenol (*p*-NP) conjugated substrate dissolved in 50 mM sodium phosphate buffer pH 7.0. Parallel reactions were incubated at 28°C and 37°C until a yellow color was observed, or for a maximum of 24 h. The assay was stopped by adding 2 ml of 1M Na₂CO₃ (final concentration 800 mM). A 1-ml sample from the reaction was centrifuged for

5 min to pellet cell debris. The absorbance was read at 410 nm (A_{410}) to determine the amount of p-NP generated from enzymatic cleavage, and also at 550 nm (A_{550}) to determine light scattering from residual cell debris. To calculate pmol of p-NP generated min⁻¹ ml⁻¹, the A_{410} reading from each sample minus the A_{550} reading for each sample was compared to a linear standard of p-NP, and this was divided by the incubation time and the 0.1 ml of lysate added to the reaction.

Squid colonization assays. *E. scolopes* was maintained in Instant Ocean (Aquarium Systems, Mantor, OH) mixed to ~36 ppt. To determine whether a mutant strain had a competitive disadvantage in the symbiosis relative to the wild-type, cultures for inoculation were grown as previously described (69), and juvenile squid were exposed to a ~1:1 mix of the wild-type and mutant strains for 14 h and then moved to *V. fischeri*-free Instant Ocean. Squid were homogenized after 48 h to determine the ratio of wild type to mutant. The relative competitive index (RCI) was determined by dividing the mutant to wild type ratio in each individual squid by the ratio in the inoculum. Log transformed data were used to calculate the average RCI and to determine statistical significance.

Bioinformatic Analyses. Protein sequence comparisons to Genbank entries were generated using BLAST-P (4). *V. salmonicida* LFI1238 sequence was obtained from the Sanger Institute (http://www.sanger.ac.uk/Projects/V_salmonicida/) as a shotgun database and homologs of specific *V. fischeri* genes were determined using Artemis (228). Genomes with similar regions surrounding the CelC ORF were found using the SEED pinned region search (196). The similarity between homologs that is reported was determined using MatGAT using the default settings (33). Phylogenetic and molecular evolutionary analyses were conducted using *MEGA*

version 4.0 using the default settings (260). Using the *MEGA* program, consensus neighbor-joining phylogenetic trees were constructed using the Amino-Poisson correction. Unweighted Pair Group Method with Arithmetic mean (UPGMA) and minimum evolution trees were also constructed with similar results (data not shown). Bootstrap values for the trees were obtained from a consensus tree based on 1,000 randomly generated trees using the *MEGA* 4.0 software (260).

Results

Mutations in *cell* reveal cryptic β-galactosidase activity in *V. fischeri*. This study was initiated by the serendipidous observation that when *V. fischeri* ES114 was mutagenized with mini-Tn5 and plated on selective media with X-gal, approximately one in 1000 colonies were dark blue, suggesting that some mutation(s) could reveal a cryptic β-galactosidase activity in this strain. We isolated ten such blue mutants and determined the location of the transposon insertion in these strains. Eight of the mutants had insertions in or directly upstream of VF0608, a gene that encodes a putative LacI-family transcriptional regulator. We have now designated VF0608 as *cell*. The other two blue mutants, DMA428 and DMA429, had insertions in VF2408, a putative LuxR-family transcriptional regulator, and VF0170, a putative O-antigen flippase, respectively. However, these mutants, like the other eight, could be complemented to the parental yellowish-white colony color on LBS X-gal by the reintroduction of *cell* on pDMA171 but not by introduction of the parent vector, pVSV107. Subsequent analyses showed that DMA428 and DMA429 each also had an identical 11-bp deletion in *cell*, which could account for their blue phenotype on LBS X-gal plates (Fig. 4.1).

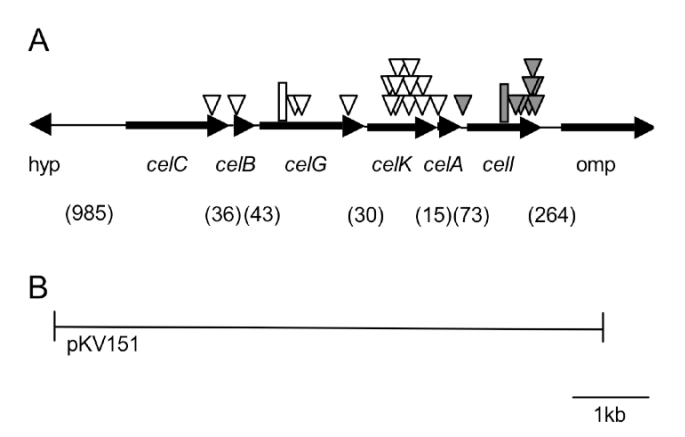


Fig. 4.1. Schematic representation of the genetic organization around the *cel* gene cluster in *V. fischeri* ES114. **A.** Arrows represent open reading frames and indicate the direction of gene transcription as well as the gene size, which is presented relative to the scale bar. Filled triangles represent transposon insertions that result in a blue colony phenotype on LBS-X-gal plates. Open triangles represent transposon insertions that result in a yellowish-white colony phenotype on LBS-X-gal cellobiose plates. A hypothetical gene is designated "hyp". The filled rectangle denotes the 11-bp deletion detected in mutants DMA428 and DMA429. The unfilled rectangle denotes the 2-bp insertion in strain KV1319. Numbers in parentheses represent the base pairs between open reading frames. **B.** Region cloned into plasmid pKV151.

Identification of cellobiose utilization gene cluster. Analysis of the genome near *cell* revealed that it was downstream of a gene cluster annotated as functioning in disaccharide uptake and catabolism, including a putative glucosidase (cellobioase) gene (Fig. 4.1). We hypothesized that the glucosidase gene encoded the enzyme responsible for the cleavage of X-gal and that *cell* repressed this operon in the absence of cellobiose. Consistent with this hypothesis, when plating wild-type ES114 on LBS supplemented with X-gal and 5 mM cellobiose, all the colonies were blue. We then repeated the mini-Tn5 mutagenesis but plated on LBS supplemented with X-gal and 5 mM cellobiose and screened for loss of blue colony color, predicting that the inability to cleave X-gal would correlate with the loss of ability to grow on cellobiose as a sole carbon source. After screening over 10,000 colonies, 16 transposon mutants were isolated based on their yellowish-white color on LBS X-gal cellobiose plates. All but one insertion was localized to the predicted cellobiose utilization gene cluster upstream of *cell* (Fig. 4.1), and all of the

mutants with insertions in this cluster grew poorly or did not grow with cellobiose as the sole carbon source. Moreover, in BCP assays none of these mutants acidified the medium in the presence of cellobiose as wild type does (Table 4.2). Each of the mutants with an insertion in the genes upstream of *cell* could be complemented to a wild-type-like phenotype upon reintroduction of this gene cluster on pKV151 (Fig. 4.1), but not by introduction of the parent vector, pVO8. In light of these data, the genes in the cluster were named based on their predicted function: PTS IIA component, *celA* (VF0607); PTS IIB component, *celB* (VF0604); PTS IIC component, *celC* (VF0603); 6-phospho-β-glucosidase, *celG* (VF0605); glucokinase, *celK* (VF0606), and, as mentioned above, LacI-like family transcriptional regulator; *celI* (VF0608) (Fig. 4.1).

The single mutant with an insertion outside this gene cluster, DMA424, had an insertion in VF1896, which is annotated as a PTS system enzyme. Visick *et al.* (284) characterized a mutation in this gene previously and determined that the VF1895 and VF1896 open reading frames were actually one gene, an ortholog to *E. coli*'s *ptsI*. Similar to the *ptsI* mutant isolated by Visick *et al.* (284), we found that our *ptsI* mutant grew poorly in minimal media with cellobiose or glucose as the sole carbon source and had a slower growth rate than wild type in LBS (data not shown). The *ptsI* gene encodes the E1 component of the PTS system, one of two proteins with essential roles as general components for all PTS systems. Because there is no other E1 encoded in *V. fischeri* ES114, the PTS II system comprised of CelA, CelB, and CelC should be severely attenuated or non-functional in mutant DMA424.

celG encodes a β -glucosidase with lesser β -galactosidase activity. To investigate whether the putative 6-phospho- β -glucosidase encoded by celG was responsible for the cleavage of

cellobiose and X-gal, we generated mutant KV1319, which contains a 2-bp insertion in *celG*. KV1319 was unable to cleave X-gal, was unable to utilize cellobiose as a sole carbon source, and did not acidify cellobiose-containing media in BCP assays. This provides further evidence that CelG is responsible for the cleavage of both cellobiose and X-gal, a supposition that is also supported by enzymatic assays described below. To test the prediction that the *celI* mutant's blue colony phenotype on LBS X-gal was due to the loss of CelI-mediated repression of *celG*, we incorporated the 2-bp frameshifting mutation in *celG* into DMA420, a *celI* transposon mutant. As predicted, the resulting strain DMA401 (*celG*, *celI*::mini-Tn5-Em) was yellowish-white in contrast to the blue color of the *celI* mutant on LBS X-gal plates (data not shown).

To further test the substrates targeted by CelG, we assayed enzymatic activity in cell lysates using sugar substrates para-linked to a nitrophenol group. We examined lysates of *celI* mutant DMA420, which should enhance CelG activity by allowing the derepression of *celG*. To test whether utilization of a particular substrate was specific to CelG and not some other enzyme in the whole cell lysate, we compared activity in *celI* mutant lysates (dark gray bars in Fig. 4.2) to that in lysates of the double *celI* and *celG* mutant, DMA401 (light gray bars in Fig. 4.2). Thus, the difference between the dark and light gray bars in Figure 4.2 represents CelG-dependent activity, and CelG-independent activity can be gleaned directly from the light gray bars.

Figure 4.2 shows that the *celG* mutant loses the ability to cleave the model substrate for cellobiose cleavage, p-NP-β-D-glucopyranoside (glu). Lower but significant CelG-dependent activity was observed with p-NP-β-D-galactopyranoside (gal), p-NP-β-D-cellobioside (cello), and p-NP-β-D-lactopyranoside (lac). We also observed modest (0.25%) residual activity toward p-NP-β-D-glucopyranoside (glu) even in *celG* mutant DMA401, which could indicate that the

frameshift in celG does not completely eliminate CelG function or that other enzymes in the lysate catalyze a relatively minor amount of hydrolysis of the substrate. To differentiate between these possibilities, we tested the celG::mini-Tn5-Em mutant, DMA425 and found it had similar activity toward p-NP- β -D-glucopyranoside (glu) as the celG frameshift mutant, supporting the idea that the residual activity is due to an unidentified enzyme rather than partial activity from the frameshift allele (data not shown).

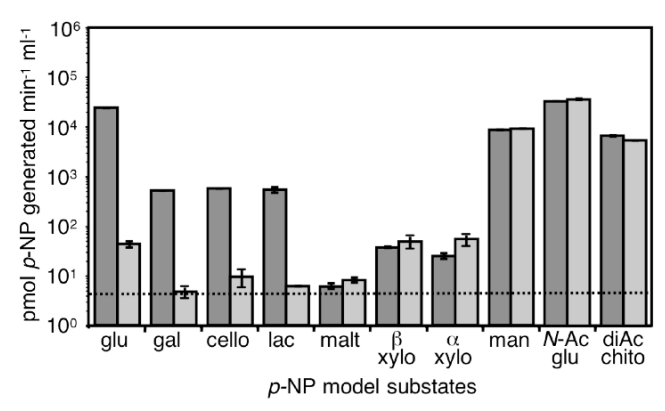


Fig. 4.2. *celG*-dependent enzymatic activity. Activities in lysates from DMA420 (*celI*::mini-Tn5-Em) are shown as dark grey bars, and activities from DMA401 lysates (*celI*::mini-Tn5-Em, *celG*) are shown as light grey bars. Activities represent the ability to cleave p-nitrophenol (*p*-NP) from the substrate. Error bars, some too small to visualize, indicate standard error (n=3). The dashed line represents the limit of detection. Results shown are representative of two experiments at 37°C and are also similar to data obtained in two experiments at 28°C. Substrate abbreviations are: glu, *p*-NP-β-D-glucopyranoside (model substrate for cellobiose); gal, *p*-NP-β-D-galactopyranoside; cello, *p*-NP-β-D-cellobioside; lac, *p*-NP-β-D-lactopyranoside; malt, *p*-NP-β-D-maltoside; β-xylo, *p*-NP-β-D-xylopyranoside; α-xylo, *p*-NP-α-D-xylopyranoside; man, *p*-NP-β-D-mannopyranoside; *N*-Ac-glu, *p*-NP-N-acetyl-β-D-glucosaminide; and diAC-chito, *p*-NP-N,N'-diacetyl-β-D-chitobioside.

Although each of the other substrates cleaved by CelG contains a β -1,4 linkage, promiscuity of the enzyme was evident in its activity as both a β -glucosidase and a β -glucosidase. The latter may reflect a coincidental and physiologically irrelevant activity. Although CelG is apparently able to cleave p-NP- β -D-lactopyranoside (lac), V. fischeri is unable to utilize lactose as a carbon source. Moreover, data below indicate that CelG is induced by the

presence of cellobiose, but not by lactose (Fig. 4.3). Given the ability of CelG to direct X-gal cleavage, the β -galactosidase activity attributed to CelG in this assay was expected; however, it is worth noting that this activity was ~50-fold lower than the β -glucosidase activity (Fig. 4.2).

The assays with other p-NP-linked substrates indicate that enzymes other than CelG in the lysates direct cleavage of p-NP- β -D-mannopyranoside (man), p-NP-N-acetyl- β -D-glucosaminide (N-Ac-glu), p-NP-N,N'-diacetyl- β -D-chitobioside (diAC-chito), p-NP- β -D-xylopyranoside (β -xylo), and p-NP- α -D-xylopyranoside (α -xylo). We saw no enzymatic activity toward p-NP- β -D-maltoside (malt).

cell, cellobiose-, and glucose-mediated control of cel expression. To determine when the cel genes are induced, we developed a transcriptional reporter plasmid, pDMA193, containing the region immediately upstream of the cel gene cluster driving expression of gfp. Without cellobiose, the reporter's fluorescence in ES114 was slightly elevated above background, but with growth in cellobiose there was an increase of almost 5-fold in fluorescence (Fig. 4.3). In the cell::mini-Tn5-Em mutant DMA420 the reporter was expressed with and without added cellobiose, further supporting our prediction that Cell represses the cel gene cluster when cellobiose is not present.

Interestingly, in the presence of cellobiose, fluorescence of the reporter in the *celI* mutant DMA420 decreases compared to growing without cellobiose. We hypothesized that generation of glucose due to the cleavage of cellobiose might cause catabolite repression of the gene cluster, resulting in this inhibitory effect of cellobiose on *cel* expression. To examine this, both wild type ES114 and *celI* mutant DMA420 containing the reporter plasmid were grown in the presence of glucose. In both strains, fluorescence from the reporter plasmid decreased substantially when

cells were grown in LBS supplemented with glucose (Fig. 4.3). Furthermore, we moved the reporter plasmid into DMA401, the *cell celG* double mutant, to assess whether the loss of CelG, which should reduce the breakdown of cellobiose to glucose, would allow induction of the gene cluster in the presence of cellobiose. In media with glucose, reporter expression in DMA401 was reduced, as it is in the other strains (Fig. 4.3). However, supplementation with cellobiose, did not affect reporter expression in DMA401 (Fig. 4.3). Thus it appears that *cel* expression is repressed by glucose that is either added exogenously or generated by CelG-dependent cleavage of cellobiose.

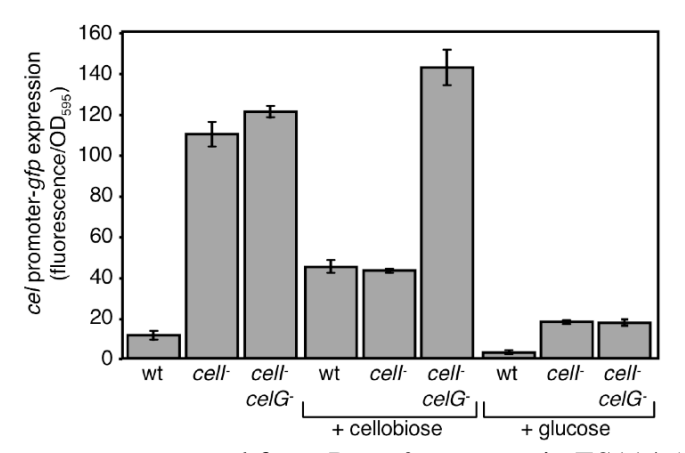


Fig. 4.3. Specific fluorescence generated from P_{cel} -gfp reporter in ES114 (wt), mutant DMA420 (cel), or mutant DMA401 (cel). Cultures of strains carrying pDMA193 were grown in LBS with and without 10 mM cellobiose or 20 mM glucose. Data represent the average specific fluorescence with standard error (n=3).

Taking advantage of the promiscuity of CelG and its ability to degrade X-gal, we next tested whether other carbon sources, besides cellobiose, could induce the expression of the *cel* gene cluster, using a disc assay with ES114 or the *celG* mutant KV1319 plated on LBS plates supplemented with X-gal. We tested glucose, galactose, lactose, chitin-hexamers, cellulose, N-acetyl-glucosamine and cellobiose and found that only cellobiose was able to induce the expression of the *cel* gene cluster, resulting in CelG-dependent cleavage of X-gal and

development of blue color in growth of ES114 around the disc (data not shown). Thus even if CelG is able to cleave other substrates besides cellobiose (as described above), the substrates above do not induce *celG* and are therefore unlikely to be physiologically relevant targets for the *cel* gene cluster.

The *celCBGKAI* gene cluster on pKV151 confers cellobiose utilization on six cellobiosenegative *Vibrio* strains. To determine whether this cellobiose-utilization gene cluster in *V. fischeri* was sufficient to confer cellobiose utilization to other Vibrios, pKV151 (Fig. 4.1) was moved into six different *Vibrio* or *Photobacterium* strains that are negative for cellobiose utilization (Table 4.2). Transconjugants were tested for growth on solid media with cellobiose as a sole carbon source, and were also tested for growth in the presence of glucose (the breakdown product of cellobiose) as a control. Both ES114 and the *celG* frameshift mutant were also included as positive and negative controls, respectively. All of the strains grew regardless of plasmid when glucose was the sole carbon source (data not shown); however, of the strains carrying the insertless vector pVO8, only ES114 grew on cellobiose (Table 4.2). Thus, for each of the other *Vibrio* or *Photobacterium* strains, the *V. fischeri cel* gene cluster on pKV151 conferred the ability to grow on cellobiose (Table 4.2).

Table 4.2. Growth and acid production of *Vibrio* strains on glucose and cellobiose.

	Growth on		Acidification of LBS-BCP in presence of			
Strain	Minimal + Cellobiose		Glucose		Cellobiose	
	pVO8	pKV151	pVO8	pKV151	pVO8	pKV151
ES114	+	+	+	+	+	+
KV1319	-	+	+	+	-	+
P. leiognathi	-	+	+	+	-	-
V. cholerae VC4103	-	+	+	+	-	+
V. cholerae VC4056	-	+	+	+	+	+
V. parahaemolyticus	-	+	+	+	-	+
V. hollisae	-	+	+	+	-	-
V. mimicus	_	+	+	+	-	+

Substrate utilization is often tested indirectly based on the production of fermentation acids in the presence of a particular sugar, resulting in a pH shift that can be detected by the colorimetric change in the dye BCP. We therefore also tested strains carrying pKV151 in BCP assays. All strains with either the control vector or pKV151 acidified glucose-containing LBS medium (Table 4.2). For *V. cholerae* VC4103, *V. mimicus*, and *V. parahaemolyticus*, pKV151 conferred not only the ability to grow on cellobiose, but also the production of acid in LBS supplemented with cellobiose. For the other strains, the ability to grow on cellobiose did not correlate with acid production in the presence of cellobiose. *P. leiognathi* and *V. hollisae* were unable to acidify the cellobiose-containing medium regardless of whether they carried the control vector or pKV151, whereas *V. cholerae* VC4056 acidified the medium regardless of whether it contained pKV151 or the control vector. Thus, although acid production is often used as an indirect indicator of sugar catabolism by *Vibrio* species (16, 72), direct testing for growth on cellobiose was a more reliable measure of this metabolic capability.

Bioinformatic analyses of the *cel* gene cluster. Using a combination of bioinformatic programs and databases (see Materials and Methods) we sought to determine whether *celCBGKAI* was an ancestral locus present in all cellobiose-utilizing members of the *Vibrionaceae*, and if this was not the case to determine the likely origin(s) of these genes. Comparisons of nucleotide or encoded-protein sequences yielded similar results, and for the most part only the latter are reported here, with nucleotide sequence used for reporting gene arrangement. We found that *V. salmonicida* strain LFI1238, which utilizes cellobiose (Nils-Peder Willassen, personal communication), has a homologous *celCBGKAI* cluster. The *cel* gene order is conserved in *V. salmonicida*, the encoded proteins were >90% similar to the respective

homologs in *V. fischeri*, and it included both the genes for cellobiose utilization (Fig. 4.4A) and the regulator *cell* (not shown).

Photobacterium profundum SS9 and V. vulnificus, which are cellobiose positive (72, 190), also had gene clusters that included PTS II system genes, a glucosidase gene and in the latter bacterium a glucokinase gene as well; however, neither had impressive similarity to the V. fischeri cel cluster. For example, the putative glucosidase and glucokinase encoded by this V. vulnificus cluster shared only 29% and 33% similarity to CelG and CelK, respectively (Fig. 4.4A). Although V. vulnificus is able to grow on cellobiose, we speculate that this might not be the gene cluster responsible for cellobiose catabolism. In support of this idea, V. cholerae and V. parahaemolyticus are both cellobiose negative, yet both have a highly homologous gene cluster to that described above in V. vulnificus (Fig. 4.4B). Partial genomic sequences are available for other cellobiose-utilizing Vibrio species, but additional clusters similar to celCBGKAI were not found. Indeed, homologs of the individual V. fischeri CelG and CelK proteins were notably absent. Taken together, our analyses suggest that celCBGKAI underpins cellobiose utilization in the V. fischeri/V. salmonicida clade, but that distinct pathways may direct cellobiose catabolism in other members of the Vibrionaceae.

Despite further analyses, the ancestry of the *celCBGKAI* genes in *V. fischeri* and *V. salmonicida* remains uncertain, and these genes may have multiple origins. It seems likely that *celI*, which encodes the LacI-family regulator, originated within the *Vibrionaceae*, as it shares high similarity with many regulators in this bacterial family (data not shown). Interestingly however, CelG and CelK clustered most closely with ORFs found in the *Firmicutes* phylum of the bacteria, particularly *Clostridium*, *Bacillus* and *Listeria* species. This is illustrated both in comparisons of similar gene clusters (Fig. 4.4) and in neighbor-joining trees comparing the

specific proteins encoded by these gene clusters (Fig. 4.5). Gene clusters in Clostridium acetobutylicum and Listeria monocytogenes were more similar to the V. fischeri cel cluster than were the gene clusters from other Vibrios (Fig. 4.4A). The closest homolog of CelG was found in C. acetobutylicum (Figs. 4.4A and 4.5D), while close homologs to CelK are found in C. acetobutylicum, L. monocytogenes and Yersinia intermedia (Figs. 4.4A and 4.5C). Although Y. intermedia is a gamma proteobacterium, it appeared exceptional in this group in that the proteins encoded by the Y. intermedia cluster group more closely with homologs in Listeria than with proteins in other proteobacteria. The gene cluster in L. monocytogenes is also similar to the V. fischeri cel cluster, and gene order is conserved with that in V. fischeri except that the PTS IIC and glucosidase genes are switched (Fig. 4.4A). Moreover, codon usage by *Listeria* is so similar to that in V. fischeri that genes transferred between the two cannot be recognized as foreign using this criterion (data not shown). The origin of the celA, celB, and celC genes is especially difficult to infer, as the PTS IIC component tends to group with homologs in the *Firmicutes* (Fig. 4.5B), whereas the PTS IIB and IIA components tend to group more closely with homologs within the Vibrionaceae (Fig. 4.5A and data not shown). The PTS IIB and IIA components must interface with other endogenous proteins and the respective genes might be expected to face greater selective pressure to adapt to a new host and therefore appear less foreign. Overall, it seems plausible that at least some of the genes for cellobiose uptake and catabolism may have been transferred horizontally from a marine Firmicute to an ancestor of the V. fischeri/V. salmonicida clade, although other scenarios remain possible.

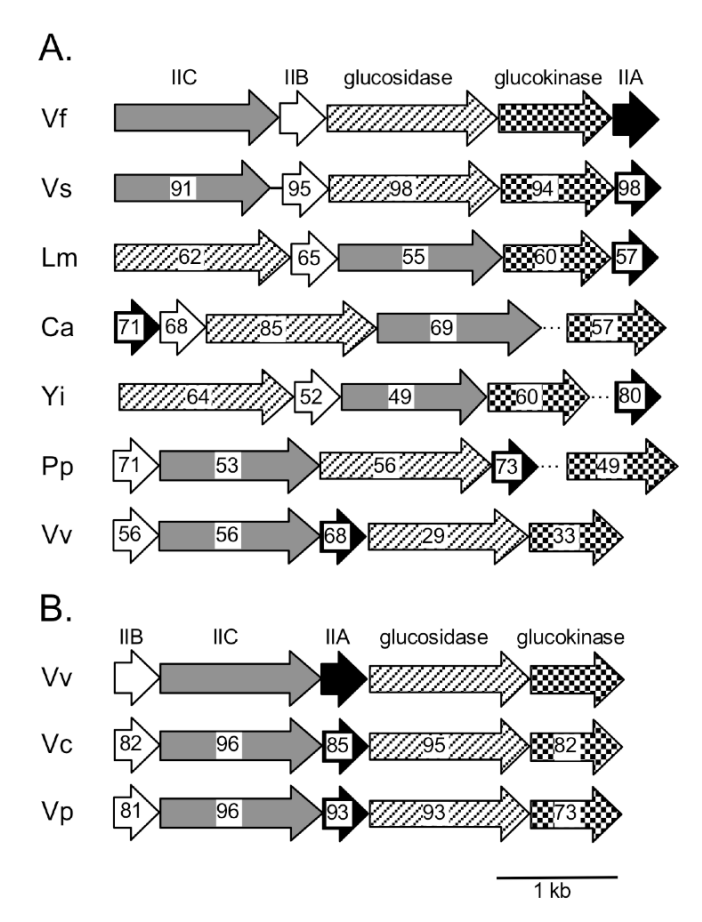


Fig. 4.4. Homologs of the *V. fischeri* cellobiose-utilization genes. Gene arrangement and orientation for each particular strain is indicated with arrows. Arrows with the same colored or patterned fill are putative homologs. Genes encoding PTS components A, B, or C are shaded black, white or grey, respectively. Genes encoding glucokinases or glucosidases are filled with checkerboard or crosshatching patterns, respectively. Broken (dotted) lines are used to indicate that glucokinase genes in these bacteria are not genetically linked to the other genes shown. Numbers within the arrows represent the overall similarity to the respective protein from *V. fischeri* (panel A) or *V. vulnificus* (panel B) as determined by MatGAT (33). Species abbreviations are: Vf, *Vibrio fischeri*; Vs, *Vibrio salmonicida*; Lm, *Listeria monocytogenes*; Ca, *Clostridium acetobutylicum*; Yi, *Yersinia intermedia*; Pp, *Photobacterium profundum*; Vv, *Vibrio vulnificus*; Vc, *Vibrio cholerae*; and Vp, *Vibrio parahaemolyticus*.

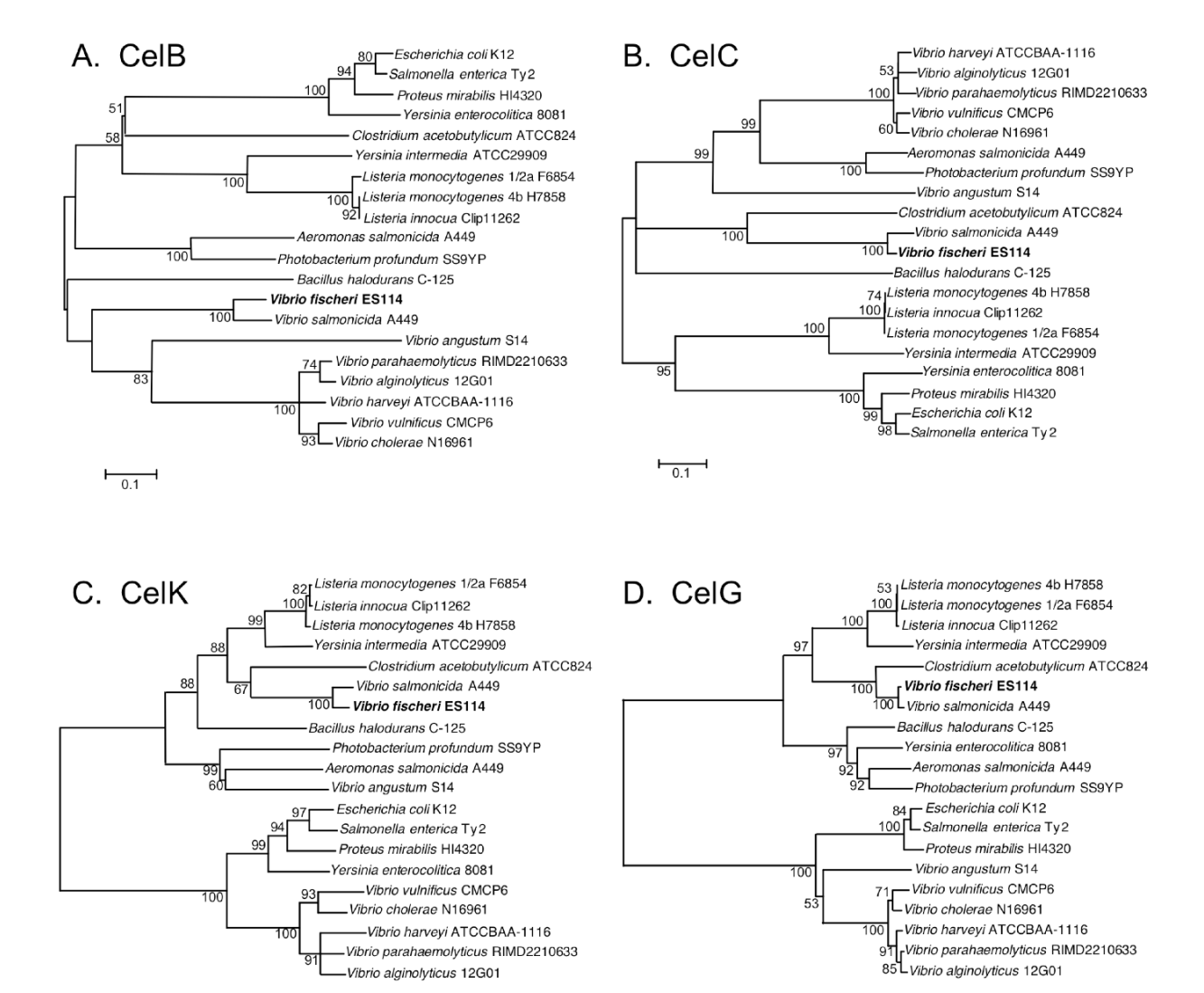


Fig. 4.5. Comparison of *V. fischeri* CelB, CelC, CelK, and CelG to proteins encoded by other bacteria with similar gene clusters. Consensus neighbor-joining trees constructed using *MEGA* 4.0 (260) are shown. Trees constructed using both UPGMA and minimum evolution algorithms were similar to the ones shown (data not shown). Bootstrap values >50% are indicated at the respective nodes. The scale bar represents corrected sequence divergence of 0.1 or 0.2 as indicated. Trees in panels A, B, C, and D include *V. fischeri* proteins CelB, CelC, CelK and CelG, respectively.

Symbiotic colonization of *E. scolopes*. Our laboratories and others study the symbiotic interaction of *V. fischeri* ES114 with the Hawaiian bobtail squid, *E. scolopes*, and we therefore investigated the symbiotic phenotype of *cel* mutants. If cellobiose utilization contributed to colonization proficiency, this would provide insight into the symbiotic nutritional environment of the host light organ. On the other hand, if mutants had no symbiotic attenuation, then mutant *cel* alleles could be useful as neutral markers with a readily scored phenotype on X-gal.

Mutants with insertions in each of the *cel* genes were checked for their ability to compete with wild type for colonization in *E. scolopes*. Mutants with an insertion in *cell* or in the non-coding region upstream of *cell* were consistently outcompeted by ~2.2 fold as indicated by RCI values ~0.45 (Table 4.3). In contrast, strains with mutations in genes responsible for the transport and degradation of cellobiose, *celA*, *celB*, *celC*, *celG*, and *celK*, had no significant competitive defect relative to wild type (Table 4.3). We competed DMA401 (*celG celI*::mini-Tn5-Em) to see if the competitive defect of a mutation in *cell* was dependent on overexpression of a functional *cel* gene cluster and cellobioase activity. This competition yielded an RCI that was essentially the same as the single *celI* mutant alone, indicating that the negative effect of knocking out *celI* on symbiotic colonization is independent of cellobioase activity. Instead, this attenuation of competitiveness may simply be from overexpression of the Cel proteins. Not surprisingly, the *ptsI* mutant, DMA424, was outcompeted by wild type; however, this mutant's slower growth in culture indicates that its defect in colonizing the host cannot be considered symbiosis-specific.

Table 4.3. Colonization competitiveness of *V. fischeri cel* mutants relative to ES114

Strain	Genotype	# of animals ^a	RCI^b
DMA420	celI::mini-Tn5-Em	42	0.40^{c}
		41	0.48 ^c
		44	0.40 ^c
DMA421	celI upstream region::Tn5	44	0.44 ^c
DMA401	<i>celI</i> ::mini-Tn5-Em, <i>celG</i> ⁻ (frameshift)	32	0.39 °
DMA425	celG::Tn5-Em	32	0.90
KV1319	<i>celG</i> (frameshift)	32	1.21
DMA422	celK::mini-Tn5-Em	26	0.68
DMA423	celA::mini-Tn5-Em	29	0.95
DMA427	celB::mini-Tn5-Em	32	1.04
DMA426	celC::mini-Tn5-Em	32	0.91
DMA424	ptsI::mini-Tn5-Em	32	0.02 ^c

^a Number of animals in individual experiment

Discussion:

In this study we describe a gene cluster that is required for the utilization of cellobiose by V. fischeri and is sufficient to confer this property on cellobiose-negative Vibrio species. The genes in this cluster encode a PTS transport system (celA, celB, and celC), a glucokinase (celK), a glucosidase (celG), and a LacI-like transcriptional regulator (celI) that inhibits expression of the cluster when cellobiose is not present (Fig. 1 and Fig. 3). Mutational analyses and enzymatic assays show that the cel cluster is responsible for cleavage of both cellobiose, which is a β -1,4-linked glucose dissacharide, and X-gal, which is a β -1,4 linked galactoside. Although CelG is promiscuous with respect to the β -1,4-linked substrates it cleaves, and theoretically it could direct catabolism of a β -1,4-galactoside such as lactose, we propose that its activity as a β -1,4-glucosidase is physiologically relevant whereas its galactosidase activity is coincidental. In support of this, CelG appeared to have greater activity as a glucosidase, and it was required for growth on cellobiose while lactose is not even utilized by V. fischeri as a carbon source.

^b Ratio of a mutant strain to the wild type in the light organ at 48 h post-inoculation divided by the ratio in the inoculum

^c Mutant is significantly outcompeted by ES114, < 0.01

Moreover, the glucoside cellobiose (or a mutation in *celI*) induced the *cel* cluster whereas several other sugars including lactose did not.

Cellobiose is a disaccharide breakdown product of cellulose, but *V. fischeri* apparently lacks cellulose-degrading capacity, and the importance of its *cel* gene cluster is unclear. There is no evidence that cellobiose is released by *E. scolopes* to symbiotic *V. fischeri*, and it seems unlikely that this predatory invertebrate would produce or accumulate cellulose or cellobiose. Moreover, losing the ability to utilize cellobiose did not result in symbiotic attenuation (Table 3). *V. fischeri* has been isolated from the water column, even in areas where symbiotic hosts are not found (151, 224), and it has also been isolated from the bacterial consortium in the guts of herbivorous marine fishes where it can survive and persist (209, 255). These observations suggest a niche where cellobioase activity may be important for *V. fischeri*. Many herbivorous fish partially digest cellulose by acid hydrolysis in their stomach (310), and it is believed that bacterial cellulases contribute to the digestion of the cellulose in the gut, as with termites and ruminants (227, 293). Although *V. fischeri* does not contain a cellulase it is possible that either the acidity of the fish stomach or other bacteria in a fish intestine could break down cellulose into cellobiose allowing *V. fischeri* to consume it.

Interestingly, other cellobiose-utilizing *Vibrios*, notably *V. vulnificus*, lack the *celCBGKAI* gene cluster, and we speculate that cellobiose catabolism may have arisen in the *Vibrionaceae* by multiple distinct events. Based on our bioinformatic data, we speculate that a *Firmicute* horizontally transferred the cellobiose degradation glucokinase and glucosidase genes, and possibly the PTS genes, to an ancestor of the *V. fischeri* and *V. salmonicida* lineage. *Firmicutes* have been found in the guts of marine fishes (123, 184) and in the marine environment (25, 219), so it seems plausible for the ancestor of *V. fischeri* to have acquired the

gene cluster from a member of the *Firmicutes* by horizontal gene transfer. Moreover, codon usage patterns of *V. fischeri* and *Listeria* species isolated from marine environments are not distinguishably different, suggesting that expression of genes transferred between these species may be readily possible. As genome sequences become available for additional marine species are sequenced, particularly *Firmicutes*, the origin of the *V. fischeri* gene cluster may become more apparent.

We and other labs use the β -galactosidase gene lacZ as a transcriptional reporter (158, 287, 306, 307) in V. fischeri, and the discovery of a cryptic β -galactosidase activity in V. fischeri strikes as a cautionary note for such applications. For example, when using lacZ as a transcriptional reporter and screening transposon mutants to find regulators of these lacZ fusions, knockouts of celI will also result in blue colonies on media containing X-gal. It may be useful in such situations to use the celG allele in KV1319 in the reporter strain, to prevent celG expression from confounding screens for lacZ activity. Alternatively, celI could be introduced on plasmid pDMA171 into strains with apparent increases in lacZ activity to eliminate the possibility that a celI mutation and concomitant celG expression are responsible for β -galactosidase activity. Whatever the experimental setup, appropriate controls and careful interpretation are warranted whenever lacZ is used in a $celG^+$ background.

lacZ has also been used as a marker in *V. fischeri*, so that the ratio of two strains in a mixed inoculum or infection can be determined by blue/white screening plating on media with X-gal. Determining strain ratios underlies competition experiments, which enable researchers to detect even subtle differences in symbiotic fitness (23, 125, 149, 157, 159, 179, 195, 251, 282, 284, 298, 306). Recently, *V. fischeri* strains have been marked for competition assays with the introduction of a stable plasmid containing *lacZ* (2, 69, 125). However, the *lacZ*-carrying

plasmids can be lost, albeit at a low rate, and their use is inconsistent with other plasmids (e.g. for complementation). Our data suggest a fresh approach that does not rely on a plasmid-borne lacZ, but retains the convenience of blue/white scoring to determine strain ratios. In this approach, one strain could be marked with the mutant celG allele present in KV1319. We have shown that this mutation has no effect on colonization competitiveness (Table 3), yet it results in loss of blue color when plated on media containing cellobiose and X-gal.

The Vibrionaceae is an important and diverse family of bacteria with new species continually being discovered (8, 133, 147, 199, 216, 233, 264) and with an apparent capacity for rapid evolution given the periodic emergence of new pathogenic biotypes (51, 77, 229, 237). Traditionally, phenotypic markers such as strains' catabolic capacities have been used to help define Vibrio species. However, as more genomes are sequenced for important Vibrios, molecular probes and DNA-based techniques will likely plan an ever-larger role in identifying and defining important species or emergent biotypes. Our bioinformatic and phenotypic analyses suggest, not surprisingly, that caution is warranted when viewing automated genome For example automated annotation of celA indicated that it directed annotations. "diacetylchitobiose-specific" transport, which seems clearly not the case given its importance in cellobiose catabolism. Similarly, PTS gene clusters were annotated as cellobiose transport systems in V. parahaemolyticus and V. cholerae, two species that are cellobiose negative. Experimental studies linking genes with taxonomically useful phenotypes, such as our dissection of the cel gene cluster reported here, will be useful in the future to improve Vibrio genome annotations and connect molecular and phenotypic identification techniques.

Acknowledgements:

We would like to thank Jeff Turner and Erin Lipp for providing strains, Larry Shimkets and Jan Mrazek for helpful discussions and Eduardo de Aquino Ximenes, Emily DeCrescenzo Henriksen, James Henriksen, Dana Cook, Nathan Montgomery, and Line Skoufos for technical assistance. We would also like to thank Nils-Peder Willassen and the Sanger Institute for allowing us access to the *V. salmonicida* genome before publication. This work was supported by the National Institutes of Health (NIH) Grant GM59690 to K.L.V., by the National Science Foundation under Grant CAREER MCB-0347317 to E.V.S., and by NIH Grant A150661 to M. McFall-Ngai.

CHAPTER 5: CONCLUSIONS AND FUTURE DIRECTIONS

The purpose of this dissertation was to examine the genes in *V. fischeri* that underlie the recognition and signaling that occurs between this bacterium and its squid host *E. scolopes*. Previous work showed that lipid A and PG monomers were important signals in the symbiosis (75, 141); however, the structural and genetic basis for these signals in *V. fischeri* was not determined. My first goal was to determine the relevance of secondary acylations on the lipid A moiety. To accomplish this goal, in Chapter 2 I mutated three genes, *htrB1*, *htrB2*, and *msbB*, and also showed that each encoded secondary acyltransferase activity. I then showed that altering the secondary acylations, especially by layering mutations, affected cell morphology and caused other unexpected pleiotropic effects in culture. Of these three genes, only the *htrB1* mutant had a transient defect in colonization.

My second goal was to investigate the genes responsible for the release of PG monomers, a known morphogen that induces regression of the squid light organ ciliated epithelial appendages. In Chapter 3, I showed that deletion of three lytic transglycosylases reduces PG monomer release to very low (< 3 nM per OD₅₉₅) levels in culture. Moreover, *V. fischeri* has a functional PG monomer permease, AmpG, suggesting that PG recycling occurs in *V. fischeri*. In an attempt to find regulators of *ampG*, I placed *lacZ* downstream of this gene, and mutagenesis of this reporter strain lead to the discovery reported in Chapter 4 that *V. fischeri* possesses a β -glucosidase involved in the catabolism of cellobiose that also has cryptic β -galactosidase activity. In this chapter, I will discuss the impact these studies have on our understanding of

signaling in the V. fischeri - E. scolopes symbiosis, and I will suggest directions for future research.

LPS and Lipid A

Foster et al. reported that LPS purified from Haemophilus influenzae when added to aposymbiotic squid induced apoptosis in the ciliated appendages at 18 h post-inoculation. In contrast, LPS purified from a H. influenzae htrB mutant did not induce significant apoptosis above background at 18 h, but by 48 h the LPS isolated from the mutant H. influenzae strain had induced cell death to similar levels as the wild-type LPS (75). These results mirror what was seen in Chapter 2 with the V. fischeri htrB1 mutant insofar as there is an initial colonization defect with this mutant that occurs in the first ~14 h that disappears by 48 h. There appears to be no difference between LPS purified from this mutant (or any of the mutants) and LPS from the wild type with respect to induction of apoptosis (Jamie Foster and Tanya Koropatnick, personal communication); however, as described in Chapter 2, the htrB1 mutant is similar to wild type in culture, and this includes indistinguishable LPS composition. This suggests that the expression of htrB1 and the subsequent acylation of lipid A may only occur during the initial events of colonization, such as in the aggregate of cells that forms on the light-organ surface. Thus LPS purified from a culture of the htrB1 mutant may structurally be no different from wild-type LPS. This may be the reason why there is no difference in apoptosis induction between the wild type and the htrB1 mutant.

LPS from the other mutants discussed in Chapter 2 was also checked for the ability to induce apoptosis; however, it is hard to tell whether there were significant differences between the treatments (Tanya Koropatnick and Margaret McFall-Ngai, personal communication)

because of the synergy that occurs between PG monomers and LPS. Only small amounts of LPS are needed to enhance the PG monomer effect on the ciliated appendages, so if the strains are producing PG monomers, and if these are contaminating LPS preparations, then the changes to the LPS may show little effect on the stimulation of apoptosis. This might not have been a complicating factor for the Foster et al. analysis of *H. influenzae* LPS, because this bacterium does not release such a high concentration of PG monomers (75). One way to re-check the mutant's LPS would be to move the *htrB1*, *htrB2*, and *msbB* mutations into the *ltgA1 ltgA2 ltgD* background (described in Chapter 3) that produces lower levels of PG monomers in culture. This may give cleaner preparations of LPS without contaminating PG monomers and allow for direct analysis of regression and apoptosis by inoculating with strains, not just purified LPS.

The observation that the *htrB1* mutant was wild-type-like in culture yet differed from wild type in the symbiosis suggests that there might be regulation of *htrB1* (e.g. it might be induced in the symbiosis). However promoter-*gfp* fusions indicated that *htrB1* is transcribed both in culture and in the symbiosis, apparently to high levels (data not shown). With these fusions, subtle regulation may not be apparent, but this suggests that there is no transcriptional induction of *htrB1* during symbiosis. An alternative explanation may be that HtrB1 competes with HtrB2 for adding a secondary acylation to the same primary acylation, so repression of *htrB2* in the squid would allow HtrB1 to attach its acyl group. The expression of a *htrB2-gfp* reporter both in culture and in squid appeared to be low, so we cannot rule this out (data not shown). LPS isolated from symbionts in the squid light organ or from the aggregate outside the light organ would help to further understand the contribution of HtrB1 to lipid A structure in the symbiosis.

Based on the work of our collaborators Nancy Phillips and Brad Gibson, the yet unsolved LPS structure of *V. fischeri* appears to have unique additions to lipid A, including a 172 Da potential phosphoglycerol moiety attached to a primary acylation and also a C_{16:1} secondary acylation. Unfortunately, attempts to isolate the genes responsible for these additions were unsuccessful, as described in Appendix A. A mutation in a phosphoglycerol transferase or a monounsaturated palmitate transferase that modify lipid A could potentially alter signaling to the squid and affect colonization. Finding such genes in a random mutant hunt would presumably be difficult if the only way to screen for such a mutant would be to purify LPS and perform MALDI-TOF on lipid A from each mutant. Because the *E. coli* strain MKV15 lacking all secondary acylations is temperature sensitive for growth, it may be worth transforming a cosmid library of *V. fischeri* DNA into this mutant and screening for rescued growth at 37°C.

Peptidoglycan

PG monomer induces the morphogenesis of the squid's ciliated appendages and the loss of three lytic transglycosylases reduced PG monomer release to low levels in culture as shown in Chapter 3. The *ltgA1 ltgA2 ltgD* triple mutant appears attenuated in induction of ciliated appendage regression, but it does still stimulate regression. This could be due to another gene that is induced during squid colonization to cleave and release PG monomers. Assessing expression (e.g. with *gfp* reporters) of each of the lytic transglycosylases listed in Table 3.2 may help to determine of which genes are transcribed in the squid. Along with mutating the rest of the lytic transglycosylase genes singly and layering mutations together, this may lead to deciphering all the genes that are responsible for the release of the PG monomer morphogen.

The experiment that I performed in Chapter 3 to look for secondary infections of precolonized light organs will also be of interest when looking at these mutants. The subtle
phenotype that the triple *ltgA1 ltgA2 ltgD* mutant has on regression was revealed more
definitively by measuring susceptibility of animals to secondary infection, and this may be
analogous to how competition experiments expose differences in relative symbiosis proficiency
that are not always apparent in comparisons of clonal infections. Previous transposon-mutant
libraries screened individually for colonization have revealed genes important for infection of
squid (307). Screening for mutants that lack or gain some the ability to prevent secondary
infections could elucidate genes important for stimulating regression of the ciliated appendages
that otherwise may not be found.

It is also possible that other PG fragments may influence the morphogenesis. *V. fischeri* releases not only the anhydrous *N*-acetylglucosaminyl-1,6-anhydro-*N*-acetylmuramylalanyl-γ-glutamyldiaminopimelylalanine but also a reduced version (William Goldman, personal communication), which has not been assessed for its potential role as a morphogen. Analysis of the amount of this reduced monomer that is released in culture, and adding it to aposymbiotic squid will allow us to determine its potential role in the regression of the ciliated appendages. Other PG fragments also might have morphogenic activity and should be investigated.

MAMP signal perception by hosts

V. fischeri lipid A and PG monomers act as signals, and the role that particular genes play in their structure and release are extremely important; however, the reception of these signals by the squid host is also vital. Work being performed in the McFall-Ngai lab is investigating the expression of lipid binding protein and peptidoglycan receptor proteins as

potential signal receivers. *V. fischeri* mutants that alter signaling either by changing the structure of the lipid A moiety or by influencing the amount of PG monomer that is released will allow for a better understanding of these host proteins and how the squid senses and identifies its symbiont.

In this dissertation, I have identified genes responsible for altering the lipid A and for the release of PG monomer. The search for genes responsible for these signal molecules is showing that pathogens and symbionts are recognized by similar means. The lines between our perceptions of symbionts and pathogens are beginning to blur and the continued work in the area of these signaling molecules will only help in deciphering how a host is able to accept signals and determine the difference between beneficial and harmful bacteria.

REFERENCES

- 1. **Aderem, A., and R. J. Ulevitch.** 2000. Toll-like receptors in the induction of the innate immune response. Nature **406:**782-787.
- 2. Adin, D. M., N. J. Phillips, B. W. Gibson, M. A. Apicella, E. G. Ruby, M. J. McFall-Ngai, D. B. Hall, and E. V. Stabb. 2008. Characterization of *htrB* and *msbB* mutants of the light organ symbiont *Vibrio fischeri*. Appl. Environ. Microbiol. **74:**633-644.
- 3. **Aeckersberg, F., C. Lupp, B. Feliciano, and E. G. Ruby.** 2001. *Vibrio fischeri* outer membrane protein OmpU plays a role in normal symbiotic colonization. J. Bacteriol. **183:**6590-6597.
- 4. **Altschul, S. F., W. Gish, W. Miller, E. W. Myers, and D. J. Lipman.** 1990. Basic local alignment search tool. J. Mol. Biol. **215**:403-410.
- 5. Anderson, M. S., H. G. Bull, S. M. Galloway, T. M. Kelly, S. Mohan, K. Radika, and C. R. Raetz. 1993. UDP-N-acetylglucosamine acyltransferase of *Escherichia coli*. The first step of endotoxin biosynthesis is thermodynamically unfavorable. J. Biol. Chem. 268:19858-19865.
- 6. **Anton, P. M., V. Theodorou, S. Roy, J. Fioramonti, and L. Bueno.** 2002. Pathways involved in mild gastrointestinal inflammation induced by a low level exposure to a food contaminant. Dig. Dis. Sci. **47:**1308-1315.
- 7. Antunes, L. C., A. L. Schaefer, R. B. Ferreira, N. Qin, A. M. Stevens, E. G. Ruby, and E. P. Greenberg. 2007. Transcriptome analysis of the *Vibrio fischeri* LuxR-LuxI regulon. J. Bacteriol. **189:**8387-8391.
- 8. **Ast, J. C., I. Cleenwerck, K. Engelbeen, H. Urbanczyk, F. L. Thompson, P. De Vos, and P. V. Dunlap.** 2007. *Photobacterium kishitanii* sp. nov., a luminous marine bacterium symbiotic with deep-sea fishes. Int. J. Syst. Evol. Microbiol. **57:**2073-2078.
- 9. **Ayouba, A., C. Chatelain, and P. Rouge.** 1991. Legume lectins interact with muramic acid and *N*-acetylmuramic acid. FEBS Lett. **289:**102-104.
- 10. **Ayouba, A., D. Martin, and P. Rouge.** 1992. Recognition of muramic acid and *N*-acetylmuramic acid by *Leguminosae* lectins: possible role in plant-bacteria interactions. FEMS Microbiol. Lett. **92:**41-46.

- 11. **Babinski, K. J., S. J. Kanjilal, and C. R. Raetz.** 2002. Accumulation of the lipid A precursor UDP-2,3-diacylglucosamine in an *Escherichia coli* mutant lacking the *lpxH* gene. J. Biol. Chem. **277:**25947-25956.
- 12. **Babinski, K. J., A. A. Ribeiro, and C. R. Raetz.** 2002. The *Escherichia coli* gene encoding the UDP-2,3-diacylglucosamine pyrophosphatase of lipid A biosynthesis. J. Biol. Chem. **277:**25937-25946.
- 13. **Barreteau, H., A. Kovac, A. Boniface, M. Sova, S. Gobec, and D. Blanot.** 2008. Cytoplasmic steps of peptidoglycan biosynthesis. FEMS Microbiol. Rev. **32:**168-207.
- 14. **Bates, J. M., J. Akerlund, E. Mittge, and K. Guillemin.** 2007. Intestinal alkaline phosphatase detoxifies lipopolysaccharide and prevents inflammation in zebrafish in response to the gut microbiota. Cell Host Microbe. **2:**371-382.
- 15. **Bates, J. M., E. Mittge, J. Kuhlman, K. N. Baden, S. E. Cheesman, and K. Guillemin.** 2006. Distinct signals from the microbiota promote different aspects of zebrafish gut differentiation. Dev. Biol. **297:**374-386.
- 16. **Baumann, P., A. L. Furniss, and J. V. Lee.** 1984. Genus I. *Vibrio* Pacini 1854., p. 518-538. *In* N. R. Kreig and J. G. Holt (ed.), Bergey's Manual of Systematic Bacteriology, vol. 1. Williams & Wilkins, Baltimore.
- 17. **Belunis, C. J., and C. R. Raetz.** 1992. Biosynthesis of endotoxins. Purification and catalytic properties of 3-deoxy-D-manno-octulosonic acid transferase from *Escherichia coli*. J. Biol. Chem. **267**:9988-9997.
- 18. **Berry, S. S.** 1914. The cephalopoda of the Hawaiian islands. Bull. U. S. Bur. Fish. **32:**257-362.
- 19. **Bishop, R. E., H. S. Gibbons, T. Guina, M. S. Trent, S. I. Miller, and C. R. Raetz.** 2000. Transfer of palmitate from phospholipids to lipid A in outer membranes of gramnegative bacteria. EMBO J. **19:**5071-5080.
- 20. **Boettcher, K. J., and E. G. Ruby.** 1990. Depressed light emission by symbiotic *Vibrio fischeri* of the sepiolid squid *Euprymna scolopes*. J. Bacteriol. **172:**3701-3706.
- 21. **Boettcher, K. J., and E. G. Ruby.** 1994. Occurrence of plasmid DNA in the sepiolid squid symbiont *Vibrio fischeri*. Curr. Microbiol. **29:**279-286.
- 22. **Boettcher, K. J., E. G. Ruby, and M. J. McFall-Ngai.** 1996. Bioluminescence in the symbiotic squid *Euprymna scolopes* is controlled by daily biological rhythm. J. Comp. Physiol. A **179:**65-73.

- 23. **Bose, J. L., U. Kim, W. Bartkowski, R. P. Gunsalus, A. M. Overley, N. L. Lyell, K. L. Visick, and E. V. Stabb.** 2007. Bioluminescence in *Vibrio fischeri* is controlled by the redox-responsive regulator ArcA. Mol. Microbiol. **65:**538-553.
- 24. **Bose, J. L., C. S. Rosenberg, and E. V. Stabb.** 2008. Enhancement of symbiotic colonization and conditional attenuation of growth in culture. Arch. Microbiol. **In press**.
- 25. **Bou-M'handi, N., C. Jacquet, A. El Marrakchi, and P. Martin.** 2007. Phenotypic and molecular characterization of *Listeria monocytogenes* strains isolated from a marine environment in Morocco. Foodborne Pathog. Dis. **4:**409-417.
- 26. **Bouhss, A., A. E. Trunkfield, T. D. Bugg, and D. Mengin-Lecreulx.** 2008. The biosynthesis of peptidoglycan lipid-linked intermediates. FEMS Microbiol. Rev. **32:**208-233.
- 27. **Boylan, M., C. Miyamoto, L. Wall, A. Grahm, and E. Meighen.** 1989. Lux C, D, and E genes of the *Vibrio fischeri* luminescence operon code for the reductase, transferase, and synthetase enzymes involved in aldehyde biosyntheses. Photochem. Photobiol. **49:**681-688.
- 28. **Braun, V.** 1975. Covalent lipoprotein from the outer membrane of *Escherichia coli*. Biochim. Biophys. Acta **415**:335-377.
- 29. **Breznak, J. A.** 1982. Intestinal microbiota of termites and other xylophagous insects. Annu. Rev. Microbiol. **36:**323-343.
- 30. **Brozek, K. A., C. E. Bulawa, and C. R. Raetz.** 1987. Biosynthesis of lipid A precursors in *Escherichia coli*. A membrane-bound enzyme that transfers a palmitoyl residue from a glycerophospholipid to lipid X. J. Biol. Chem. **262:**5170-5179.
- 31. **Brozek, K. A., and C. R. Raetz.** 1990. Biosynthesis of lipid A in *Escherichia coli*. Acyl carrier protein-dependent incorporation of laurate and myristate. J. Biol. Chem. **265:**15410-15417.
- 32. **Buist, G., A. Steen, J. Kok, and O. P. Kuipers.** 2008. LysM, a widely distributed protein motif for binding to (peptido)glycans. Mol. Microbiol. **68:**838-847.
- 33. **Campanella, J. J., L. Bitincka, and J. Smalley.** 2003. MatGAT: an application that generates similarity/identity matrices using protein or DNA sequences. BMC Bioinformatics **4:**29.
- 34. Caroff, M., L. Aussel, H. Zarrouk, A. Martin, J. C. Richards, H. Therisod, M. B. Perry, and D. Karibian. 2001. Structural variability and originality of the *Bordetella* endotoxins. J. Endotoxin Res. 7:63-68.

- 35. **Caroff, M., and D. Karibian.** 2003. Structure of bacterial lipopolysaccharides. Carbohydr. Res. **338:**2431-2447.
- 36. Carty, S. M., K. R. Sreekumar, and C. R. H. Raetz. 1999. Effect of Cold Shock on Lipid A Biosynthesis in *Escherichia coli*. J. Biol. Chem. **274**:9677-9685.
- 37. **Cerda-Cuellar, M., J. Jofre, and A. R. Blanch.** 2000. A selective medium and a specific probe for detection of *Vibrio vulnificus*. Appl. Environ. Microbiol. **66:**855-859.
- 38. **Chahboune, A., M. Decaffmeyer, R. Brasseur, and B. Joris.** 2005. Membrane topology of the *Escherichia coli* AmpG permease required for recycling of cell wall anhydromuropeptides and AmpC beta-lactamase induction. Antimicrob. Agents Chemother. **49:**1145-1149.
- 39. Chen, C. Y., K. M. Wu, Y. C. Chang, C. H. Chang, H. C. Tsai, T. L. Liao, Y. M. Liu, H. J. Chen, A. B. Shen, J. C. Li, T. L. Su, C. P. Shao, C. T. Lee, L. I. Hor, and S. F. Tsai. 2003. Comparative genome analysis of *Vibrio vulnificus*, a marine pathogen. Genome Res. 13:2577-2587.
- 40. **Cheng, Q., H. Li, K. Merdek, and J. T. Park.** 2000. Molecular characterization of the beta-*N*-acetylglucosaminidase of *Escherichia coli* and its role in cell wall recycling. J. Bacteriol. **182:**4836-4840.
- 41. **Cheng, Q., and J. T. Park.** 2002. Substrate specificity of the AmpG permease required for recycling of cell wall anhydro-muropeptides. J. Bacteriol. **184:**6434-6436.
- 42. Chow, J. C., D. W. Young, D. T. Golenbock, W. J. Christ, and F. Gusovsky. 1999. Toll-like receptor-4 mediates lipopolysaccharide-induced signal transduction. J. Biol. Chem. 274:10689-10692.
- 43. Chun, C. K., T. E. Scheetz, F. Bonaldo Mde, B. Brown, A. Clemens, W. J. Crookes-Goodson, K. Crouch, T. DeMartini, M. Eyestone, M. S. Goodson, B. Janssens, J. L. Kimbell, T. A. Koropatnick, T. Kucaba, C. Smith, J. J. Stewart, D. Tong, J. V. Troll, S. Webster, J. Winhall-Rice, C. Yap, T. L. Casavant, M. J. McFall-Ngai, and M. B. Soares. 2006. An annotated cDNA library of juvenile *Euprymna scolopes* with and without colonization by the symbiont *Vibrio fischeri*. BMC Genomics 7:154-163.
- 44. **Claes, M. F., and P. V. Dunlap.** 2000. Aposymbiotic culture of the sepiolid squid *Euprymna scolopes*: role of the symbiotic bacterium *Vibrio fischeri* in host animal growth, development, and light organ morphogenesis. J. Exp. Zool. **286**:280-296.
- 45. **Clementz, T., J. J. Bednarski, and C. R. H. Raetz.** 1996. Function of the *htrB* high temperature requirement gene of *Escherchia coli* in the acylation of lipid A. J. Biol. Chem. **271**:12095-12102.

- 46. **Clementz, T., and C. R. Raetz.** 1991. A gene coding for 3-deoxy-D-manno-octulosonic-acid transferase in *Escherichia coli*. Identification, mapping, cloning, and sequencing. J. Biol. Chem. **266:**9687-9696.
- 47. **Clementz, T., Z. Zhou, and C. R. H. Raetz.** 1997. Function of the *Escherichia coli msbB* Gene, a multicopy suppressor of *htrB* knockouts, in the acylation of lipid A. J. Biol. Chem. **272**:10353-10360.
- 48. **Cloud, K. A.** 2004. Lytic transglycosylases are responsible for the production of peptidoglycan-derived cytotoxin in *Neisseria gonorrhoeae*. Ph.D. thesis. University of Wisconsin, Madison.
- 49. **Cloud, K. A., and J. P. Dillard.** 2002. A lytic transglycosylase of *Neisseria gonorrhoeae* is involved in peptidoglycan-derived cytotoxin production. Infect. Immun. **70**:2752-2757.
- 50. Cloud-Hansen, K. A., S. B. Peterson, E. V. Stabb, W. E. Goldman, M. J. McFall-Ngai, and J. Handelsman. 2006. Breaching the great wall: peptidoglycan and microbial interactions. Nat. Rev. Microbiol. 4:710-716.
- 51. **Cohen, A. L., J. D. Oliver, A. DePaola, E. J. Feil, and E. F. Boyd.** 2007. Emergence of a virulent clade of *Vibrio vulnificus* and correlation with the presence of a 33-kilobase genomic island. Appl. Environ. Microbiol. **73:**5553-5565.
- 52. Cookson, B. T., H.-L. Cho, L. A. Herwaldt, and W. E. Goldman. 1989. Biological activities and chemical composition of purified tracheal cytotoxin of *Bordetella pertussis*. Infect. Immun. 57:2223-2229.
- 53. **Cookson, B. T., A. N. Tyler, and W. E. Goldman.** 1989. Primary structure of the peptidoglycan-derived tracheal cytotoxin of *Bordetella pertussis*. Biochemistry **28:**1744-1749.
- 54. **Cox, A. D., J. Li, J. R. Brisson, E. R. Moxon, and J. C. Richards.** 2002. Structural analysis of the lipopolysaccharide from *Neisseria meningitidis* strain BZ157 *galE*: localisation of two phosphoethanolamine residues in the inner core oligosaccharide. Carbohydr. Res. **337:**1435-1444.
- 55. **D'Hauteville, H., S. Khan, D. J. Maskell, A. Kussak, A. Weintraub, J. Mathison, R. J. Ulevitch, N. Wuscher, C. Parsot, and P. J. Sansonetti.** 2002. Two *msbB* genes encoding maximal acylation of lipid A are required for invasive *Shigella flexneri* to mediate inflammatory rupture and destruction of the intestinal epithelium. J. Immunol. **168:**5240-5251.
- 56. **Darveau, R. P.** 1998. Lipid A diversity and the innate host responses to bacterial infection. Curr. Opin. Microbiol. **1:**36-42.

- 57. **Davidson, S. K., T. A. Koropatnick, R. Kossmehl, L. Sycuro, and M. J. McFall-Ngai.** 2004. NO means 'yes' in the squid-vibrio symbiosis: nitric oxide (NO) during the initial stages of a beneficial association. Cell. Microbiol. **6:**1139-1151.
- 58. Dazzo, F. B., G. L. Truchet, R. I. Hollingsworth, E. M. Hrabak, H. S. Pankratz, S. Philip-Hollingsworth, J. L. Salzwedel, K. Chapman, L. Appenzeller, A. Squartini, and et al. 1991. *Rhizobium* lipopolysaccharide modulates infection thread development in white clover root hairs. J. Bacteriol. 173:5371-5384.
- 59. **DeLoney, C. R., T. M. Bartley, and K. L. Visick.** 2002. Role for phosphoglucomutase in *Vibrio fischeri-Euprymna scolopes* symbiosis. J. Bacteriol. **184:**5121-5129.
- 60. **DeLoney-Marino, C. R., A. J. Wolfe, and K. L. Visick.** 2003. Chemoattraction of *Vibrio fischeri* to serine, nucleosides, and *N*-acetylneuraminic acid, a component of squid light-organ mucus. Appl. Environ. Microbiol. **69:**7527-7530.
- 61. **Demchick, P., and A. L. Koch.** 1996. The permeability of the wall fabric of *Escherichia coli* and *Bacillus subtilis*. J. Bacteriol. **178:**768-773.
- 62. **Doerrler, W. T., H. S. Gibbons, and C. R. Raetz.** 2004. MsbA-dependent translocation of lipids across the inner membrane of *Escherichia coli*. J. Biol. Chem. **279:**45102-45109.
- 63. **Doerrler, W. T., M. C. Reedy, and C. R. Raetz.** 2001. An *Escherichia coli* mutant defective in lipid export. J. Biol. Chem. **276:**11461-11464.
- 64. **Doino, J. A., and M. J. McFall-Ngai.** 1995. A transient exposure to symbiosiscompetent bacteria induces light organ morphogenesis in the host squid. Biol. Bull. **189:**347-355.
- 65. **Donovan, T. J., and P. van Netten.** 1995. Culture media for the isolation and enumeration of pathogenic *Vibrio* species in foods and environmental samples. Int. J. Food. Microbiol. **26:**77-91.
- 66. **Downie, J. A.** 2007. Plant science. Infectious heresy. Science **316:**1296-1297.
- 67. **Dryselius, R., K. Kurokawa, and T. Iida.** 2007. *Vibrionaceae*, a versatile bacterial family with evolutionarily conserved variability. Res. Microbiol. **158:**479-486.
- 68. **Dunn, A. K., M. O. Martin, and E. V. Stabb.** 2005. Characterization of pES213, a small mobilizable plasmid from *Vibrio fischeri*. Plasmid **54:**114-134.
- 69. **Dunn, A. K., D. S. Millikan, D. M. Adin, J. L. Bose, and E. V. Stabb.** 2006. New *rfp*-and pES213-derived tools for analyzing symbiotic *Vibrio fischeri* reveal patterns of infection and *lux* expression *in situ*. Appl. Environ. Microbiol. **72:**802-810.

- 70. **Dziarski, R.** 2004. Peptidoglycan recognition proteins (PGRPs). Mol. Immunol. **40:**877-886.
- 71. **Fallon, P. G., R. L. Allen, and T. Rich.** 2001. Primitive Toll signalling: bugs, flies, worms and man. Trends Immunol. **22:**63-66.
- 72. **Farmer, J. J. I., and F. W. Hickman-Brenner.** 2006. The genera *Vibrio* and *Photobacterium*, p. 508-563. *In* M. Dworkin, S. Falkow, E. Rosenberg, K. Schleifer, and E. Stackenbrandt (ed.), The Prokaryotes, 3rd ed, vol. 6. Springer, New York.
- 73. **Ferguson, G. P., A. Datta, J. Baumgartner, R. M. Roop, 2nd, R. W. Carlson, and G. C. Walker.** 2004. Similarity to peroxisomal-membrane protein family reveals that *Sinorhizobium* and *Brucella* BacA affect lipid-A fatty acids. Proc. Natl. Acad. Sci. USA **101:**5012-5017.
- 74. **Ferguson, G. P., A. Datta, R. W. Carlson, and G. C. Walker.** 2005. Importance of unusually modified lipid A in *Sinorhizobium* stress resistance and legume symbiosis. Mol. Microbiol. **56:**68-80.
- 75. **Foster, J. S., M. A. Apicella, and M. J. McFall-Ngai.** 2000. *Vibrio fisheri* lipopolysaccharide induces developmental apoptosis, but not complete morphogenesis, of the *Euprymna scolopes* symbiotic light organ. Dev. Biol. **226:**242-254.
- 76. **Foster, J. S., and M. J. McFall-Ngai.** 1998. Induction of apoptosis by cooperative bacteria in the morphogenesis of host epithelial tissues. Dev. Genes Evol. **208:**295-303.
- 77. **Fouz, B., F. J. Roig, and C. Amaro.** 2007. Phenotypic and genotypic characterization of a new fish-virulent *Vibrio vulnificus* serovar that lacks potential to infect humans. Microbiology **153:**1926-1934.
- 78. Galanos, C., O. Luderitz, E. T. Rietschel, O. Westphal, H. Brade, L. Brade, M. Freudenberg, U. Schade, M. Imoto, H. Yoshimura, S. Kusumoto, and T. Shiba. 1985. Synthetic and natural *Escherichia coli* free lipid A express identical endotoxic activities. Eur. J. Biochem. **148:**1-5.
- 79. **Garcia, D. L., and J. P. Dillard.** 2008. Mutations in *ampG* or *ampD* affect peptidoglycan fragment release from *Neisseria gonorrhoeae*. J. Bacteriol. **190**:3799-3807.
- 80. **Garrett, T. A., J. L. Kadrmas, and C. R. Raetz.** 1997. Identification of the gene encoding the *Escherichia coli* lipid A 4'-kinase. Facile phosphorylation of endotoxin analogs with recombinant LpxK. J. Biol. Chem. **272:**21855-64.
- 81. **Garrett, T. A., N. L. Que, and C. R. Raetz.** 1998. Accumulation of a lipid A precursor lacking the 4'-phosphate following inactivation of the *Escherichia coli lpxK* gene. J. Biol. Chem. **273**:12457-12465.

- 82. **Gelius, E., C. Persson, J. Karlsson, and H. Steiner.** 2003. A mammalian peptidoglycan recognition protein with *N*-acetylmuramoyl-L-alanine amidase activity. Biochem. Biophys. Res. Com. **306:**988-994.
- 83. **Gibbons, H. S., S. R. Kalb, R. J. Cotter, and C. R. Raetz.** 2005. Role of Mg²⁺ and pH in the modification of *Salmonella* lipid A after endocytosis by macrophage tumour cells. Mol. Microbiol. **55:**425-440.
- 84. **Gibbons, H. S., S. Lin, R. J. Cotter, and C. R. Raetz.** 2000. Oxygen requirement for the biosynthesis of the S-2-hydroxymyristate moiety in *Salmonella typhimurium* lipid A. Function of LpxO, A new Fe²⁺/α-ketoglutarate-dependent dioxygenase homologue. J. Biol. Chem. **275**:32940-32949.
- 85. **Gibbons, H. S., C. M. Reynolds, Z. Guan, and C. R. Raetz.** 2008. An Inner Membrane Dioxygenase that Generates the 2-Hydroxymyristate Moiety of *Salmonella* Lipid A. Biochemistry **47:**2814-2825.
- 86. **Gil-Turnes, M. S., and W. Fenical.** 1992. Embryos of *Homarus americanus* are protected by epibiotic bacteria. Biol. Bull. **182:**105-108.
- 87. **Gil-Turnes, M. S., M. E. Hay, and W. Fenical.** 1989. Symbiotic marine bacteria chemically defend crustacean embryos from a pathogenic fungus. Science **246**:116-118.
- 88. Girardin, S. E., I. G. Boneca, L. A. Carneiro, A. Antignac, M. Jehanno, J. Viala, K. Tedin, M. K. Taha, A. Labigne, U. Zahringer, A. J. Coyle, P. S. DiStefano, J. Bertin, P. J. Sansonetti, and D. J. Philpott. 2003. Nod1 detects a unique muropeptide from gram-negative bacterial peptidoglycan. Science 300:1584-1587.
- 89. Girardin, S. E., I. G. Boneca, J. Viala, M. Chamaillard, A. Labigne, G. Thomas, D. J. Philpott, and P. J. Sansonetti. 2003. Nod2 is a general sensor of peptidoglycan through muramyl dipeptide (MDP) detection. J. Biol. Chem. 278:8869-8872.
- 90. **Girardin, S. E., and D. J. Philpott.** 2004. Mini-review: the role of peptidoglycan recognition in innate immunity. Eur. J. Immunol. **34:**1777-1782.
- 91. **Girardin, S. E., L. H. Travassos, M. Herve, D. Blanot, I. G. Boneca, D. J. Philpott, P. J. Sansonetti, and D. Mengin-Lecreulx.** 2003. Peptidoglycan molecular requirements allowing detection by Nod1 and Nod2. J. Biol. Chem. **278**:41702-41708.
- 92. Giraud, E., L. Moulin, D. Vallenet, V. Barbe, E. Cytryn, J. C. Avarre, M. Jaubert, D. Simon, F. Cartieaux, Y. Prin, G. Bena, L. Hannibal, J. Fardoux, M. Kojadinovic, L. Vuillet, A. Lajus, S. Cruveiller, Z. Rouy, S. Mangenot, B. Segurens, C. Dossat, W. L. Franck, W. S. Chang, E. Saunders, D. Bruce, P. Richardson, P. Normand, B. Dreyfus, D. Pignol, G. Stacey, D. Emerich, A. Vermeglio, C. Medigue, and M. Sadowsky. 2007. Legumes symbioses: absence of *Nod* genes in photosynthetic bradyrhizobia. Science 316:1307-1312.

- 93. **Gittins, J. R., D. A. Phoenix, and J. M. Pratt.** 1994. Multiple mechanisms of membrane anchoring of *Escherichia coli* penicillin-binding proteins. FEMS Microbiol. Rev. **13:**1-12.
- 94. **Goldman, W. E., D. G. Klapper, and J. B. Baseman.** 1982. Detection, isolation, and analysis of a released *Bordetella pertussis* product toxic to cultured tracheal cells. Infect. Immun. **36:**782-794.
- 95. Golenbock, D. T., R. Y. Hampton, N. Qureshi, K. Takayama, and C. R. Raetz. 1991. Lipid A-like molecules that antagonize the effects of endotoxins on human monocytes. J. Biol. Chem. **266**:19490-19498.
- 96. **Goodell, E. W.** 1985. Recycling of murein by *Escherichia coli*. J. Bacteriol. **163:**305-310.
- 97. **Goodell, E. W., and C. F. Higgins.** 1987. Uptake of cell wall peptides by *Salmonella typhimurium* and *Escherichia coli*. J. Bacteriol. **169:**3861-3865.
- 98. **Goodell, E. W., and U. Schwarz.** 1985. Release of cell wall peptides into culture medium by exponentially growing *Escherichia coli*. J. Bacteriol. **162:**391-397.
- 99. **Goodson, M. S., W. J. Crookes-Goodson, J. R. Kimbell, and M. J. McFall-Ngai.** 2006. Characterization and role of p53 family members in the symbiont-induced morphogenesis of the *Euprymna scolopes* light organ. Biol. Bull. **211:**7-17.
- 100. Goodson, M. S., M. Kojadinovic, J. V. Troll, T. E. Scheetz, T. L. Casavant, M. B. Soares, and M. J. McFall-Ngai. 2005. Identifying components of the NF-κB pathway in the beneficial *Euprymna scolopes-Vibrio fischeri* light organ symbiosis. Appl. Environ. Microbiol. **71:**6934-6946.
- 101. **Graf, J., P. V. Dunlap, and E. G. Ruby.** 1994. Effect of transposon-induced motility mutations on colonization of the host light organ by *Vibrio fischeri*. J. Bacteriol. **176:**6986-6991.
- 102. **Graf, J., and E. G. Ruby.** 1998. Host-derived amino acids support the proliferation of symbiotic bacteria. Proc. Natl. Acad. Sci. USA **95**:1818-1822.
- 103. **Graf, J., and E. G. Ruby.** 2000. Novel effects of a transposon insertion in the *Vibrio fischeri glnD* gene: defects in iron uptake and symbiotic persistence in addition to nitrogen utilization. Mol. Microbiol. **37:**168-179.
- 104. Gueguen, Y., J. P. Cadoret, D. Flament, C. Barreau-Roumiguiere, A. L. Girardot, J. Garnier, A. Hoareau, E. Bachere, and J. M. Escoubas. 2003. Immune gene discovery by expressed sequence tags generated from hemocytes of the bacteria-challenged oyster, *Crassostrea gigas*. Gene 303:139-145.

- 105. **Gunn, J. S.** 2001. Bacterial modification of LPS and resistance to antimicrobial peptides. J. Endotoxin Res. **7:**57-62.
- 106. **Gunn, J. S., K. B. Lim, J. Krueger, K. Kim, L. Guo, M. Hackett, and S. I. Miller.** 1998. PmrA-PmrB-regulated genes necessary for 4-aminoarabinose lipid A modification and polymyxin resistance. Mol. Microbiol. **27:**1171-1182.
- 107. **Guo, L., K. B. Lim, J. S. Gunn, B. Bainbridge, R. P. Darveau, M. Hackett, and S. I. Miller.** 1997. Regulation of lipid A modifications by *Salmonella typhimurium* virulence genes *phoP-phoQ*. Science **276:**250-253.
- 108. Guo, L., K. B. Lim, C. M. Poduje, M. Daniel, J. S. Gunn, M. Hackett, and S. I. Miller. 1998. Lipid A acylation and bacterial resistance against vertebrate antimicrobial peptides. Cell 95:189-198.
- 109. **Hanahan, D.** 1983. Studies on transformation of *Escherichia coli* with plasmids. J. Mol. Biol. **166:**557-580.
- 110. **Harvey, N. E.** 1952. Bioluminescence. Academic Press, Inc., New York.
- 111. **Hastings, J. W., and K. H. Nealson.** 1981. The symbiotic luminous bacteria, p. 1332-1345. *In* M. P. Starr, H. Stolp, H. G. Truper, A. Balows, and H. G. Schlegel (ed.), The procaryotes. Springer-Verlag, New York.
- 112. Heidelberg, J. F., J. A. Eisen, W. C. Nelson, R. A. Clayton, M. L. Gwinn, R. J. Dodson, D. H. Haft, E. K. Hickey, J. D. Peterson, L. Umayam, S. R. Gill, K. E. Nelson, T. D. Read, H. Tettelin, D. Richardson, M. D. Ermolaeva, J. Vamathevan, S. Bass, H. Qin, I. Dragoi, P. Sellers, L. McDonald, T. Utterback, R. D. Fleishmann, W. C. Nierman, O. White, S. L. Salzberg, H. O. Smith, R. R. Colwell, J. J. Mekalanos, J. C. Venter, and C. M. Fraser. 2000. DNA sequence of both chromosomes of the cholera pathogen Vibrio cholerae. Nature 406:477-483.
- 113. **Heidrich, C., M. F. Templin, A. Ursinus, M. Merdanovic, J. Berger, H. Schwarz, M. A. de Pedro, and J. V. Höltje.** 2001. Involvement of *N*-acetylmuramyl-L-alanine amidases in cell separation and antibiotic-induced autolysis of *Escherichia coli*. Mol. Microbiol. **41:**167-178.
- 114. **Heidrich, C., A. Ursinus, J. Berger, H. Schwarz, and J. V. Höltje.** 2002. Effects of multiple deletions of murein hydrolases on viability, septum cleavage, and sensitivity to large toxic molecules in *Escherichia coli*. J. Bacteriol. **184:**6093-6099.
- 115. **Helander, I. M., I. Kilpelainen, and M. Vaara.** 1994. Increased substitution of phosphate groups in lipopolysaccharides and lipid A of the polymyxin-resistant *pmrA* mutants of *Salmonella typhimurium*: a 31P-NMR study. Mol. Microbiol. **11:**481-487.

- 116. **Henikoff, S., and J. G. Henikoff.** 1992. Amino acid substitution matrices from protein blocks. Proc. Natl. Acad. Sci. USA **89:**10915-10919.
- 117. **Henneke, P., and D. T. Golenbock.** 2002. Innate immune recognition of lipopolysaccharide by endothelial cells. Crit. Care Med. **30:**207-213.
- 118. **Hensey, S., and M. J. McFall-Ngai.** 1992. A surface peptide of the bacterium *Vibrio fischeri* plays a key role in specificity and recognition in the symbiosis with the squid *Euprymna scolopes*. Amer. Zool. **32:**37A.
- 119. **Herrero, M., V. de Lorenzo, and K. N. Timmis.** 1990. Transposon vectors containing non-antibiotic resistance selection markers for cloning and stable chromosomal insertion of foreign genes in gram-negative bacteria. J. Bacteriol. **172:**6557-6567.
- 120. **Herring, P. J.** 1977. Luminescence in cephalopods and fish. Symp. Zool. Soc. Lond. **38:**127-159.
- 121. **Heumann, D., and T. Roger.** 2002. Initial responses to endotoxins and Gram-negative bacteria. Clin. Chim. Acta. **323:**59-72.
- 122. **Hoffmann, J. A., F. C. Kafatos, C. A. Janeway, and R. A. Ezekowitz.** 1999. Phylogenetic perspectives in innate immunity. Science **284:**1313-1318.
- 123. Holben, W. E., P. Williams, M. A. Gilbert, M. Saarinen, L. K. Sarkilahti, and J. H. Apajalahti. 2002. Phylogenetic analysis of intestinal microflora indicates a novel *Mycoplasma phylotype* in farmed and wild salmon. Microb. Ecol. 44:175-185.
- 124. **Höltje, J. V., D. Mirelman, N. Sharon, and U. Schwarz.** 1975. Novel type of murein transglycosylase in *Escherichia coli*. J. Bacteriol. **124:**1067-1076.
- 125. **Hussa, E. A., T. M. O'Shea, C. L. Darnell, E. G. Ruby, and K. L. Visick.** 2007. Two-component response regulators of *Vibrio fischeri*: identification, mutagenesis, and characterization. J. Bacteriol. **189:**5825-5838.
- 126. **Ichige, A., and G. C. Walker.** 1997. Genetic analysis of the *Rhizobium meliloti bacA* gene: functional interchangeability with the *Escherichia coli sbmA* gene and phenotypes of mutants. J. Bacteriol. **179:**209-216.
- 127. Inohara, N., T. Koseki, L. del Peso, Y. Hu, C. Yee, S. Chen, R. Carrio, J. Merino, D. Liu, J. Ni, and G. Nunez. 1999. Nod1, an Apaf-1-like activator of caspase-9 and nuclear factor-κB. J. Biol. Chem. 274:14560-14567.
- 128. Inohara, N., Y. Ogura, A. Fontalba, O. Gutierrez, F. Pons, J. Crespo, K. Fukase, S. Inamura, S. Kusumoto, M. Hashimoto, S. J. Foster, A. P. Moran, J. L. Fernandez-Luna, and G. Nunez. 2003. Host recognition of bacterial muramyl dipeptide mediated through NOD2. Implications for Crohn's disease. J. Biol. Chem. 278:5509-5512.

- 129. **Jacobs, C., L. J. Huang, E. Bartowsky, S. Normark, and J. T. Park.** 1994. Bacterial cell wall recycling provides cytosolic muropeptides as effectors for beta-lactamase induction. EMBO J. **13**:4684-4694.
- 130. **Johannsen, L.** 1993. Biological properties of bacterial peptidoglycan. APMIS **101:**337-344.
- 131. **Jones, B. D., W. A. Nichols, B. W. Gibson, M. G. Sunshine, and M. A. Apicella.** 1997. Study of the role of the *htrB* gene in *Salmonella typhimurium* virulence. Infect. Immun. **65:**4778-4783.
- 132. **Jones, B. W., and M. K. Nishiguchi.** 2004. Counterillumination in the Hawaiian bobtail squid, *Euprymna scolopes* Berry (Mollusca: Cephalopoda). Mar. Biol. **144:**1151-1155.
- 133. **Jung, S. Y., Y. T. Jung, T. K. Oh, and J. H. Yoon.** 2007. *Photobacterium lutimaris* sp. nov., isolated from a tidal flat sediment in Korea. Int. J. Syst. Evol. Microbiol. **57:**332-336.
- 134. **Kanipes, M. I., S. Lin, R. J. Cotter, and C. R. Raetz.** 2001. Ca²⁺-induced phosphoethanolamine transfer to the outer 3-deoxy-D-manno-octulosonic acid moiety of *Escherichia coli* lipopolysaccharide. A novel membrane enzyme dependent upon phosphatidylethanolamine. J. Biol. Chem. **276:**1156-1163.
- 135. **Kavanagh, K., and E. P. Reeves.** 2007. Insect and mammalian innate immune responses are much alike. Microbe **2:**596-599.
- 136. **Kelly, T. M., S. A. Stachula, C. R. Raetz, and M. S. Anderson.** 1993. The *firA* gene of *Escherichia coli* encodes UDP-3-O-(R-3-hydroxymyristoyl)-glucosamine N-acyltransferase. The third step of endotoxin biosynthesis. J. Biol. Chem. **268:**19866-19874.
- 137. Kim, Y. R., S. E. Lee, C. M. Kim, S. Y. Kim, E. K. Shin, D. H. Shin, S. S. Chung, H. E. Choy, A. Progulske-Fox, J. D. Hillman, M. Handfield, and J. H. Rhee. 2003. Characterization and pathogenic significance of *Vibrio vulnificus* antigens preferentially expressed in septicemic patients. Infect. Immun. 71:5461-5471.
- 138. **Kimbell, J. R., T. A. Koropatnick, and M. J. McFall-Ngai.** 2006. Evidence for the participation of the proteasome in symbiont-induced tissue morphogenesis. Biol. Bull. **211:**1-6.
- 139. **Kimbell, J. R., and M. J. McFall-Ngai.** 2004. Symbiont-induced changes in host actin during the onset of a beneficial animal-bacterial association. Appl. Environ. Microbiol. **70**:1434-1441.

- 140. **Klena, J. D., R. S. Ashford, 2nd, and C. A. Schnaitman.** 1992. Role of *Escherichia coli* K-12 *rfa* genes and the *rfp* gene of *Shigella dysenteriae* 1 in generation of lipopolysaccharide core heterogeneity and attachment of O antigen. J. Bacteriol. **174:**7297-7307.
- 141. Koropatnick, T. A., J. T. Engle, M. A. Apicella, E. V. Stabb, W. E. Goldman, and M. J. McFall-Ngai. 2004. Microbial factor-mediated development in a host-bacterial mutualism. Science 306:1186-1188.
- 142. **Koropatnick, T. A., J. R. Kimbell, and M. J. McFall-Ngai.** 2007. Responses of host hemocytes during the initiation of the squid-*Vibrio* symbiosis. Biol. Bull. **212:**29-39.
- 143. **Kreig, N. R.** 1984. Bergey's Manual of Systematic Bacteriology, vol. I. Williams & Wilkins, Baltimore.
- 144. **Lamarcq, L. H., and M. J. McFall-Ngai.** 1998. Induction of a gradual, reversible morphogenesis of its host's epithelial brush border by *Vibrio fischeri*. Infect. Immun. **66:**777-785.
- 145. Lane, M. C., V. Lockatell, G. Monterosso, D. Lamphier, J. Weinert, J. R. Hebel, D. E. Johnson, and H. L. Mobley. 2005. Role of motility in the colonization of uropathogenic *Escherichia coli* in the urinary tract. Infect. Immun. 73:7644-7656.
- 146. **Laviña, M., A. P. Pugsley, and F. Moreno.** 1986. Identification, mapping, cloning and characterization of a gene (*sbmA*) required for microcin B17 action on *Escherichia coli* K12. J. Gen. Microbiol. **132:**1685-1693.
- 147. Le Roux, F., A. Goubet, F. L. Thompson, N. Faury, M. Gay, J. Swings, and D. Saulnier. 2005. *Vibrio gigantis* sp. nov., isolated from the haemolymph of cultured oysters (*Crassostrea gigas*). Int. J. Syst. Evol. Microbiol. 55:2251-2255.
- 148. **Lee, H., F. F. Hsu, J. Turk, and E. A. Groisman.** 2004. The PmrA-regulated pmrC gene mediates phosphoethanolamine modification of lipid A and polymyxin resistance in *Salmonella enterica*. J. Bacteriol. **186:**4124-4133.
- 149. **Lee, K.-H., and E. G. Ruby.** 1994. Competition between *Vibrio fischeri* strains during initiation and maintenance of a light organ symbiosis. J. Bacteriol. **176:**1985-1991.
- 150. **Lee, K.-H., and E. G. Ruby.** 1992. Detection of the light organ symbiont, *Vibrio fischeri*, in Hawaiian seawater by using *lux* gene probes. Appl. Environ. Microbiol. **58:**942-947.
- 151. **Lee, K.-H., and E. G. Ruby.** 1994. Effect of the squid host on the abundance and distribution of symbiotic *Vibrio fischeri* in nature. Appl. Environ. Microbiol. **60:**1565-1571.

- 152. **Lemus, J. D., and M. J. McFall-Ngai.** 2000. Alterations in the Proteome of the *Euprymna scolopes* Light Organ in Response to Symbiotic *Vibrio fischeri*. Appl. Environ. Microbiol. **66:**4091-4097.
- 153. Leulier, F., C. Parquet, S. Pili-Floury, J. H. Ryu, M. Caroff, W. J. Lee, D. Mengin-Lecreulx, and B. Lemaitre. 2003. The *Drosophila* immune system detects bacteria through specific peptidoglycan recognition. Nat. Immunol. 4:478-484.
- 154. Lindquist, S., K. Weston-Hafer, H. Schmidt, C. Pul, G. Korfmann, J. Erickson, C. Sanders, H. H. Martin, and S. Normark. 1993. AmpG, a signal transducer in chromosomal beta-lactamase induction. Mol. Microbiol. 9:703-715.
- 155. Liu, C., E. Gelius, G. Liu, H. Steiner, and R. Dziarski. 2000. Mammalian peptidoglycan recognition protein binds peptidoglycan with high affinity, is expressed in neutrophils, and inhibits bacterial growth. J. Biol. Chem. 275:24490-24499.
- 156. Loppnow, H., H. Brade, I. Durrbaum, C. A. Dinarello, S. Kusumoto, E. T. Rietschel, and H. D. Flad. 1989. IL-1 induction-capacity of defined lipopolysaccharide partial structures. J. Immunol. 142:3229-3238.
- 157. **Lupp, C., R. E. Hancock, and E. G. Ruby.** 2002. The *Vibrio fischeri sapABCDF* locus is required for normal growth, both in culture and in symbiosis. Arch. Microbiol. **179:**57-65.
- 158. **Lupp, C., and E. G. Ruby.** 2005. *Vibrio fischeri* uses two quorum-sensing systems for the regulation of early and late colonization factors. J. Bacteriol. **187:**3620-3629.
- 159. **Lupp, C., M. Urbanowski, E. P. Greenberg, and E. G. Ruby.** 2003. The *Vibrio fischeri* quorum-sensing systems *ain* and *lux* sequentially induce luminescence gene expression and are important for persistence in the squid host. Mol. Microbiol. **50:**319-331.
- 160. **Lyon, R. S.** 2001. Tracheal cytotoxin production by the *Bordetellae*. Ph.D. thesis. Washington University, St. Louis.
- Mackinnon, F. G., A. D. Cox, J. S. Plested, C. M. Tang, K. Makepeace, P. A. Coull, J. C. Wright, R. Chalmers, D. W. Hood, J. C. Richards, and E. R. Moxon. 2002. Identification of a gene (*lpt-3*) required for the addition of phosphoethanolamine to the lipopolysaccharide inner core of *Neisseria meningitidis* and its role in mediating susceptibility to bactericidal killing and opsonophagocytosis. Mol. Microbiol. 43:931-943.
- 162. Madsen, E. B., L. H. Madsen, S. Radutoiu, M. Olbryt, M. Rakwalska, K. Szczyglowski, S. Sato, T. Kaneko, S. Tabata, N. Sandal, and J. Stougaard. 2003. A receptor kinase gene of the LysM type is involved in legume perception of rhizobial signals. Nature 425:637-640.

- 163. Makino, K., K. Oshima, K. Kurokawa, K. Yokoyama, T. Uda, K. Tagomori, Y. Iijima, M. Najima, M. Nakano, A. Yamashita, Y. Kubota, S. Kimura, T. Yasunaga, T. Honda, H. Shinagawa, M. Hattori, and T. Iida. 2003. Genome sequence of Vibrio parahaemolyticus: a pathogenic mechanism distinct from that of Vibrio cholerae. Lancet 361:743-749.
- 164. **Martin, S. A., R. S. Rosenthal, and K. Biemann.** 1987. Fast atom bombardment mass spectrometry and tandem mass spectrometry of biologically active peptidoglycan monomers from *Neisseria gonorrhoeae*. J. Biol. Chem. **262:**7514-7522.
- 165. **Massad, G., and J. D. Oliver.** 1987. New selective and differential medium for *Vibrio cholerae* and *Vibrio vulnificus*. Appl. Environ. Microbiol. **53:**2262-2264.
- Mathis, R., F. Van Gijsegem, R. De Rycke, W. D'Haeze, E. Van Maelsaeke, E. Anthonio, M. Van Montagu, M. Holsters, and D. Vereecke. 2005. Lipopolysaccharides as a communication signal for progression of legume endosymbiosis. Proc. Natl. Acad. Sci. USA 102:2655-2660.
- 167. Mattiuzzo, M., A. Bandiera, R. Gennaro, M. Benincasa, S. Pacor, N. Antcheva, and M. Scocchi. 2007. Role of the *Escherichia coli* SbmA in the antimicrobial activity of proline-rich peptides. Mol. Microbiol. **66:**151-163.
- 168. **McCann, J., E. V. Stabb, D. S. Millikan, and E. G. Ruby.** 2003. Population dynamics of *Vibrio fischeri* during infection of *Euprymna scolopes*. Appl. Environ. Microbiol. **69:**5928-5934.
- 169. **McFall-Ngai, M.** 2007. Adaptive immunity: care for the community. Nature **445:**153.
- 170. **McFall-Ngai, M. J.** 1994. Animal-bacterial interactions in the early life history of marine invertebrates: The *Euprymna scolopes/Vibrio fischeri* symbiosis. Amer. Zool. **34:**554-561.
- 171. **McFall-Ngai, M. J.** 2002. Review: Unseen Forces: The Influence of Bacteria on Animal Development. Dev. Biol. **242:**1-14.
- 172. **McFall-Ngai, M. J., and M. K. Montgomery.** 1990. The anatomy and morphology of the adult bacterial light organ of *Euprymna scolopes* Berry (Cephalopoda:Sepiolidae). Biol. Bull. **179:**332-339.
- 173. **McFall-Ngai, M. J., and E. G. Ruby.** 1998. *Sepiolids* and *Vibrios*: When first they meet. BioScience **48:**257-265.
- 174. **McFall-Ngai, M. J., and E. G. Ruby.** 1991. Symbiont recognition and subsequent morphogenesis as early events in an animal-bacterial mutualism. Science **254**:1491-1494.

- 175. **Melly, M. A., Z. A. McGee, and R. S. Rosenthal.** 1984. Ability of monomeric peptidoglycan fragments from *Neisseria gonorrhoeae* to damage human fallopian-tube mucosa. J. Infect. Dis. **149:**378-386.
- 176. **Miller, J. H.** 1992. A short course in bacterial genetics. Cold Spring Harbor Laboratory Press, Cold Spring Harbor, N.Y.
- 177. **Millikan, D. S., and E. G. Ruby.** 2002. Alterations in *Vibrio fischeri* motility correlate with a delay in symbiosis initiation and are associated with additional symbiotic colonization defects. Appl. Environ. Microbiol. **68:**2519-2528.
- 178. **Millikan, D. S., and E. G. Ruby.** 2003. FlrA, a sigma54-dependent transcriptional activator in *Vibrio fischeri*, is required for motility and symbiotic light-organ colonization. J. Bacteriol. **185:**3547-3557.
- 179. **Millikan, D. S., and E. G. Ruby.** 2004. *Vibrio fischeri* flagellin A is essential for normal motility and for symbiotic competence during initial squid light organ colonization. J. Bacteriol. **186:**4315-4325.
- 180. **Montagnani, C., C. Kappler, J. M. Reichhart, and J. M. Escoubas.** 2004. Cg-Rel, the first Rel/NF-κB homolog characterized in a mollusk, the Pacific oyster *Crassostrea gigas*. FEBS Lett. **561:**75-82.
- 181. **Montagnani, C., Y. Labreuche, and J. M. Escoubas.** 2008. Cg-IκB, a new member of the IκB protein family characterized in the pacific oyster *Crassostrea gigas*. Dev. Comp. Immunol. **32:**182-190.
- 182. **Montgomery, M. K., and M. J. McFall-Ngai.** 1994. Bacterial symbionts induce host organ morphogenesis during early postembryonic development of the squid *Euprymna scolopes*. Development **120:**1719-1729.
- 183. **Montgomery, M. K., and M. J. McFall-Ngai.** 1993. Embryonic development of the light organ of the sepiolid squid *Euprymna scolopes* Berry. Biol. Bull. **184:**296-308.
- 184. **Moran, D., S. J. Turner, and K. D. Clements.** 2005. Ontogenetic development of the gastrointestinal microbiota in the marine herbivorous fish *Kyphosus sydneyanus*. Microb. Ecol. **49:**590-597.
- 185. **Moynihan, M.** 1982. Notes on the behavior of *Euprymna scolopes* (Cephalopoda: Sepiolidae). Behavior **85:**25-41.
- 186. **Murray, G. L., S. R. Attridge, and R. Morona.** 2003. Regulation of *Salmonella typhimurium* lipopolysaccharide O-antigen chain length is required for virulence; identification of FepE as a second Wzz. Mol. Microbiol. **47:**1395-1406.

- 187. **Nelson, D. E., A. S. Ghosh, A. L. Paulson, and K. D. Young.** 2002. Contribution of membrane-binding and enzymatic domains of penicillin binding protein 5 to maintenance of uniform cellular morphology of *Escherichia coli*. J. Bacteriol. **184:**3630-3639.
- 188. **Netea, M. G., M. van Deuren, B. J. Kullberg, J.-M. Cavaillon, and J. W. M. Van der Meer.** 2002. Does the shape of lipid A determine the interaction of LPS with Toll-like receptors? Trends Immunol. **23:**135-139.
- 189. Niwa, S., M. Kawaguchi, H. Imazumi-Anraku, S. A. Chechetka, M. Ishizaka, A. Ikuta, and H. Kouchi. 2001. Responses of a model legume *Lotus japonicus* to lipochitin oligosaccharide nodulation factors purified from *Mesorhizobium loti* JRL501. Mol. Plant-Microbe Interact. 14:848-856.
- 190. **Nogi, Y., N. Masui, and C. Kato.** 1998. *Photobacterium profundum* sp. nov., a new, moderately barophilic bacterial species isolated from a deep-sea sediment. Extremophiles **2:1**-7.
- 191. **Nyholm, S. V., B. Deplancke, H. R. Gaskins, M. A. Apicella, and M. J. McFall-Ngai.** 2002. Roles of *Vibrio fischeri* and nonsymbiotic bacteria in the dynamics of mucus secretion during symbiont colonization of the *Euprymna scolopes* light organ. Appl. Environ. Microbiol. **68:**5113-5122.
- 192. **Nyholm, S. V., and M. J. McFall-Ngai.** 2003. Dominance of *Vibrio fischeri* in secreted mucus outside the light organ of *Euprymna scolopes*: the first site of symbiont specificity. Appl. Environ. Microbiol. **69:**3932-3937.
- 193. **Nyholm, S. V., and M. J. McFall-Ngai.** 1998. Sampling the light-organ microenvironment of *Euprymna scolopes*: description of a population of host cells in association with the bacterial symbiont *Vibrio fischeri*. Biol. Bull. **195**:89-97.
- 194. **Nyholm, S. V., and M. J. McFall-Ngai.** 2004. The winnowing: establishing the squid-vibrio symbiosis. Nat. Rev. Microbiol. **2:**632-642.
- 195. **Nyholm, S. V., E. V. Stabb, E. G. Ruby, and M. J. McFall-Ngai.** 2000. Establishment of an animal-bacterial association: Recruiting symbiotic vibrios from the environment. Proc. Natl. Acad. Sci. USA **97:**10231-10235.
- 196. Overbeek, R., T. Begley, R. M. Butler, J. V. Choudhuri, H. Y. Chuang, M. Cohoon, V. de Crecy-Lagard, N. Diaz, T. Disz, R. Edwards, M. Fonstein, E. D. Frank, S. Gerdes, E. M. Glass, A. Goesmann, A. Hanson, D. Iwata-Reuyl, R. Jensen, N. Jamshidi, L. Krause, M. Kubal, N. Larsen, B. Linke, A. C. McHardy, F. Meyer, H. Neuweger, G. Olsen, R. Olson, A. Osterman, V. Portnoy, G. D. Pusch, D. A. Rodionov, C. Ruckert, J. Steiner, R. Stevens, I. Thiele, O. Vassieva, Y. Ye, O. Zagnitko, and V. Vonstein. 2005. The subsystems approach to genome annotation and its use in the project to annotate 1000 genomes. Nucleic Acids Res. 33:5691-5702.

- 197. **Parducz, B.** 1967. Ciliary movement and coordination in ciliates. Int. Rev. Cytol. **21:**91-128.
- 198. **Park, J. T., and T. Uehara.** 2008. How bacteria consume their own exoskeletons (turnover and recycling of cell wall peptidoglycan). Microbiol. Mol. Biol. Rev. **72:**211-227.
- 199. **Park, Y. D., K. S. Baik, C. N. Seong, K. S. Bae, S. Kim, and J. Chun.** 2006. *Photobacterium ganghwense* sp. nov., a halophilic bacterium isolated from sea water. Int. J. Syst. Evol. Microbiol. **56:**745-749.
- 200. **Parquet, C., B. Flouret, M. Leduc, Y. Hirota, and J. van Heijenoort.** 1983. *N*-acetylmuramoyl-L-alanine amidase of *Escherichia coli* K12. Possible physiological functions. Eur. J. Biochem. **133:**371-377.
- 201. Persing, D. H., R. N. Coler, M. J. Lacy, D. A. Johnson, J. R. Baldridge, R. M. Hershberg, and S. G. Reed. 2002. Taking toll: lipid A mimetics as adjuvants and immunomodulators. Trends Microbiol. 10:S32-37.
- 202. **Phillips, N. J., B. Schilling, M. K. McLendon, M. A. Apicella, and B. W. Gibson.** 2004. Novel modification of lipid A of *Francisella tularensis*. Infect. Immun. **72:**5340-5348.
- 203. **Pinheiro, J. C., and D. M. Bates.** 2000. Mixed-effects models in S and S-PLUS. Springer, New York.
- 204. Poltorak, A., X. He, I. Smirnova, M. Y. Liu, C. Van Huffel, X. Du, D. Birdwell, E. Alejos, M. Silva, C. Galanos, M. Freudenberg, P. Ricciardi-Castagnoli, B. Layton, and B. Beutler. 1998. Defective LPS signaling in C3H/HeJ and C57BL/10ScCr mice: mutations in Tlr4 gene. Science 282:2085-2088.
- 205. **Post, D. M., N. J. Phillips, J. Q. Shao, D. D. Entz, B. W. Gibson, and M. A. Apicella.** 2002. Intracellular survival of *Neisseria gonorrhoeae* in male urethral epithelial cells: importance of a hexaacyl lipid A. Infect. Immun. **70:**909-920.
- 206. **Radika, K., and C. R. Raetz.** 1988. Purification and properties of lipid A disaccharide synthase of *Escherichia coli*. J. Biol. Chem. **263**:14859-14867.
- 207. **Raetz, C. R., C. M. Reynolds, M. S. Trent, and R. E. Bishop.** 2007. Lipid A modification systems in gram-negative bacteria. Annu. Rev. Biochem. **76:**295-329.
- 208. **Raetz, C. R. H., and C. Whitfield.** 2002. Lipopolysaccharide Endotoxins. Annu. Rev. Microbiol. **71:**635-700.
- 209. **Ramesh, A., and V. K. Venugopalan.** 1988. Cellulolytic activity of luminous bacteria. World J. Microbiol. Biotechnol. **4:**227-230.

- 210. **Rawls, J. F., M. A. Mahowald, R. E. Ley, and J. I. Gordon.** 2006. Reciprocal gut microbiota transplants from zebrafish and mice to germ-free recipients reveal host habitat selection. Cell **127:**423-433.
- 211. **Rawls, J. F., B. S. Samuel, and J. I. Gordon.** 2004. Gnotobiotic zebrafish reveal evolutionarily conserved responses to the gut microbiota. Proc. Natl. Acad. Sci. USA **101:**4596-4601.
- 212. **Ray, B. L., G. Painter, and C. R. Raetz.** 1984. The biosynthesis of gram-negative endotoxin. Formation of lipid A disaccharides from monosaccharide precursors in extracts of *Escherichia coli*. J. Biol. Chem. **259**:4852-4859.
- 213. **Reynolds, C. M., S. R. Kalb, R. J. Cotter, and C. R. Raetz.** 2005. A phosphoethanolamine transferase specific for the outer 3-deoxy-D-manno-octulosonic acid residue of *Escherichia coli* lipopolysaccharide. Identification of the *eptB* gene and Ca²⁺ hypersensitivity of an *eptB* deletion mutant. J. Biol. Chem. **280**:21202-21211.
- 214. **Reynolds, C. M., A. A. Ribeiro, S. C. McGrath, R. J. Cotter, C. R. Raetz, and M. S. Trent.** 2006. An outer membrane enzyme encoded by *Salmonella typhimurium lpxR* that removes the 3'-acyloxyacyl moiety of lipid A. J. Biol. Chem. **281:**21974-21987.
- 215. Rietschel, E. T., T. Kirikae, F. U. Schade, U. Mamat, G. Schmidt, H. Loppnow, A. J. Ulmer, U. Zähringer, U. Seydel, F. Di Padova, M. Schreier, and H. Brade. 1994. Bacterial endotoxin: molecular relationships of structure to activity and function. FASEB J. 8:217-225.
- 216. Rivas, R., P. Garcia-Fraile, P. F. Mateos, E. Martinez-Molina, and E. Velazquez. 2006. *Photobacterium halotolerans* sp. nov., isolated from Lake Martel in Spain. Int. J. Syst. Evol. Microbiol. **56:**1067-1071.
- 217. Roach, J. C., G. Glusman, L. Rowen, A. Kaur, M. K. Purcell, K. D. Smith, L. E. Hood, and A. Aderem. 2005. The evolution of vertebrate Toll-like receptors. Proc. Natl. Acad. Sci. USA 102:9577-9582.
- 218. **Robey, M., W. O'Connell, and N. P. Cianciotto.** 2001. Identification of *Legionella pneumophila rcp*, a *pagP*-like gene that confers resistance to cationic antimicrobial peptides and promotes intracellular infection. Infect. Immun. **69:**4276-4286.
- 219. Rodas-Suarez, O. R., J. F. Flores-Pedroche, J. M. Betancourt-Rule, E. I. Quinones-Ramirez, and C. Vazquez-Salinas. 2006. Occurrence and antibiotic sensitivity of *Listeria monocytogenes* strains isolated from oysters, fish, and estuarine water. Appl. Environ. Microbiol. **72:**7410-7412.
- 220. **Rosenthal, R. S.** 1979. Release of soluble peptidoglycan from growing gonococci: Hexaminidase and amidase activities. Infect. Immun. **24:**869-878.

- 221. **Rosenthal, R. S., W. Nogami, B. T. Cookson, W. E. Goldman, and W. J. Folkening.** 1987. Major fragment of soluble peptidoglycan released from growing *Bordetella pertussis* is tracheal cytotoxin. Infect. Immun. **55:**2117-2120.
- 222. **Ruby**, **E. G.** 1996. Lessons from a cooperative bacterial-animal association: The *Vibrio fisheri-Euprymna scolopes* light organ symbiosis. Annu. Rev. Microbiol. **50:**591-624.
- 223. **Ruby, E. G., and L. M. Asato.** 1993. Growth and flagellation of *Vibrio fischeri* during initiation of the sepiolid squid light organ symbiosis. Arch. Microbiol. **159**:160-167.
- 224. **Ruby, E. G., E. P. Greenberg, and J. W. Hastings.** 1980. Planktonic marine luminous bacteria: Species distribution in the water column. Appl. Environ. Microbiol. **39:**302-306.
- 225. **Ruby, E. G., and M. J. McFall-Ngai.** 1992. A squid that glows in the night: Development of an animal-bacterial mutualism. J. Bacteriol. **174:**4865-4870.
- 226. Ruby, E. G., M. Urbanowski, J. Campbell, A. Dunn, M. Faini, R. Gunsalus, P. Lostroh, C. Lupp, J. McCann, D. Millikan, A. Schaefer, E. Stabb, A. Stevens, K. Visick, C. Whistler, and E. P. Greenberg. 2005. Complete genome sequence of *Vibrio fischeri*: a symbiotic bacterium with pathogenic congeners. Proc. Natl. Acad. Sci. USA 102:3004-3009.
- 227. **Russell, J. B., and J. L. Rychlik.** 2001. Factors that alter rumen microbial ecology. Science **292:**1119-1122.
- 228. Rutherford, K., J. Parkhill, J. Crook, T. Horsnell, P. Rice, M. A. Rajandream, and B. Barrell. 2000. Artemis: sequence visualization and annotation. Bioinformatics 16:944-945.
- 229. Safa, A., N. A. Bhuyian, S. Nusrin, M. Ansaruzzaman, M. Alam, T. Hamabata, Y. Takeda, D. A. Sack, and G. B. Nair. 2006. Genetic characteristics of Matlab variants of *Vibrio cholerae* O1 that are hybrids between classical and El Tor biotypes. J. Med. Microbiol. 55:1563-1569.
- 230. Salzman, A. L., T. Eaves-Pyles, S. C. Linn, A. G. Denenberg, and C. Szabo. 1998. Bacterial induction of inducible nitric oxide synthase in cultured human intestinal epithelial cells. Gastroenterology 114:93-102.
- 231. **Sambrook, J., E. F. Fritsch, and T. Maniatis.** 1989. Molecular Cloning: A Laboratory Manual, Second ed, vol. 3. Cold Spring Harbor Laboratory Press.
- 232. Sauvage, E., F. Kerff, M. Terrak, J. A. Ayala, and P. Charlier. 2008. The penicillin-binding proteins: structure and role in peptidoglycan biosynthesis. FEMS Microbiol. Rev. 32:234-258.

- 233. **Sawabe, T., Y. Fujimura, K. Niwa, and H. Aono.** 2007. *Vibrio comitans* sp. nov., *Vibrio rarus* sp. nov. and *Vibrio inusitatus* sp. nov., from the gut of the abalones *Haliotis discus discus*, *H. gigantea*, *H. madaka* and *H. rufescens*. Int. J. Syst. Evol. Microbiol. **57:**916-922.
- 234. **Scheidle, H., A. Gross, and K. Niehaus.** 2005. The Lipid A substructure of the *Sinorhizobium meliloti* lipopolysaccharides is sufficient to suppress the oxidative burst in host plants. New Phytol. **165**:559-565.
- 235. **Scheurwater, E., C. W. Reid, and A. J. Clarke.** 2008. Lytic transglycosylases: Bacterial space-making autolysins. Int. J. Biochem. Cell. Biol. **40:**586-591.
- 236. Schromm, A. B., K. Brandenburg, H. Loppnow, U. Zahringer, E. T. Rietschel, S. F. Carroll, M. H. Koch, S. Kusumoto, and U. Seydel. 1998. The charge of endotoxin molecules influences their conformation and IL-6-inducing capacity. J. Immunol. 161:5464-5471.
- 237. Serichantalergs, O., N. A. Bhuiyan, G. B. Nair, O. Chivaratanond, A. Srijan, L. Bodhidatta, S. Anuras, and C. J. Mason. 2007. The dominance of pandemic serovars of *Vibrio parahaemolyticus* in expatriates and sporadic cases of diarrhoea in Thailand, and a new emergent serovar (O3: K46) with pandemic traits. J. Med. Microbiol. 56:608-613.
- 238. Seshadri, R., S. W. Joseph, A. K. Chopra, J. Sha, J. Shaw, J. Graf, D. Haft, M. Wu, Q. Ren, M. J. Rosovitz, R. Madupu, L. Tallon, M. Kim, S. Jin, H. Vuong, O. C. Stine, A. Ali, A. J. Horneman, and J. F. Heidelberg. 2006. Genome sequence of *Aeromonas hydrophila* ATCC 7966T: jack of all trades. J. Bacteriol. 188:8272-8282.
- 239. Sharypova, L. A., K. Niehaus, H. Scheidle, O. Holst, and A. Becker. 2003. *Sinorhizobium meliloti acpXL* mutant lacks the C28 hydroxylated fatty acid moiety of lipid A and does not express a slow migrating form of lipopolysaccharide. J. Biol. Chem. 278:12946-12954.
- 240. **Shockman, G. D., and J. V. Höltje.** 1994. Microbial peptidoglycan (murein) hydrolases, p. 131-166. *In* J.-M. Ghuysen and R. Hackenbeck (ed.), Bacterial cell wall. Elsevier, Amsterdam, New York.
- 241. **Silverman, N., and T. Maniatis.** 2001. NF-κB signaling pathways in mammalian and insect innate immunity. Genes Dev. **15**:2321-2342.
- 242. **Sinha, R. K., and R. S. Rosenthal.** 1980. Release of soluble peptidoglycan from growing gonococci: Demonstration of anhydro-muramyl-containing fragments. Infect. Immun. **29:**914-925.
- 243. **Small, A. L., and M. J. McFall-Ngai.** 1999. Halide peroxidase in tissues that interact with bacteria in the host squid *Euprymna scolopes*. J. Cell. Biochem. **72:**445-457.

- 244. **Somerville, J. E., Jr, L. Cassiano, B. Bainbridge, M. D. Cunningham, and R. P. Darveau.** 1996. A novel *Escherichia coli* lipid A mutant that produces an antiinflammatory lipolysaccharide. J. Clin. Invest. **97:**359-365.
- 245. **Somerville, J. E., Jr, L. Cassiano, and R. P. Darveau.** 1999. *Escherichia coli msbB* gene as a virulence factor and a therapeutic target. Infect. Immun. **67:**6583-6590.
- 246. Spaink, H. P., D. M. Sheeley, A. A. van Brussel, J. Glushka, W. S. York, T. Tak, O. Geiger, E. P. Kennedy, V. N. Reinhold, and B. J. Lugtenberg. 1991. A novel highly unsaturated fatty acid moiety of lipo-oligosaccharide signals determines host specificity of *Rhizobium*. Nature **354**:125-130.
- 247. **Stabb, E. V.** 2005. Shedding light on the bioluminescence "paradox". ASM News **71**:223-229.
- 248. **Stabb, E. V.** 2006. The *Vibrio fischeri-Euprymna scolopes* light organ symbiosis, p. 204-218. *In* F. L. Thompson, B. Austin, and J. Swings (ed.), The Biology of Vibrios. ASM Press, Washington D.C.
- 249. **Stabb, E. V., M. S. Butler, and D. M. Adin.** 2004. Correlation between osmolarity and luminescence of symbiotic *Vibrio fischeri* strain ES114. J. Bacteriol. **186:**2906-2908.
- 250. **Stabb, E. V., K. A. Reich, and E. G. Ruby.** 2001. *Vibrio fischeri* genes *hvnA* and *hvnB* encode secreted NAD⁺-glycohydrolases. J. Bacteriol. **183:**309-317.
- 251. **Stabb, E. V., and E. G. Ruby.** 2003. Contribution of *pilA* to competitive colonization of the squid *Euprymna scolopes* by *Vibrio fischeri*. Appl. Environ. Microbiol. **69:**820-826.
- 252. **Stabb, E. V., and E. G. Ruby.** 2002. RP4-based plasmids for conjugation between *Escherichia coli* and members of the Vibrionaceae. Meth. Enzymol. **358:**413-426.
- 253. **Stabb, E. V., K. L. Visick, D. S. Millikan, A. A. Corcoran, L. Gibson, S. V. Nyholm, M. McFall-Ngai, and E. G. Ruby.** 2001. The *Vibrio fischeri-Euprymna scolopes* symbiosis: A model marine animal-bacteria interaction, p. 269-277. *In* N. K. Saxena (ed.), Recent Advances in Marine Science and Technology, 2000. PACON International, Honolulu, Hawaii.
- 254. **Stecher, B., S. Hapfelmeier, C. Muller, M. Kremer, T. Stallmach, and W. D. Hardt.** 2004. Flagella and chemotaxis are required for efficient induction of *Salmonella enterica* serovar Typhimurium colitis in streptomycin-pretreated mice. Infect. Immun. **72:**4138-4150.
- 255. **Sugita, H., and Y. Ito.** 2006. Identification of intestinal bacteria from Japanese flounder (*Paralichthys olivaceus*) and their ability to digest chitin. Lett. Appl. Microbiol. **43:**336-342.

- 256. **Swords, W. E., D. L. Chanc, L. A. Cohn, J. Shao, M. A. Apicella, and A. L. Smith.** 2002. Acylation of the lipooligosaccharide of *Haemophilus influenzae* and colonization: an *htrB* mutation diminishes the colonization of human airway epithelial cells. Infect. Immun. **70**:4661-4668.
- 257. **Sycuro, L. K., E. G. Ruby, and M. McFall-Ngai.** 2006. Confocal microscopy of the light organ crypts in juvenile *Euprymna scolopes* reveals their morphological complexity and dynamic function in symbiosis. J. Morphol. **267:**555-568.
- 258. **Tam, C., and D. Missiakas.** 2005. Changes in lipopolysaccharide structure induce the σ^E-dependent response of *Escherichia coli*. Mol. Microbiol. **55:**1403-1412.
- 259. **Tamayo, R., B. Choudhury, A. Septer, M. Merighi, R. Carlson, and J. S. Gunn.** 2005. Identification of *cptA*, a PmrA-regulated locus required for phosphoethanolamine modification of the *Salmonella enterica* serovar typhimurium lipopolysaccharide core. J. Bacteriol. **187:**3391-3399.
- 260. **Tamura, K., J. Dudley, M. Nei, and S. Kumar.** 2007. *MEGA4*: Molecular Evolutionary Genetics Analysis (MEGA) software version 4.0. Mol. Biol. Evol. **24:**1596-1599.
- 261. **Tellström, V., B. Usadel, O. Thimm, M. Stitt, H. Küster, and K. Niehaus.** 2007. The lipopolysaccharide of *Sinorhizobium meliloti* suppresses defense-associated gene expression in cell cultures of the host plant *Medicago truncatula*. Plant Physiol. **143:**825-837.
- 262. **Templin, M. F., A. Ursinus, and J. V. Höltje.** 1999. A defect in cell wall recycling triggers autolysis during the stationary growth phase of *Escherichia coli*. EMBO J. **18:**4108-4117.
- 263. **Thompson, F. L., B. Austin, and J. G. Swings.** 2006. The Biology of Vibrios. Blackwell Publishing.
- 264. Thompson, F. L., B. Hoste, C. C. Thompson, J. Goris, B. Gomez-Gil, L. Huys, P. De Vos, and J. Swings. 2002. *Enterovibrio norvegicus* gen. nov., sp. nov., isolated from the gut of turbot (*Scophthalmus maximus*) larvae: a new member of the family *Vibrionaceae*. Int. J. Syst. Evol. Microbiol. **52:**2015-2022.
- 265. **Thompson, F. L., and K. E. Klose.** 2006. Vibrio2005: the First International Conference on the Biology of Vibrios. J. Bacteriol. **188:**4592-4596.
- 266. **Tinnert, A. S., M. Mansson, H. H. Yildirim, D. W. Hood, and E. K. Schweda.** 2005. Structural investigation of lipopolysaccharides from nontypeable *Haemophilus influenzae*: investigation of inner-core phosphoethanolamine addition in NTHi strain 981. Carbohydr. Res. **340**:1900-1907.

- 267. **Tobias, P. S., K. Soldau, and R. J. Ulevitch.** 1989. Identification of a lipid A binding site in the acute phase reactant lipopolysaccharide binding protein. J. Biol. Chem. **264:**10867-10871.
- 268. **Tobias, P. S., K. Soldau, and R. J. Ulevitch.** 1986. Isolation of a lipopolysaccharide-binding acute phase reactant from rabbit serum. J. Exp. Med. **164:**777-793.
- 269. Tomarev, S. I., R. D. Zinovieva, V. M. Weis, A. B. Chepelinsky, J. Piatigorsky, and M. J. McFall-Ngai. 1993. Abundant mRNAs in the squid light organ encode proteins with a high similarity to mammalian peroxidases. Gene 132:219-226.
- 270. **Touzé, T., A. X. Tran, J. V. Hankins, D. Mengin-Lecreulx, and M. S. Trent.** 2008. Periplasmic phosphorylation of lipid A is linked to the synthesis of undecaprenyl phosphate. Mol. Microbiol. **67:**264-277.
- 271. **Trent, M. S., W. Pabich, C. R. Raetz, and S. I. Miller.** 2001. A PhoP/PhoQ-induced Lipase (PagL) that catalyzes 3-O-deacylation of lipid A precursors in membranes of *Salmonella typhimurium*. J. Biol. Chem. **276:**9083-9092.
- 272. **Trent, M. S., A. A. Ribeiro, S. Lin, R. J. Cotter, and C. R. Raetz.** 2001. An inner membrane enzyme in *Salmonella* and *Escherichia coli* that transfers 4-amino-4-deoxy-L-arabinose to lipid A: induction on polymyxin-resistant mutants and role of a novel lipid-linked donor. J. Biol. Chem. **276:**43122-43131.
- 273. **Uehara, T., and J. T. Park.** 2007. An anhydro-*N*-acetylmuramyl-L-alanine amidase with broad specificity tethered to the outer membrane of *Escherichia coli*. J. Bacteriol. **189:**5634-5641.
- 274. **Ulitzur, S., and J. W. Hastings.** 1979. Evidence for tetradecanal as the natural aldehyde in bacterial bioluminescence. Proc. Natl. Acad. Sci. USA **76:**265-267.
- 275. **van der Ley, P., L. Steeghs, H. jan Hamstra, J. ten Hove, B. Zomer, and L. van Alphen.** 2001. Modification of lipid A biosynthesis in *Neisseria meningitidis lpxL* mutants: Influence on lipopolysaccharide structure, toxicity, and adjuvant activity. Infect. Immun. **69:**5981-5990.
- 276. **van Heijenoort, J., C. Parquet, B. Flouret, and Y. van Heijenoort.** 1975. Envelope-bound N-acetylmuramyl-L-alanine amidase of *Escherichia coli* K 12. Purification and properties of the enzyme. Eur. J. Biochem. **58:**611-619.
- 277. **Van Heijenoort, Y., and J. Van Heijenoort.** 1971. Study of the *N*-acetylmuramyl-L-alanine amidase activity in *Escherichia coli*. FEBS Lett. **15:**137-141.

- 278. **Vedam, V., J. G. Haynes, E. L. Kannenberg, R. W. Carlson, and D. J. Sherrier.** 2004. A *Rhizobium leguminosarum* lipopolysaccharide lipid A mutant induces nitrogenfixing nodules with delayed and defective bacteroid formation. Mol. Plant-Microbe Interact. **17:**283-291.
- 279. **Vedam, V., E. Kannenberg, A. Datta, D. Brown, J. G. Haynes-Gann, D. J. Sherrier, and R. W. Carlson.** 2006. The pea nodule environment restores the ability of a *Rhizobium leguminosarum* lipopolysaccharide *acpXL* mutant to add 27-hydroxyoctacosanoic acid to its lipid A. J. Bacteriol. **188:**2126-2133.
- 280. Vedam, V., E. L. Kannenberg, J. G. Haynes, D. J. Sherrier, A. Datta, and R. W. Carlson. 2003. A *Rhizobium leguminosarum acpXL* mutant produces lipopolysaccharide lacking 27-hydroxyoctacosanoic acid. J. Bacteriol. **185**:1841-1850.
- Vezzi, A., S. Campanaro, M. D'Angelo, F. Simonato, N. Vitulo, F. M. Lauro, A. Cestaro, G. Malacrida, B. Simionati, N. Cannata, C. Romualdi, D. H. Bartlett, and G. Valle. 2005. Life at depth: *Photobacterium profundum* genome sequence and expression analysis. Science 307:1459-1461.
- 282. Visick, K. L., J. Foster, J. Doino, M. McFall-Ngai, and E. G. Ruby. 2000. Vibrio fischeri lux genes play an important role in colonization and development of the host light organ. J. Bacteriol. 182:4578-4586.
- 283. **Visick, K. L., and M. J. McFall-Ngai.** 2000. An exclusive contract: specificity in the *Vibrio fischeri-Euprymna scolopes* partnership. J. Bacteriol. **182:**1779-1787.
- 284. Visick, K. L., T. M. O'Shea, A. H. Klein, K. Geszvain, and A. J. Wolfe. 2007. The sugar phosphotransferase system of *Vibrio fischeri* inhibits both motility and bioluminescence. J. Bacteriol. **189:**2571-2574.
- 285. **Visick, K. L., and E. G. Ruby.** 1998. The periplasmic, group III catalase of *Vibrio fischeri* is required for normal symbiotic competence and is induced both by oxidative stress and by approach to stationary phase. J. Bacteriol. **180:**2087-2092.
- 286. **Visick, K. L., and E. G. Ruby.** 2006. *Vibrio fischeri* and its host: it takes two to tango. Curr. Opin. Microbiol. **9:**632-638.
- 287. **Visick, K. L., and L. M. Skoufos.** 2001. Two-component sensor required for normal symbiotic colonization of *Euprymna scolopes* by *Vibrio fischeri*. J. Bacteriol. **183:**835-842.
- 288. **Vollmer, W., D. Blanot, and M. A. de Pedro.** 2008. Peptidoglycan structure and architecture. FEMS Microbiol. Rev. **32:**149-167.
- 289. **Vollmer, W., B. Joris, P. Charlier, and S. Foster.** 2008. Bacterial peptidoglycan (murein) hydrolases. FEMS Microbiol. Rev. **32:**259-286.

- 290. **Vorachek-Warren, M. K., S. Ramirez, R. J. Cotter, and C. R. H. Raetz.** 2002. A triple mutant of *Escherichia coli* lacking secondary acyl chains on lipid A. J. Biol. Chem. **277:**14194-14205.
- 291. **Votsch, W., and M. F. Templin.** 2000. Characterization of a β-*N*-acetylglucosaminidase of *Escherichia coli* and elucidation of its role in muropeptide recycling and β-lactamase induction. J. Biol. Chem. **275:**39032-39038.
- 292. Wang, Z. M., X. Li, R. R. Cocklin, M. Wang, K. Fukase, S. Inamura, S. Kusumoto, D. Gupta, and R. Dziarski. 2003. Human peptidoglycan recognition protein-L is an *N*-acetylmuramoyl-L-alanine amidase. J. Biol. Chem. **278**:49044-49052.
- 293. Warnecke, F., P. Luginbuhl, N. Ivanova, M. Ghassemian, T. H. Richardson, J. T. Stege, M. Cayouette, A. C. McHardy, G. Djordjevic, N. Aboushadi, R. Sorek, S. G. Tringe, M. Podar, H. G. Martin, V. Kunin, D. Dalevi, J. Madejska, E. Kirton, D. Platt, E. Szeto, A. Salamov, K. Barry, N. Mikhailova, N. C. Kyrpides, E. G. Matson, E. A. Ottesen, X. Zhang, M. Hernandez, C. Murillo, L. G. Acosta, I. Rigoutsos, G. Tamayo, B. D. Green, C. Chang, E. M. Rubin, E. J. Mathur, D. E. Robertson, P. Hugenholtz, and J. R. Leadbetter. 2007. Metagenomic and functional analysis of hindgut microbiota of a wood-feeding higher termite. Nature 450:560-565.
- 294. **Wei, S. L., and R. E. Young.** 1989. Development of symbiotic bacterial bioluminescence in a nearshore cephalopod, *Euprymna scolopes*. Mar. Biol. **103:**541-546.
- 295. **Weimer, P. J.** 1998. Manipulating ruminal fermentation: a microbial ecological perspective. J. Anim. Sci. **76:**3114-3122.
- 296. **Weis, V. M., A. L. Small, and M. J. McFall-Ngai.** 1996. A peroxidase related to the mammalian antimicrobial protein myeloperoxidase in the *Euprymna-Vibrio* mutualism. Proc. Natl. Acad. Sci. USA **93:**13683-13688.
- 297. Whistler, C. A., T. A. Koropatnick, A. Pollack, M. J. McFall-Ngai, and E. G. Ruby. 2007. The GacA global regulator of *Vibrio fischeri* is required for normal host tissue responses that limit subsequent bacterial colonization. Cell. Microbiol. 9:766-778.
- 298. **Whistler, C. A., and E. G. Ruby.** 2003. GacA regulates symbiotic colonization traits of *Vibrio fischeri* and facilitates a beneficial association with an animal host. J. Bacteriol. **185:**7202-7212.
- 299. White, K. A., I. A. Kaltashov, R. J. Cotter, and C. R. Raetz. 1997. A mono-functional 3-deoxy-D-manno-octulosonic acid (Kdo) transferase and a Kdo kinase in extracts of *Haemophilus influenzae*. J. Biol. Chem. 272:16555-16563.

- 300. White, K. A., S. Lin, R. J. Cotter, and C. R. Raetz. 1999. A *Haemophilus influenzae* gene that encodes a membrane bound 3-deoxy-D-manno-octulosonic acid (Kdo) kinase. Possible involvement of Kdo phosphorylation in bacterial virulence. J. Biol. Chem. **274:**31391-31400.
- 301. **Wientjes, F. B., C. L. Woldringh, and N. Nanninga.** 1991. Amount of peptidoglycan in cell walls of gram-negative bacteria. J. Bacteriol. **173:**7684-7691.
- 302. **Wolfe, A. J., and H. C. Berg.** 1989. Migration of bacteria in semisolid agar. Proc. Natl. Acad. Sci. USA **86:**6973-6977.
- 303. Wright, J. C., D. W. Hood, G. A. Randle, K. Makepeace, A. D. Cox, J. Li, R. Chalmers, J. C. Richards, and E. R. Moxon. 2004. *lpt6*, a gene required for addition of phosphoethanolamine to inner-core lipopolysaccharide of *Neisseria meningitidis* and *Haemophilus influenzae*. J. Bacteriol. **186**:6970-6982.
- 304. Wright, S. D., R. A. Ramos, P. S. Tobias, R. J. Ulevitch, and J. C. Mathison. 1990. CD14, a receptor for complexes of lipopolysaccharide (LPS) and LPS binding protein. Science **249**:1431-1433.
- 305. Wright, S. D., P. S. Tobias, R. J. Ulevitch, and R. A. Ramos. 1989. Lipopolysaccharide (LPS) binding protein opsonizes LPS-bearing particles for recognition by a novel receptor on macrophages. J. Exp. Med. 170:1231-1241.
- 306. **Yip, E. S., K. Geszvain, C. R. DeLoney-Marino, and K. L. Visick.** 2006. The symbiosis regulator *rscS* controls the *syp* gene locus, biofilm formation and symbiotic aggregation by *Vibrio fischeri*. Mol. Microbiol. **62:**1586-1600.
- 307. **Yip, E. S., B. T. Grublesky, E. A. Hussa, and K. L. Visick.** 2005. A novel, conserved cluster of genes promotes symbiotic colonization and sigma-dependent biofilm formation by *Vibrio fischeri*. Mol. Microbiol. **57:**1485-1498.
- 308. **Yorgey, P., J. Lee, J. Kordel, E. Vivas, P. Warner, D. Jebaratnam, and R. Kolter.** 1994. Posttranslational modifications in microcin B17 define an additional class of DNA gyrase inhibitor. Proc. Natl. Acad. Sci. USA **91:**4519-4523.
- 309. Young, K., L. L. Silver, D. Bramhill, P. Cameron, S. S. Eveland, C. R. Raetz, S. A. Hyland, and M. S. Anderson. 1995. The *envA* permeability/cell division gene of *Escherichia coli* encodes the second enzyme of lipid A biosynthesis. UDP-3-O-(R-3-hydroxymyristoyl)-N-acetylglucosamine deacetylase. J. Biol. Chem. 270:30384-30391.
- 310. **Zemke-White, W. L., K. D. Clements, and P. J. Harris.** 1999. Acid lysis of macroalgae by marine herbivorous fishes: myth or digestive mechanism? J. Exp. Mar. Biol. Ecol. **233:**95-113.

- 311. **Zhou, Z., A. A. Ribeiro, S. Lin, R. J. Cotter, S. I. Miller, and C. R. Raetz.** 2001. Lipid A modifications in polymyxin-resistant *Salmonella typhimurium*: PMRA-dependent 4-amino-4-deoxy-L-arabinose, and phosphoethanolamine incorporation. J. Biol. Chem. **276:**43111-43121.
- 312. **Zhou, Z., K. A. White, A. Polissi, C. Georgopoulos, and C. R. Raetz.** 1998. Function of *Escherichia coli* MsbA, an essential ABC family transporter, in lipid A and phospholipid biosynthesis. J. Biol. Chem. **273**:12466-12475.

Appendix A

CHARACTERIZATION OF GENES THAT ALTER VIBRIO FISCHERI LPS 4

⁴ Adin, D.M., Phillips, N.J., Gibson, B.W., Apicella, M.A., Stabb, E.V. Unpublished.

Introduction

The lipid A of *Vibrio fischeri* is thought to have unusual structural modifications, although the complete structure is not yet known. The major lipid A species are hexa-acylated to octa-acylated and appear to have the novel additions of an N-linked 3-OH C_{14:1}, a C_{16:1}, and a 172 Da moiety (Nancy Phillips, personal communication). This 172 Da moiety is removable by a mild hydrazine treatment that is used to remove O-linked fatty acids from the LPS. This observation and the molecular weight suggest that the 172 Da moiety may be a phosphoglycerol. The importance of this and the other modifications during symbiotic colonization are untested.

Some bacteria modify their lipid A in ways that increase resistance to antimicrobial peptides and enable full colonization of hosts (207). In certain *Salmonella* strains, there can be significant remodeling of the lipid A moiety (e.g. see Figure 1.5 in Chapter 1). For example, PmrC/EptA (148) and ArnT (272) decorate lipid A with phosphoethanolamine (PEA) and aminoarabinose (L-Ara4N), respectively, leading to increased polymyxin resistance. PagP is activated by PhoPQ, and adds a palmitate acylation to lipid A in the presence of low Mg^{2+} , also increaseing polymyxin resistance (108). LpxO attaches a hydroxyl group to an acyl chain on lipid A and transcription of lpxO is induced by low pH and Mg^{2+} levels, conditions like those within macrophages; however, lipid A species under a variety of conditions still contain this hydroxyl group (84, 85). The PagL deacylase removes a primary acylation at the 3-position and is PhoPQ dependent (271). LpxR is a Ca^{2+} dependent deacylase that removes the primary acylation containing the myristate secondary acylation at the 1-position of the lipid A (214, 271).

Our goals in this project were to identify transferases responsible for adding the putative phosphoglycerol or the $C_{16:1}$ acylation to lipid A. We also sought to test the importance of such modifications during symbiotic colonization. We searched the *V. fischeri* genome for potential

phosphogylcerol transferases and transporters of acylations, and found three potential candidate genes for a phosphoglycerol transferase and one candidate for a long chain fatty acid transporter. Mutations in each of these genes affected LPS structure; however, none of the genes was required for the addition of the putative phosphoglycerol (172 Da) moiety or the long chain fatty acid to lipid A, and none had an apparent symbiosis-specific role for *V. fischeri*.

Materials and Methods

Bacterial strains, plasmids and growth conditions. *V. fischeri* strains used in this study are listed in Table 1. *Escherichia coli* strains DH5αλpir (68) and TOP10 (Invitrogen, Carlsbad, CA) were used for cloning R6K-based and pCR-BluntII-TOPO derived vectors, respectively, while CC118λpir (119) carrying pEVS104 (252) was used as a conjugative helper in triparental matings. All *E. coli* strains were incubated at 37°C. Genotypes of these *E. coli* strains are provided in Chapter 2 (Table 1.1). When added to LB medium (176) for selection of *E. coli*, kanamycin (Kn) was used at a concentration of 40 μg ml⁻¹. For selection of *E. coli* with erythromycin (Em), 150 μg ml⁻¹ was added to BHI medium (Difco, Sparks, MD). *V. fischeri* was grown at 28°C in LBS (250) or at 24°C in SWT (24). When added to LBS for selection of *V. fischeri*, Em was used at a concentration of 5 μg ml⁻¹. Agar was added to a final concentration of 1.5% for solid media.

DNA and plasmid manipulations. Plasmids were generated using standard cloning methods, as described in Chapter 3.

Table A.1. V. fischeri strains, select plasmids, and oligonucleotides

Strain, plasmid, or oligonucleotide				
V. fischeri strains				
DMA370	ES114 bacA::pDMA49; EmR	This study		
DMA390	ES114 pgtA1::pDMA64; EmR	This study		
DMA391	ES114 pgtA2::pDMA87; EmR	This study		
DMA392	ES114 pgtA3::pDMA88; EmR	This study		
ES114	Wild-type isolate from <i>E. scolopes</i>	(20)		
<u>Plasmids</u>		. , ,		
pCR-BluntII-TOPO	TOPO PCR-cloning vector; KnR	Invitrogen		
pDMA46	internal bacA fragment (PCR product; primers dma32 and	This study		
	dma33, ES114 template) in pCR-BluntII TOPO; KnR	, ,		
pDMA49	pDMA46 BglII fragment in BamHI-digested pEVS122;	This study		
•	internal bacA fragment; oriV _{R6Ky} oriT _{RP4} EmR			
pDMA64	internal pgtA1fragment (PCR product; primers dma64 and	This study		
	dma65, ES114 template) BglII-digested in BamHI-			
	digested pEVS122; EmR			
pDMA79	internal pgtA2 fragment (PCR product; primers dma69 and	This study		
	dma70, ES114 template) in pCR-BluntII TOPO;			
	KnR			
pDMA80	internal pgtA3 fragment (PCR product; primers dma71 and	This study		
1	dma72, ES114 template) in pCR-BluntII TOPO;			
	KnR			
pDMA87	pDMA79 <i>Bgl</i> II fragment in <i>Bam</i> HI-digested pEVS122;	This study		
	internal $pgtA2$ fragment; $oriV_{R6K_{\gamma}}$ $oriT_{RP4}$ EmR			
pDMA88	pDMA80 <i>Bgl</i> II fragment in <i>Bam</i> HI-digested pEVS122;	This study		
	internal $ptgA3$ fragment; $oriV_{R6K_{\gamma}}$ $oriT_{RP4}$ EmR			
pEVS122	$oriV_{ m R6K_{Y}}$ $oriT_{ m RP4}$ EmR lac Z $lpha$	(68)		
Oligonucleotides ^b				
dma32	5' GGC <u>AGATCT</u> GCGCCATGAACGAGCACTATACAA 3'	This study		
dma33	5' CGG <u>AGATCT</u> GTTGTGGCGCACATCATCAAACAG 3'	This study		
dma64	5' GGC <u>AGATCT</u> GGTATTTGCCCAATACCGATTCCAT 3'	This study		
dma65	5' CGG <u>AGATCT</u> CCATAGATTTGGGGTGTTCTCAGC 3'	This study		
dma69	5' GGC <u>AGATCT</u> CCCCAAATGGCATTATTGCGCTTGAATGGGC 3'	This study		
dma70	5' CGG <u>AGATCT</u> GCCGGTAAGTAGTTCGCGACATTACGCCAC 3'	This study		
dma71	5' GGC <u>AGATCT</u> GCGCGCTACATTCCCGCTCTCTTACC 3'	This study		
dma72	5' GCC <u>AGATCT</u> CGAAATCGGCGCAGCGTCATCGTATTCAGAAAC 3'	This study		

^a Abbreviations used: EmR, erythromycin resistance; KnR, kanamycin resistance; StrR, streptomycin resistance.

^b Underlined sequences indicate restriction enzyme recognition sites added to primers ($Bgl\Pi$; A/GATCT).

Mutant construction. Descriptions of select plasmids and the primers used in mutant construction are provided in Table A.1. To generate mutants, an internal fragment of each targeted gene was PCR amplified and either cloned directly into pEVS122 (a mobilizable vector that does not replicate in *V. fischeri*) or cloned into pCR-BluntII-TOPO vector and subsequently subcloned into pEVS122. The resulting plasmids were mobilized into *V. fischeri* using triparental matings (252), and homologous recombination between the genome and the internal gene fragment resulted in insertion of this fragment and the rest of the plasmid into the gene of interest, generating vector integration mutants of the wild-type strain ES114.

Bioinformatic Analyses. Protein sequence comparisons to Genbank entries were generated using BLAST-P (4). Genomes with similar regions surrounding each gene were found using the SEED pinned region search (196).

Luminescence and motility Assays. Motility and luminescence were assessed as described in Chapter 2.

Squid colonization assays. For infection with individual *V. fischeri* strains, *E. scolopes* juveniles were inoculated within 4 h of hatching as previously described (223). *E. scolopes* were maintained in Instant Ocean (Aquarium Systems, Mentor, OH) mixed to ~36 ppt. *E. scolopes* were exposed to inocula for up to 14 h before being rinsed in *V. fischeri*-free Instant Ocean. Infection kinetics and competition experiments were assessed as described in Chapter 2.

LPS and lipid A purification and analysis. LPS was purified from V. fischeri strains as described previously (205) except for samples from DMA370 (bacA). DMA370 (bacA) LPS partitioned into the phenol phase instead of the water phase in the phenol-water separation step in the previous method (205). To isolate the LPS from DMA370 (bacA), bacteria were collected from plates and washed three times with distilled water to lyse the cells. The washed pellet was resuspended in 20 ml distilled water and French pressed (14,000 psi) three times. The resulting fluid was centrifuged at 15,000 x g for 20 min to remove large debris and any intact cells. The resulting supernatant was exposed to 10 mg ml⁻¹ Staphylococcal nuclease and was incubated overnight at 37°C. SDS and Proteinase K were added at 2% final concentration and 10 µg ml⁻¹, respectively, and placed at 56°C for 1 h and then 37°C overnight. To remove the SDS, 2 ml of 3M sodium acetate and 30 ml -20°C ethanol was added to the proteinase K extract and the LPS was precipitated at -20°C overnight. The precipitate was collected by centrifugation (5000 x g for 15 min) and resuspended in 5 ml distilled water. This was reprecipitated twice using 0.5 ml of 3 M sodium acetate and 10 ml -20°C ethanol overnight at -20°C. The pellet was reconstituted in 20 ml distilled water and centrifuged at 160,000 x g for 2 hours. The translucent pellet of LPS at the bottom of the tube was collected, reconstituted in distilled water, and recentrifuged two additional times to remove any final contaminating proteins and nucleotides. After the final centrifugation, the pellet was reconstituted in 3 ml distilled water and lyophilized. For lipid A analysis, LPS samples were treated with a 1% total concentration acetic acid that hydrolyzes the lipid A from the intact LPS. Lipid A samples were analyzed by matrix-assisted laser desorption ionization-time-of-flight mass spectrometry (MALDI-TOF MS) on a Voyager DESTR Plus (Applied Biosystems, Framingham, MA) equipped with a 337 nm nitrogen laser as previously described (2).

Preparation of O-deacylated lipid A and lipopolysaccharides (O-LPS). Typically, ~0.3 mg of V. fischeri LPS or ~0.3 mg of lipid A was treated with 60 μl of anhydrous hydrazine (Sigma Chemical Co, St. Louis, MO) at 37°C for 40 min, with occasional vortexing. Samples were then cooled in an ice bath, treated with 5 volumes (300 μl) of ice-cold acetone added drop-wise, and allowed to sit at -20°C for 1-2 h to precipitate the O-LPS. The reaction mixtures were then centrifuged at $12,000 \times g$ for 30 minutes at 4°C. Supernatants were removed and the O-LPS pellets were washed with 100 μl of chilled acetone and centrifuged a second time. Finally, the O-LPS pellets were dissolved in 40 μl of HPLC-grade water (Fisher Scientific, Fair Lawn, NJ) and evaporated to dryness on a speed-vac concentrator. To remove salts and other low molecular weight contaminants, the O-LPS samples were dissolved in 20 μl of HPLC-grade water, and 5-μl aliquots were desalted by drop dialysis on VSWP 0.025-μm pore size nitrocellulose membranes (Millipore, Billerica, MA) over Milli-Q de-ionized water (Millipore, Billerica, MA) for 1 h. Dialyzed samples were then evaporated to dryness.

Prior to MALDI-TOF mass spectrometric analysis, the dialyzed O-LPS samples were redissolved in 5 μl of HPLC-grade water and 1-μl aliquots were desalted with cation-exchange resin (Dowex 50W-X8, NH₄⁺ form; BioRad, Hercules, CA) and then mixed 1:1 with matrix (a saturated solution of 2,5-dihydroxybenzoic acid in acetone). Samples were spotted on a stainless steel MALDI target, allowed to air dry, and then analyzed on a Voyager DESTR Plus mass spectrometer (Applied Biosystems, Framingham, MA) equipped with a 337-nm nitrogen laser. All spectra were recorded in the negative-ion linear mode with delayed extraction and an accelerating voltage of 20 kV. Approximately 200 laser shots were acquired for each sample. The spectra were smoothed with a 19-point Savitsky-Golay function and mass calibrated with an

external mass calibrant consisting of renin substrate tetradecapeptide, insulin chain B (oxidized), and bovine insulin (Sigma Chemical Co, St. Louis, MO).

Results

Targeting of potential phosphoglycerol transferase genes in V. fischeri. To identify potential phosphoglycerol transferases, we searched the V. fischeri genome for genes that encoded proteins similar to both phosphoglycerol transferases (226) and to enzymes known to decorate the ketodeoxyoctonate (KDO) portion of lipid A, such as ArnT and PmrC (148, 272). Three possible candidate ORFs were found, VF0137, VF0131 and VF1650. Each of these encode proteins with significant homology to phosphoglycerol transferases and putative sulfatases when compared to the Genbank database using BLAST-P (4). The three genes were named pgtA1 (VF0137), pgtA2 (VF0131), and pgtA3 (VF1650). The three genes and the proteins that they encode have poor homology to each other. ptgA1 is embedded in a gene cluster that appears to direct KDO incorporation into LPS alongwith KDO phosphorylation, and ptgA2 is just upstream of this gene cluster. pgtA3 does not appear to be closely linked to any genes for LPS By analyzing the surrounding genes using the SEED program (196), we biosynthesis. determined that pgtA3 is found in a similar genetic context in other Vibrios, including Vibrio cholerae, V. parahaemolyticus, and V. vulnificus. pgtA1 and pgtA2 have significant homology to genes found in V. vulnificus, V. harveyi and V. cholerae, but are not found in a similar genetic context on the chromosome.

Targeting potential C_{16} acyltransferase genes in V. fischeri. The genome of V. fischeri also possesses a homolog of BacA, which is important in the addition of the unusual very-long-chain

fatty acid of Sinorhizobium meliloti and Brucella abortus (73). Comparisons of O-deacylated to non-deacylated lipid A suggested that the lipid A of V. fischeri contained a C_{16:0} acylation, and we hypothesized that BacA may be responsible for the incorporation of the apparent $C_{16:0}$ acylation in V. fischeri lipid A. We therefore also targeted bacA for analysis and mutation. The BacA homolog in V. fischeri (VFA0673) is not found in any other sequenced Vibrios except V. angustum (49% identity, 72% similarity); however, the genetic context of the two Vibrios homologs is different. BLAST-P searches showed that the V. fischeri BacA homolog is similar to not only the BacA from S. meliloti and B. abortus but also to SbmA homologs in E. coli, Shigella flexneri and Salmonella species. SbmA is an inner membrane protein predicted to be part of an ABC-transporter for the transport of proline-rich antimicrobial peptides as well as bleomycin and microcin J25 (146, 167, 308), and S. meliloti BacA is a functional homolog of the E. coli SbmA (126). S. meliloti BacA also shares sequence homology to a family of peroxisomal-membrane proteins, which are important for the transport of long-chain fatty acids to the cytoplasm (73). AcpXL may then directly attach the long-chain fatty acid to the lipid A (280).

Construction of mutants in VF0137, VF0131, VF1650, and VFA0673. To assess whether BacA, PgtA1, PgtA2, or PgtA3 contributed to the lipid A structure, we targeted each of the genes for mutagenesis. To mutate these genes, we cloned an internal portion of each of the genes into a suicide vector, pEVS122, marked with Em resistance. Recombination of these constructs into the *V. fischeri* chromosome should result in two truncated copies of the genes. All genes were easily mutated using this technique, and the resulting mutants were subsequently named DMA370 (*bacA*), DMA390 (*pgtA1*), DMA391 (*pgtA2*), and DMA392 (*pgtA3*).

Impact of mutations in VF0137, VF0131, VF1650, and VFA0673 on growth, motility and luminescence. In Chapter 2, I showed that mutations altering *V. fischeri* lipid A affected the growth, cell morphology, motility, and luminescence of mutants (2). To colonize *E. scolopes* fully, *V. fischeri* must be able to grow rapidly (101), swim (223), and luminescence (282). Therefore, before testing symbiotic colonization, we assayed the effect of each mutation on these phenotypes.

We first assessed the ability of the mutants to swim through soft agar. The *bacA* mutant DMA370 (*bacA*) had no detectable difference in swimming rate relative to wild type. All three *pgtA* mutants displayed an attenuation of motility with the most dramatic and significant effect being with *pgtA3* mutant DMA392 (*pgtA3*) (Figure A.1). Motility defects with DMA390 (*ptgA1*) were significant for one experiment (Figure A.1) but not for the second (data not shown). Microscopic observations offered an explanation for the motility defect of DMA392 (*pgtA3*). DMA392 (*pgtA3*) appears to form chains of cells, and at higher densities in SWT it forms large groups of cells adhered together (Figure A.2). It is possible that cells linked together may not be able to swim as efficiently as free individual cells.

Growth of DMA370 (bacA), DMA390 (pgtA1) and DMA391 (pgtA2) was wild-type-like. However, DMA392 (pgtA3) began to form clumps in culture after an OD₅₉₅ ~1.0, making the relevance and accuracy of OD₅₉₅ readings and CFU determinations suspect (Figure A.2).

We also assayed bioluminescence of all the mutants. DMA370 (*bacA*), DMA390 (*pgtA1*) and DMA391 (*pgtA2*) each exhibited wild-type-like luminescence, however we found that DMA392 (*pgtA3*) had approximately 4-fold less luminescence than ES114. The reason for this decreased bioluminescence is unknown but could be an effect of the outer membrane stability.

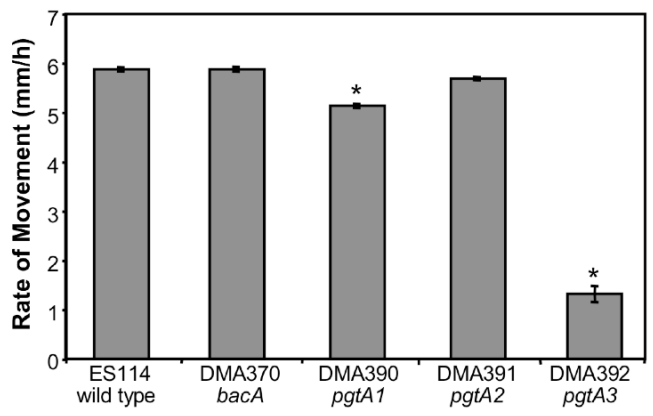


Figure A.1. Motility of *pgtA1*, *pgtA2*, *pgtA3*, and *bacA* mutants. Average rate of movement was measured through 0.25% agar plates. Representative data from one experiment of two are shown. Standard error (n=4) is shown. Asterisk represents significant difference (p<0.01) from wild type.

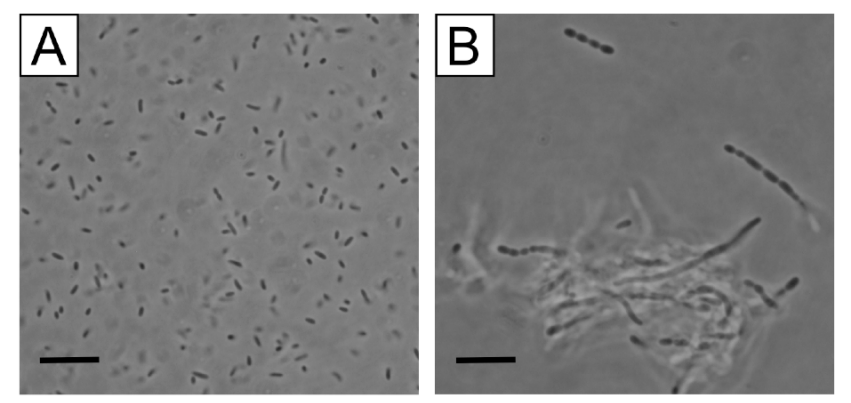


Figure A.2. Morphology of pgtA3 mutant. Phase contrast images of (A) ES114 (wild type) and (B) DMA393 (pgtA3) taken at OD ~1. Size bars represent 10 μ m.

Symbiotic colonization of *E. scolopes* by the mutants. DMA370 (*bacA*) had no defect in colonization over 48 h. Despite the slight defect in motility, DMA390 (*pgtA1*) and DMA391 (*pgtA2*) also had no apparent defect in colonization over the first 48 h. Squid colonized by DMA362 (*pgtA3*) had less luminescence over the first 48 h, which was accounted for by these animals having 10- to 100-fold fewer CFUs than the wild type at both 24 and 48 h. This result may simply be due to the motility defect, and/or the clumping phenotype of this mutant that we see in culture.

Competition experiments have been used previously in our lab and others as a measure of relative symbiotic proficiency, and such experiments have revealed colonization defects not apparent in single-strain inoculations (23, 125, 149, 157, 159, 179, 195, 251, 282, 284, 298, 306). However, we saw no significant competitive defect for DMA370 (*bacA*), DMA390 (*pgtA1*) or DMA391 (*pgtA2*) relative to wild type 48 h after inoculation (data not shown). When DMA392 (*pgtA3*) was competed with ES114 most animals were clonally infected with ES114, which is not surprising considering the motility defect of this mutant and its defect in early stages of infection even when not forced to compete with wild type (data not shown).

Effects of pgtA1, pgtA2, pgtA3 and bacA on LPS of V. fischeri. To test whether the genes we targeted have an effect on the structure of the lipid A, or other parts of the LPS, the LPS and lipid A was purified for each mutant and examined by MALDI-TOF MS. All the mutants' lipid A preparations still contained a species bearing a phosphoglycerol moiety based on comparisons of the mutant preparations to wild-type lipid A preparations (data not shown). Although we had failed to identify an enzyme responsible for adding the 172 Da moiety to lipid A, we were nonetheless interested in whether the mutants we had generated had altered LPS. To examine this, we O-deacylated the intact LPS from each of the mutants, thereby breaking all the ester linkages on the intact LPS. This results in O-deacylated LPS that contains the lipid A, minus all ester-linked fatty acids and acetyl groups, attached to the KDO and the core as well as the O-antigen. In this process, a small portion of the lipid A is also broken from the overall O-deacylated LPS structure. This O-deacylated LPS from each mutant strain was subjected to mass spectrometric analyses. MALDI spectra from O-deacylated LPS from both DMA390 (pgtA1) and DMA391 (pgtA2) both showed major species shifted to lower mass by 123 Da, which is

consistent with a phosphoethanolamine (PEA) moiety (Figure A.3). Because there was no PEA loss to the lipid A in the previously prepared deacylated lipid A structure (data not shown) and in the lipid A fragment found in the O-deacylated LPS (Figure A.3), this suggests that the PEA added is attached to the KDO or one of the core sugars. Interestingly *pgtA1* may be in an operon with a gene encoding KDO kinase, implicating KDO as the target for this PEA decoration.

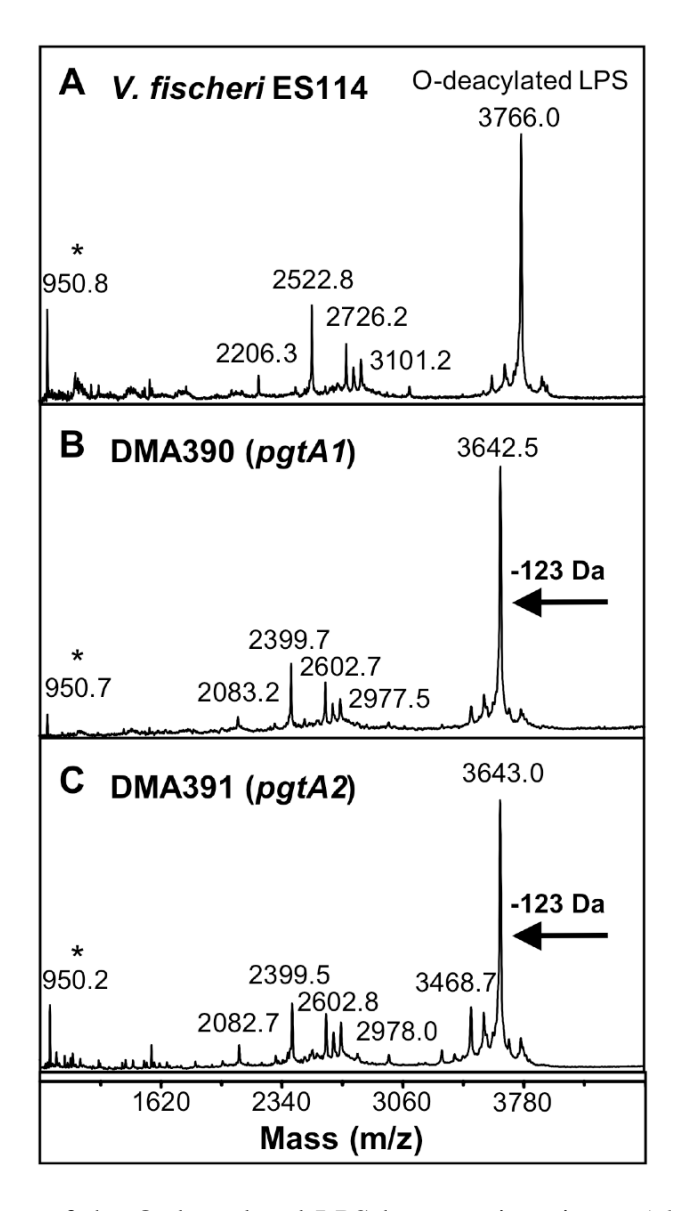


Figure A.3. Alterations of the O-deacylated LPS by mutations in *pgtA1* and *pgtA2*. LPS was purified from cultures grown on LBS plates. Samples were analyzed by MALDI-TOF mass spectrometer. Arrows in panels B and C indicate the molecular weight shift the major 3766 Da species caused by the mutation. "*" represents the ~950 Da lipid A fragment.

The DMA392 (*pgtA3*) mutant had a subtle effect on the lipid A moiety. The *V. fischeri* O-deacylated lipid A is believed to have two N-linked fatty acids, 3-OH C_{14:1} and a 3-OH C_{14:0}. While DMA392 (*ptgA3*) lipid A resembles the wild type as indicated by MALDI MS analysis, a slight difference from ES114 lipid A was detected upon analysis of the O-deacylated LPS. In addition to the expected fragment ion for the O-deacylated lipid A (~950 Da), an additional fragment ion was observed with a 2 Da increase in mass. This fragment could correspond to an O-deacylated lipid A with the N-linked 3-OH C_{14:1} fatty acid replaced by a second 3-OH C_{14:0} fatty acid. This suggests that PgtA3 may exhibit some influence over the incorporation of an N-linked fatty acid onto the lipid A.

LPS from DMA370 (*bacA*) proved difficult to purify, because it was much more hydrophobic than LPS from ES114. SDS-PAGE analysis suggested that the mass of the LPS from DMA370 was higher than that from ES114. MALDI and FAME analysis of the lipid A fraction showed that there was an increase in the relative abundance of C₁₆, C_{16:1}, and C_{18:1} fatty acids and a decrease in the relative abundance of C₁₄ and C₁₂ fatty acids, compared to the levels found in wild-type lipid A (Table A.2); however, no alterations were found that would explain the large apparent difference in SDS-PAGE mobility between LPS purified from the mutant and the wild type.

Table A.2. Percent fatty acid composition of partially purified lipid A from *V. fischeri* ES114 and DMA370 (*bacA*)

Strain	C _{12:0}	C _{14:0}	C _{16:0}	C _{16:1}	C _{16:1}	3-OH	$C_{18:0}$	C _{18:1}	$C_{18:1}$	3-OH	3-OH
				a	b	$C_{12:0}$		a	b	$C_{14:0}$	$C_{14:1}$
ES114	5.2	10.6	14.5	3.7	15.6	20.0	4.4	0.9	1.2	15.4	8.4
DMA370	1.8	4.2	22.4	15.7	14.4	12.4	2.9	0.6	9.2	11.2	5.2
(bacA)											

Discussion

Despite our attempts, we were unable to identify a gene that affected the 172 Da (putative phosphoglycerol) moiety found on the *V. fischeri* lipid A. However, the four genes that we did mutate each altered the LPS of *V. fischeri* either by the addition of PEA to the core (Figure A.3) or by subtle changes to the secondary acylations on the lipid A. Mutation of these genes resulted in few noteworthy phenotypes in culture or in the squid host, except for the mutation of *pgtA3* in DMA392, which was attenuated in motility and colonization.

Where PEA is added to core by PgtA1 and PgtA2 is unknown. Indeed, the structure of *V. fischeri* LPS is yet unsolved. A mutation in either *pgtA1* or *pgtA2* results in the loss of a PEA, and this suggests that either a PEA addition requires both of these genes, or that there are at least two PEA additions. Several bacteria have additions of PEA to their core region of LPS. In *Neisseria meningitidis*, there are two genes, *lpt3* and *lpt6*, which each direct addition of PEA to the inner core (54, 161, 303). *Haemophilus influenzae* also has two additions of PEA, one by *lpt6* (303), and the other by an unknown gene (266). *Salmonella enterica* has an addition of PEA to core that is added by *cptA* and regulated by PmrAB, and this PEA decoration has a modest effect on resistance to the cationic antimicrobial polymyxin B (259). Solving the *V. fischeri* LPS structure should reveal on how many PEA decorations are present, and ultimately relate to how *ptgA1* and *pgtA2* play a part in the additions.

The *pgtA3* mutant is an interesting strain even though it had only a subtle change in lipid A, with altered incorporation of N-linked fatty acids. Although the changes are not as drastic as one would expect given its obvious motility defect (Figure A.1) and chaining defect (Figure A.2), the small changes do reflect how subtle alterations to the lipid A moiety can affect the

morphology, motility and potentially affect the fluidity of the outer membrane of the bacterial cell.

Acknowledgements

I would like to thank Anthony Zaleski for purifying the LPS from the mutant strains.